BROADBAND WIDE COVERAGE UNIPLANAR ANTENNA

A thesis submitted by

BYBI P.C.

in partial fulfillment of the requirements for the degree of

DOCTOR OF PHILOSOPHY

Under the guidance of

Prof. P.Mohanan

COCHIN UNIVERSITY OF
SCIENCE AND TECHNOLOGY

**DEPARTMENT OF ELECTRONICS
FACULTY OF TECHNOLOGY
COCHIN UNIVERSTIY OF SCIENCE AND TECHNOLOGY
COCHIN-22, INDIA**

JANUARY 2009

Dedicated

to

The Almighty

CERTIFICATE

Certified that this thesis entitled "**BROADBAND WIDE COVERAGE UNIPLANAR ANTENNA**" is a bona fide record of the research work carried by Mrs. Bybi P.C. under my supervision in the Centre for Research in ElectroMagnetics and Antennas, Department of Electronics, Cochin University of Science and Technology. The results presented in this thesis or part of it have not been presented for the award of any other degree.

Cochin - 22   **Dr. P Mohanan**
26th January 2009   Supervising Teacher.

DECLARATION

I hereby declare that the work presented in this thesis entitled "**BROADBAND WIDE COVERAGE UNIPLANAR ANTENNA**" is a bona fide record of the research work done by me under the supervision of Prof. P. Mohanan, Department of Electronics, Cochin University of Science and Technology, India and that no part thereof has been presented for the award of any other degree.

Cochin-22   **BYBI P.C.**
26th January 2009

Acknowledgement

I remember with gratitude,

Bybi P.C.

CONTENTS

Chapter **4**

Numerical and Experimental Results…………………..81

Chapter 5

Conclusion and Future perspective...........................181

Appendix:

Chapter one

INTRODUCTION

"You see, wire telegraph is a kind of a very, very long cat. You pull his tail in New York and his head is meowing in Los Angeles. Do you understand this? And radio operates exactly the same way: you send signals here, they receive them there. The only difference is that there is no cat."

- Albert Einstein

  Wireless and mobile communication is one of the fastest growing areas of modern life. The main driving force behind wireless communication is the promise of portability, mobility and accessibility. It has an enormous impact almost every aspect of our daily life. A world of ubiquitous wireless devices is merging from wireless sensors and tag to mobile terminals. Mobile phones give us more freedom such that we can talk with each other at any time and in any place. The majority of modern portable computers already incorporate WLAN and Bluetooth solutions. New generation of wireless mobile radio systems provide flexible data rates and integrates a wide verity of applications like Television, GPS etc. This explosive growth of wireless communication is expected to continue in the future, as the demand for all type of wireless services is increasing.

  In any wireless communication system, the antenna plays a major role in the reliability and performance of the system. Today's small handheld devices challenge antenna designers for ultrathin, portable and high performance devices that have the ability to meet multi standards. This chapter serves to explore the historical advancements in the wireless communication technology with special emphasis to antenna research. It concludes with the motivation of the work and a brief description of the thesis organization.

1

1.1 Glimpse of wireless communication history

The wireless communication technology was established in 1864 when James Clerk Maxwell had procured a theoretical foundation for electromagnetic radiation. He stated that *"the energy, by the engagement of electric and magnetic waves could be transported through materials and space at a finite velocity"* [1]. His work was first published in 1873 [2]. Two decades later in 1888 another great scientist, Heinrich Hertz, demonstrated Maxwell's theory of electromagnetic radiation by launching electromagnetic waves using a spark gap generator. Hertz proved that electricity can be transmitted in the form of electromagnetic waves, which travel at the speed of light and which possess many other properties of light. His experiments with these electromagnetic waves led to the development of the wireless telegraph and the radio [3].

During 1894-1900 Jagadish Chandra Bose of Residency College in India, successfully made the first measurements at 60 GHz [4]. As a source, he used a spark gap having platinum electrodes with a special shape to emphasize the radiation at millimeter waves. In 1897 Marconi demonstrated the practical applications of wireless communication by establishing the continuous radio contact between the shore and ships travelling in the English Channel [5]. The possibility of international wireless communication opened up by the mid-December 1901, when the first transatlantic transmission between England and Canada was accomplished by Marconi[6]. The transmitting antenna used in this experiment consists of 50 vertical wires in the form of a fan connected to ground through a spark transmitter. The receiving antenna was a 200m wire pulled and supported by a kite. This was the beginning of antenna era.

Since then, the wireless communications technology has seen drastic progress and advancing rapidly. The invention of vacuum tube sparked another revolution in wireless communication. During this period of advancement in wireless

communications technology, Edwin Armstrong designed and created the super-heterodyne receiver circuit, which is used for the actual voice or music transmission [4]. This initial success of wireless communications shortly began to be a reality and further exploration was made towards today's booming area of personal communications. The milestones of wireless communication history are illustrated in Table 1.1.

1887	Heinrich Hertz verified the existence of electromagnetic waves
1901	First wireless transmission by Guglielmo Marconi.
1905	Marconi Patents his directive horizontal antenna.
1906	Lee de Forest's Radio Telephone company sold the first radio
1915	Direct telephone communications opened for service.
1924	Directive Yagi antenna is developed by Prof.Hidetsugu Yagi
1927	First television transmission.
1933	Demonstration of Frequency Modulation
1943	The first telephone line from Calcutta, India to China.
1944	Telephone cable is laid across the English channel
1947	First Mobile phone demonstration
1953	Deep space communication is proposed by John Pierce.
1957	Soviet Union launches Sputnik, humanity's first artificial satellite.
1958	Invention of Integrated Circuit
1979	A 62,000 mile telecommunications system is implemented in Saudi Arabia
1981	Beginning of first commercial cellular mobile communication
1982	Two way video teleconferencing service is started
1986	Integrated Service Digital Network is deployed
1995	CDMA is introduced
2000	3G Standard is proposed.

Table 1.1 Milestones of wireless communication history

1.2 Mobile communication systems

Table 1.2 illustrates the landmarks of mobile communication systems [7].

Generations	1G	2G	2.5G	3G
Year	1985	1992	1995	2002
Standards	AMPS,TACS,NMT	DAMPS, GSM900, CDMA TDMA	GPRS EDGE	Wideband CDMA, CDMA 2000, TD-CDMA
Access Techniques	FDMA	TDMA, CDMA	TDMA, CDMA	CDMA
Services	Analog voice	Voice(digital) and low rate data	High data rate	High capacity broadband data.

Table 1.2 Mobile communication systems

The first generation mobile communication systems of 1980's are based on analog transmission techniques, whereas second generation systems in the 1990's are digital. In digital systems, more efficient use of the available spectrum is achieved by digital encoding of the analog data. GSM (Global System for Mobile communications), TDMA (Time Division Multiple Access) and CDMA (Code Division Multiple Access) are the main mobile standards used in 2nd generation. Third generation systems evolved in early years of 20th century are providing services like wireless access to the Internet and high data rate applications like real time video transmission. In the near future, the fourth generation technology will be able to provide on-demand high quality services including voice and video.

1.3 The Antenna

The Antennas are one of the most essential components of any wireless communication system. The word antenna is derived from the Latin word '*antemna*' which became, in Latin language, antenna. The term antenna was first used by Marconi in a lecture in 1909[6]. The IEEE standard Definition of terms for Antennas defines the antenna or aerial as "a means for radiating or receiving radio waves"[8]. All antennas operate on the same basic principles of electromagnetic theory. In general, the antenna is the transitional structure between guided wave and a free space wave. In other words , a transmit antenna is a device that takes the signal from a transmission line, convert them into electromagnetic waves and then broadcast them into the free space, while operating in the receiver mode the antenna collects the incident electromagnetic waves and convert them back into electric signals.

In advanced wireless systems the antenna provides synthesized radiation characteristics depending up on the requirement of the communication equipment. In order to meet the particular requirement, it must take various forms. Wire antennas, reflector antennas, lens antennas, traveling wave antennas, frequency independent antennas, horn antennas and conformal antennas are used for different applications[9]. In addition antennas are also used in array configurations to improve the overall radiation characteristics.

- **The Ancient times**

The history of antennas dates back to James Clerk Maxwell who unified the theories of electricity and magnetism. In 1940's antennas technology was primarily related on wire related radiating elements which operates in frequencies up to in UHF. The II World War launched a new era in modern antenna technology with elements such as waveguide, apertures horn antennas and reflectors[10]. The

invention of microwave sources such as klystron and magnetron accelerated this new era of microwave communication.

Soon after II word war, antenna technology witnessed drastic improvement in its impedance bandwidth as great as 40:1 or more. These wideband antennas had the geometries specified by angles instead of linear dimensions and they are referred to as frequency independent antennas [11]. The major applications of these wideband antennas include TV reception, point to point communication, and feed for reflectors

Patch antenna is invented almost twenty years later [12], which find many applications with much ease of fabrication compared to the earlier designs. The major attractions of these designs were easy integration with active components and various antenna characteristics such as gain, electronic control of radiation pattern etc. Major advances in millimeter wave antennas have been made in recent years including integrated antennas where active and passive circuits are combined with the radiating elements in one compact unit.

Smart antennas also known as adaptive arrays, are introduced during the recent years which incorporates signal processing algorithms embedded with the antennas. These techniques result pattern synthesis and easy integration with recent mobile communication systems [13].

▪ **The selection**

The selection of the particular type of antenna to be used for a given application is determined by electrical and mechanical constrains and operating costs. The electrical parameters of the antenna are the frequency of operation, gain, polarization, radiation pattern, impedance, etc. The mechanical parameters of importance are the size, weight, reliability, manufacturing process etc. In addition, the environment under which the antenna is to be used also needs to be taken into

consideration like the effect of temperature, rain, wind vibrations, etc. A good design of the antenna can relax system requirements and improve the system performance.

▪ **The Applications**

Antennas enjoy a very broad range of application, both in the military and commercial world. Today's antennas find extensive use in biomedicine, radar, remote sensing, astronomy, collision avoidance, air traffic control, global positioning systems, pagers, WLAN etc[9]. The IEEE slandered frequency allocation for various applications in the microwave band is illustrated in Table 1.3.

Band Designation	Frequency range	Usage
VHF	3-30KHz	Long distance telegraphy and navigation
LF	30-300 KHz	Aeronautical navigation services, Radio broadcasting, Long distance communication,
MF	300-3000	Regional broadcasting, AM radio
HF	3-30MHz	Communications, broadcasting, surveillance, CB radio
VHF	30-300 MHz	Surveillance, TV broadcasting, FM radio
UHF	30-1000MHz	Cellular communications
L	1-2 GHz	Long range surveillance, remote sensing
S	2-4 GHz	Weather detection, Long range tracking
C	4-8 GHz	Weather detection, long-range tracking
X	8-12 GHz	Satellite communications, missile guidance, mapping
Ku	12-18 GHz	Satellite communications, altimetry, high resolution mapping
K	18-27 GHz	Very high resolution mapping
Ka	27-40 GHz	Air port surveillance

Table 1.3 Frequency bands allocated for various applications

1.4 Challenges in future Antenna Design

One of the trends in wireless communication technology in the last decade has been to dramatically decrease the size and the weight of the handheld communication devices. This remarkable reduction in weight and volume has necessitated a rapid evolution of the antennas used for the handsets. Accordingly, antenna designers encountered difficulty in designing antennas that could maintain their performance unchanged, even though the antenna size become smaller; since a degradation of the gain and bandwidth was inherently observed in small antennas.

In conjunction with such recent trends in mobile communications as personalization, mobile terminals have advanced to be not only smaller, but also instrumental for acquiring various voice and non-voice information, without regard to time and place. In view of the progress of small mobile terminals, the design of antennas is acquiring great importance. The antennas are required to be small, and yet to have prescribed characteristics and performance, such as wide bandwidth, operation in dual or triple frequency bands, diversity, and so forth. In addition, further advanced design is required for improving the antenna's performance in recent, small mobile systems.

The ground plane is the return path for the current in the system and its role in wireless communication devices is very much important. In the early days of mobile communications, the case, being made of metal, was simply treated as a ground plane, because radiation currents flow on it as well as on the antenna element. Conventional antenna design uses image technique to provide the infinite ground plane. This theory is not possible while designing electrically small ground plane antennas. In the case of a whip type antenna, the ground plane can be treated as the other half of the dipole to the antenna.

The characteristics of small antennas mounted on the handheld devices are get affected by the antenna position on the terminal chases and the dimensions of the chases due to the existence of radiating surface currents on the terminal ground plane induced by the antenna element. Therefore the design of an antenna with suitable ground plane is very much important.

In the case of large antennas, the challenges in design are mainly to realize ultra-low side lobes, reduce EMI, achieve superior EMC characteristics etc. The modeling of the large antennas to predict its performance is another difficult task. Currently, commercial softwares are quite limited in their ability to handle the structures which require a problem description with a very large number of meshes because of their complexity, multiscale characteristics and homogeneous nature.

1.5 Planar Antenna Technologies

The demand for broadband antennas that are capable of supporting high data speeds and multiband operations of modern wireless communication systems have significantly increased. Commonly these systems need low-cost solutions with desired performance in terms of impedance bandwidth, polarization and gain. Planar antennas are playing important roles in various wireless communication applications owing to unique merits such as small volume or low profile, low manufacturing cost, and easy integration into planar circuits [14,15].

The planar antennas can be usually be categorized in terms of radiation performance into microstrip patch antenna, Suspended Plate Antenna (SPA), planar inverted–L/F antenna and planar monopole/dipole antenna [16]. Generally the changes in such antenna design are from the specific requirements of applications. The microstrip patch antenna in its basic forms has a low profile, which is conductive to conformal design, but suffers narrow impedance

bandwidth on order of 1 percent. In contrast, the planar monopoles usually have a high profile above a ground plane but enjoy broad bandwidth.

Considering the antenna profile, impedance,and radiation performance, the SPAs are good option for fixed base stations in wireless communication systems, and planar monopole/dipoles for mobile wireless terminals. A verity of techniques has long been developed to further enhance the broadband performance of the SPAs and planar monopoles. Due to the merits of acceptable performance, low profile and in particular low manufacturing cost, the SPAs and planar monopoles have widely been applied in high-speed wireless communication systems.

1.5.1 Microstrip Antenna

As shown in Fig.1.1, conventional microstrip antenna consists of a pair of parallel conducting layers separating a dielectric medium, referred as the substrate [17]. In this configuration, the upper conducting layer or "patch" is the source of radiation where electromagnetic energy fringes off the edges of the patch and into the substrate. This patch is fed with a microstrip transmission line. The lower conducting layer acts as a perfectly reflecting ground plane, bouncing energy back through the substrate and into free space.

Physically, the patch is a thin conductor that is an appreciable fraction of a wavelength in extent, parallel to a ground plane and a small fraction of a wavelength above the ground plane. The patch will radiate effectively if the length of the patch is typically about a half guide-wavelength in size. In most practical applications, patch antennas are rectangular or circular in shape; however, in general, any geometry is possible.
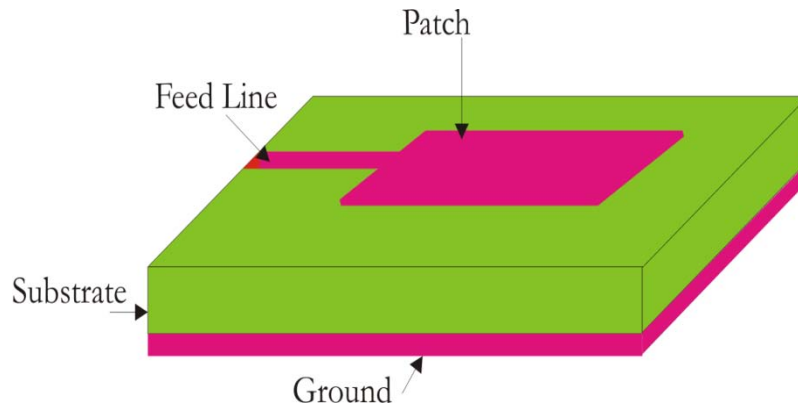
Fig.1.1. Typical geometry of a microstrip antenna

Microstrip patch antennas are increasing in popularity for use in many modern systems because

- Light weight and low volume.

- Low profile planar configuration which can be easily made conformal to host surface.

- Low fabrication cost, hence can be manufactured in large quantities.

- Supports both, linear as well as circular polarization.

- Can be easily integrated with microwave integrated circuits (MICs).

- Capable of dual and triple frequency operations.

- Mechanically robust when mounted on rigid surfaces.

Microstrip patch antennas suffer from a number of disadvantages as compared to conventional antennas.

- Narrow bandwidth

- Low efficiency

- Low Gain

- Unwanted radiation from feeds and junctions

- Poor end fire radiation except in tapered slot antennas

- Low power handling capacity.

- Surface wave excitation

The large antenna quality factor, Q, of the microstrip antenna leads to narrow bandwidth and low efficiency. Q can be reduced by increasing the thickness of the dielectric substrate. So the thickness of the substrate is of considerable importance when designing microstrip antennas. The most desirable substrates for antenna performance are the ones that are thick with a low dielectric constant. This results in an antenna with a large bandwidth and high efficiency due to the loosely bounded fringing fields that originate from the patch and propagate into the substrate. However, this comes at the expense of a large volume antenna and an increased probability of surface wave formation. On the other hand, thin substrates with high dielectric constant reduce the overall size of the antenna and are compatible with MMIC devices, since the fringing fields are tightly bound to the substrate. With thin substrates, coupling and electromagnetic interference (EMI) issues are less prone.

However, because of the relatively higher loss tangents (dissipation factors), they are less efficient and has relatively smaller bandwidth. Therefore, there is a fundamental tradeoff that must be evaluated in the initial stages of the microstrip antenna design, to obtain loosely bound fields to radiate into the free space, while keeping the fields tightly bound for the feeding circuitry.

1.5.2 Suspended Plate Antennas(SPA)

The SPA with a thick, low-permittivity dielectric substrate can be considered as a variation of microstrip patch antenna [18], as shown in Fig.1.2. The planar radiator may be of any shape above the ground plane. The dielectric substrate may be multilayered partially with air. The substrate thickness h is usually around 0.06 times the operating wave length. The operating frequency f_0 of the SPA can be estimated by

$$f_0 = c/\lambda_0 = c/ 2* \sqrt{\varepsilon r}(l+h)$$

where λ_0 denotes the operating wave length at the frequency f_0, c is the speed of light and εr is the relative dielectric constant. The legth l, distance d and thickness h are in meters.
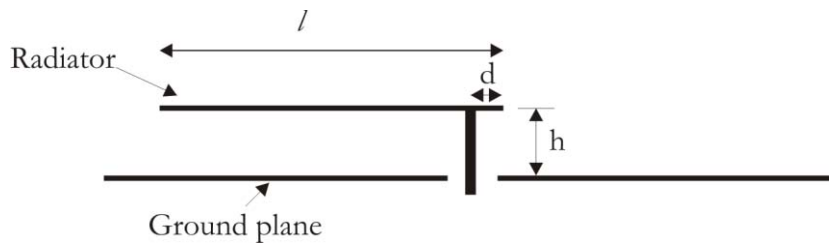
Fig.1.2 Suspended plate antenna geometry

Mainly the SPAs can be excited by a microstrip line, a probe and an aperture-coupled feeding structure, in which both the strip line and coaxial probe feeds may cause narrow impedance bandwidth due to the narrow band impedance transition between the strip line or probe and radiators. Fig. 1.3 illustrates different feeding schemes used in SPAs.
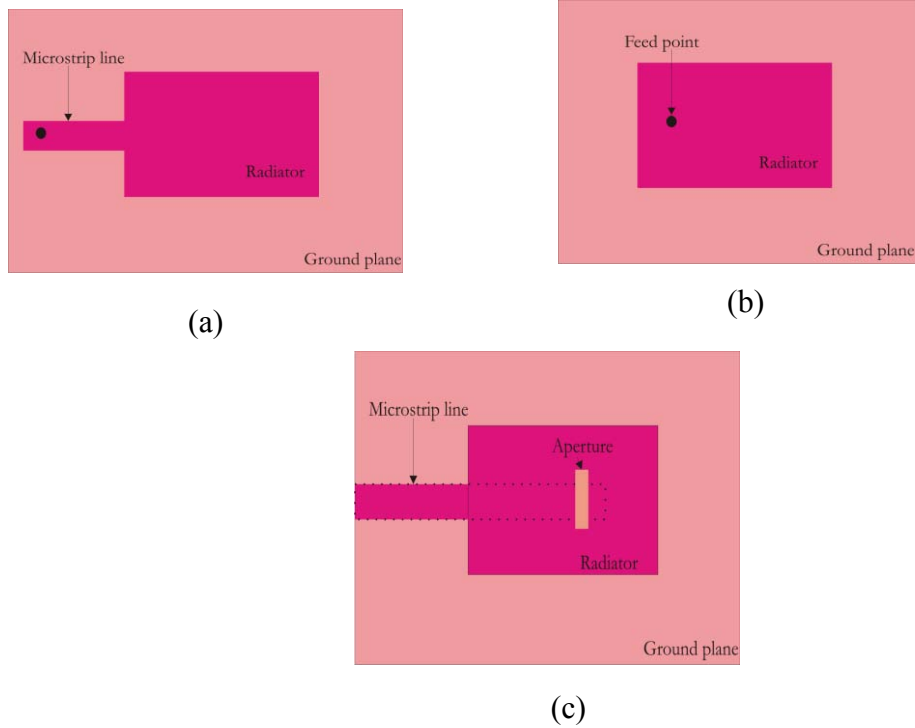
Fig.1.3. Different types of Feeding structures for SPAs (a) Microstrip (b) Probe (c) Aperture

However, the asymmetric feeding structures degrade the radiation performance especially at higher frequencies with the high cross-polarization level and beam distortion. In the case of electromagnetically coupled feeding mechanism, the symmetric configuration of the antenna improved the radiation performance by suppressing the high cross-polarized radiation. This transition structure also improves the impedance bandwidth to some extent.

1.5.3 Planar inverted F antenna

The origin of the planar inverted-F Antenna can be traced all the way back to the Inverted-L Antenna (ILA). The antenna has a structure as shown in Fig. 1.4., and may be categorized as a physically constrained small antenna. It consists of a short monopole as a vertical element and a wire horizontal element attached at the end of the monopole.
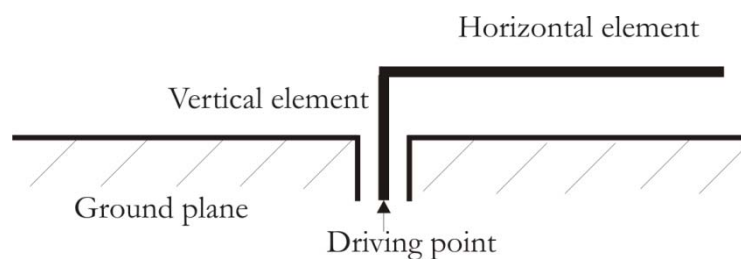
Fig. 1.4. Fundamental structure of the inverted-L Antenna(ILA).

The ILA is basically a low profile structure, due to the fact that the height of the vertical element is usually constrained to a fraction of the wavelength. The horizontal element is not necessarily very short, and usually has a length of about a quarter wave length. The ILA has inherently low impedance, since the antenna is essentially a vertical short monopole loaded with a long horizontal wire at the end of the monopole. The input impedance is comparable to that of the short monopole, in addition the reactance of the horizontal wire, which is closely placed to the ground plane. Hence to increase the radiation impedance, another inverted-L element is attached to the end of the vertical element and this is how the inverted-F Antenna (IFA), as depicted in Fig. 1.5, is formed from the ILA.
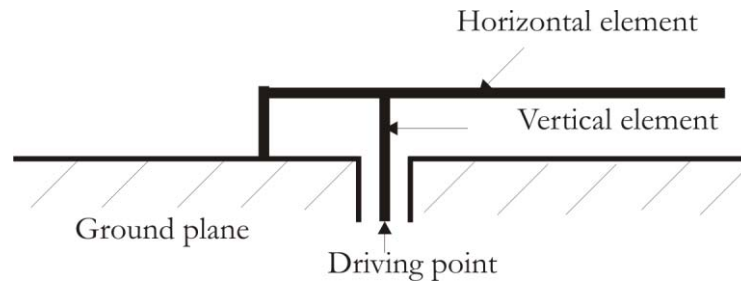
Fig. 1.5. The inverted-F antenna (IFA) modified from ILA.

This adjustment can be vital because the input impedance of an IFA can be set to have an appropriate value to match the load impedance, without using any additional circuit between the antenna and the load. For this reason, the IFA, rather than the ILA, has been used practically and applied often to moving bodies such as rockets and aircraft due to its low profile structure. In addition to the above-mentioned features, its performance with two polarizations would be useful for urban environmental use. This is especially true for application on mobile equipment like the hand-held transceiver.

To obtain broad bandwidth characteristics, the horizontal wire element is replaced by a plate, hence called the Planar Inverted F Antenna(PIFA). Fig. 1.6 shows how the PIFA looks like when mounted on a ground plane. They are good candidates as internal antennas and have important features like compact size, broad bandwidth, and moderate gain. This intern results reduction in the height of the antenna while maintaining the resonant length. The bandwidth is affected very much by the size of the ground plane. For example, reducing the ground plane can effectively broaden the bandwidth of the antenna. PIFAs are famous for multiband applications in handheld devices such as mobile handsets, notebook PCs, PDAs [19, 20, 21, 22, 23, 24].
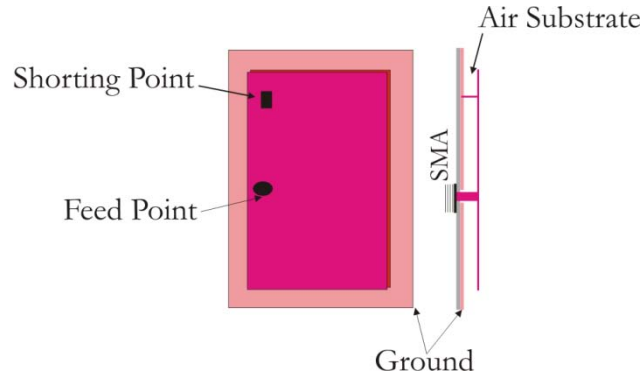
Fig.1.6. Planar inverted F antenna

1.5.4   Planar monopole Antennas

Planar monopole or disc antennas have been used in wireless communications due to its large bandwidth, moderate gain with nearly Omni-directional radiation characteristics. The earliest planar dipole may be the bow-tie antenna invented by Brown-Woodward . A general radiator mounted above a large ground plane forms a planar monopole.

The triangular monopole antenna can be considered as the planar versions of bi-conical antenna. The rectangular monopole antenna is the planar version of cylindrical monopole antenna. The monopole performance is mainly determined by the shape and size of the planar radiator as well as the feeding section. The overall size of the monopole and shape of the radiator dominate the frequency corresponding to the lower edge of the impedance bandwidth. The feed gap, the location of the feed point, and shape of the radiator greatly affect the impedance matching. Theoretically the radiating element of the planar monopole can be of any shape for broad operating bandwidth. The elliptical planar monopole antenna

is one of the important types of the planar monopole due to its broad impedance bandwidth.

(a)

(b)
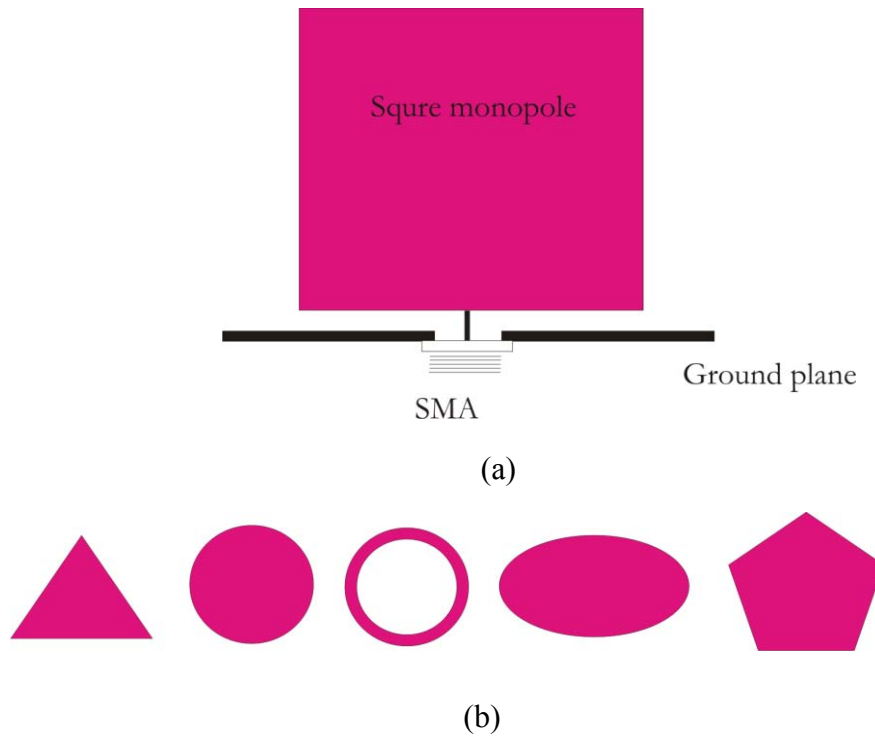
Fig. 1.7. (a) Planar square monopole antenna geometry (b) other possible patch configurations.

Printed antennas are the most promising design for mobile wireless applications since the antennas are expected to be embeddable or easy to be integrated into wireless devices. The antennas are usually constructed by etching the radiator onto the dielectric substrate with a ground plane around the radiator.
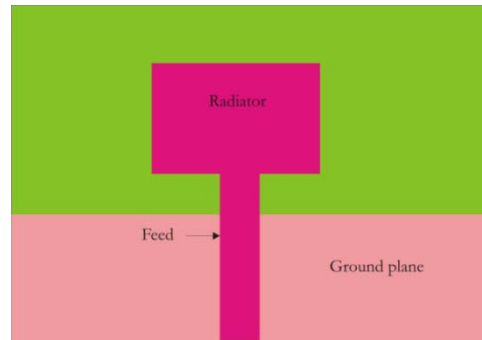
Fig. 1.8 Printed rectangular monopole antenna

The printed antennas can be fed by a microstrip transmission line, a coplanar waveguide structure or directly by a RF cable, where the inner conductor is connected to the upper radiator and the out conductor is grounded into a system ground. In the case of a microstrip transmission line, the ground plane is usually etched on opposite side, which is connected to the system ground. In the case of CPW-fed printed monopole antenna, the ground planes are etched close to the feeding strip on the same surface. The directly fed monopoles are often used where the printed monopole is not close to the main board and an RF cable is used to connect the antenna into the main board as in the case of a laptop. The different feeding techniques are illustrated in Fig. 1.9.

(a)   (b)

(c)
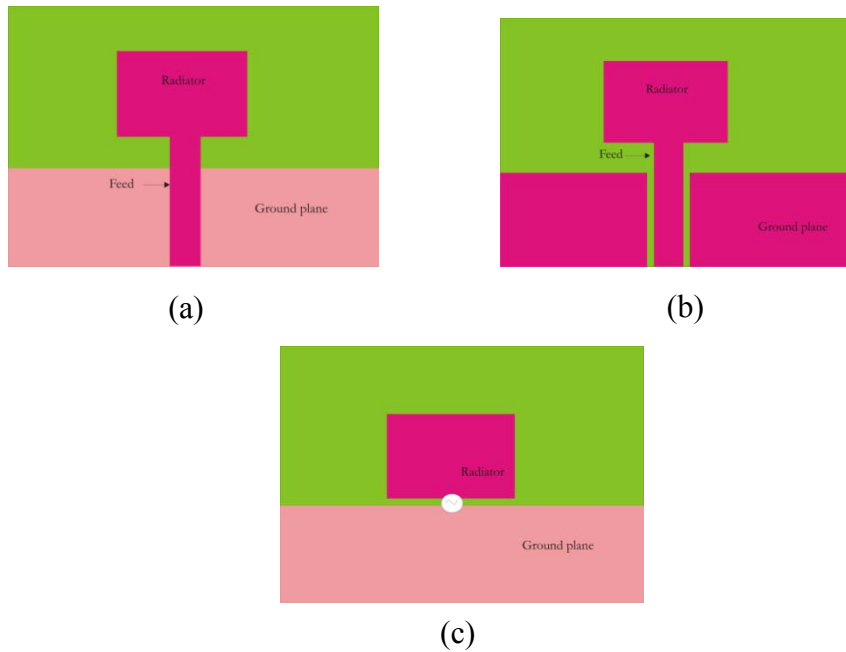
Fig. 1.9 Feeding techniques for printed antennas (a) microstrip (b) coplanar (c) RF cable

1.6 Coplanar wave guide and its application in antennas

A conventional CPW consists of a centre strip conductor with semi-infinite ground planes on either side on a dielectric substrate as illustrated in Fig.1.10. The coplanar waveguide was invented by C.P. Wen in 1969 [25]. This structure supports a quasi-TEM mode of propagation. Over a microstrip line the CPW provides many advantages like simple to fabrication, easy shunt as well as series surface mounting of active and passive devices [26,27,28,29,30]eliminates the need for wraparound and via holes [13] and [31], and reduces radiation loss[13]. More over in the case of a CPW the size reduction is possible since aspect ratio determines the characteristic impedance. In addition due to the presence of the ground plane between any two adjacent lines cross talk effects between adjacent lines are very week [13]. So, CPW circuits can be made denser than conventional

microstrip circuits. These, as well as several other advantages, make CPW ideally suited for MIC as well as MMIC applications. Generally coplanar waveguides can be classified as conventional CPW, conductor backed CPW and micro-machined CPW
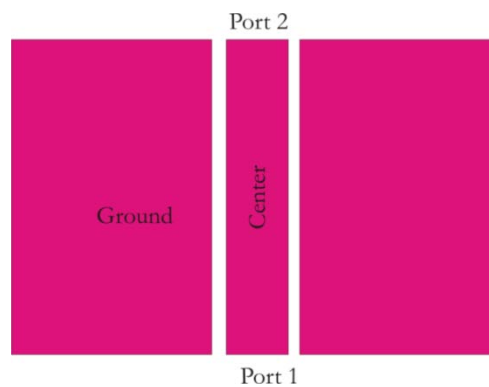
Fig. 1.10. CPW line

In a conventional CPW, the ground planes are of semi-infinite extent on either side. However, in a practical circuit the ground planes are made of finite extent. The conductor-backed CPW has an additional ground plane at the bottom surface of the substrate. This lower ground plane provides mechanical support to the substrate and acts as a heat sink for circuits with active devices. The micro-machined CPWs are of two types, namely, the micro-shield line [32] and the CPW suspended by a silicon dioxide membrane above a micro-machined groove [33].

Nowadays monopole antennas with CPW feed are more popular for dual band and wideband applications due to their attractive features such as low radiation loss, less dispersion, wide bandwidth, uni-planar structure and easy integration with active devices without via holes. Recently asymmetric coplanar strip line and slot line are also used to feed the monopole antenna. The main

advantage of using coplanar waveguide in the feed includes the capability of CPW to mount components without via holes. At the same time it helps integration of MMIC circuit's such as phase shifters using solder bumps and flip chip techniques.

1.7   Motivation of the work

With the development of wireless communications, there are growing demand for both voice and data services. The service providers are upgrading their networks with advanced technologies since the number of mobile phone subscribers, as well as usage rate is growing tremendously. Recently, FCC licensed a spectrum designated 'Advanced Wireless Services' (AWS) that offers a variety of wireless services including the broadband 3G mobile. Leading mobile telephone manufacturers are integrating features like satellite radio and TV to the hand held devices. These systems need an antenna with wideband or multi-band characteristics to cater the forthcoming mobile communication.

One technique to provide such feature is to integrate a multi-band antenna that operates over specific narrowband frequencies. However, it would be extremely difficult to accurately achieve the frequency requirements of all future communication systems. Alternately, a single antenna that covers a wide range of frequencies with same polarization would be an ideal candidate not only for present multi-band applications but also for future communication systems.

One of the most popular antennas employed in wireless and mobile communication systems is the printed monopole antenna because of simple structure and powerful merits such as wide impedance bandwidth, omni-directional radiation pattern and moderate gain. In the case of a printed monopole antenna the radiating geometry is printed on a substrate and the ground plane is printed parallel to the radiating structure. The ground plane is a crucial factor for

these printed monopoles. The shape and size of the planar radiator as well as the feeding section determines the characteristic of the printed monopole antenna. At the same time the overall size of the monopole and shape of the radiator govern the lower cut off frequency. The band width of the antenna greatly depends up on the feed gap, the location of the feed point, and shape of the radiator. The key idea behind the work is the enhancement of bandwidth by properly tuning the radiating element.

1.8 Thesis Organization

Chapter 1 gives the introduction of the thesis. It includes the history of research in the field of microwave electronics especially in antenna research. The chapter provides basic information about monopole antennas and other planar antennas. The motivation of the work and the thesis organization are also included in this chapter.

Chapter 2 covers the review of literature about the present work. Recent developments in the field of printed antennas with special attention to the printed monopoles are provided. The review also includes works in wideband and dual band antennas around the world. It briefly narrates the developments in the Coplanar Waveguide Antennas.. The development of FDTD technique and its progress is also referred at the end of this chapter.

Chapter 3 covers the experimental and theoretical analysis methodology employed for the characterization of the antenna. Simulation and parametric analysis using commercial package Ansoft-HFSS is incorporated.

Chapter 4 cover the experimental as well as numerical results. The major part of the work includes the development and characterization of wideband antennas from conversational transmission lines. A strip monopole and Finite Ground Coplanar Waveguide are utilized for the development of wideband antennas.

Detailed results of parametric analysis and optimization of various antenna parameters are included in this chapter.

Chapter 5 is the concluding session of this thesis. It describes the important inferences on results and salient features of the proposed wideband antenna. The scope of future work is also discussed in this chapter.

A detailed description of FDTD methodology and its implementation using Matlab is described in the Appendix.

References:

[1] K. Fujimoto and J.R. James, " Mobile Antenna Systems Handbook, Artech House, 1994.

[2] J. C. Maxwell, "A Treatise on Electricity and Magnetism, Oxford University Press, London, UK, 1873, 1904.

[3] W.J.G Beynon," Marconi, radio waves and the ionosphere", radio science, vol.10, no.7, pp 657-664, July 1975.

[4] John D. Kraus, "Antennas since Hertz and Marconi", IEEE Trans. Antennas and Propagat. vol.33, no.2, pp 131-136, February 1985.

[5] T. S. Rappaport, Wireless Communications, Principles and practice, Prentice Hall, 1996.

[6] Garratt, G.R.M. The Early History of Radio from Faraday to Marconi (London: Institution of Electrical Engineers, 1994).

[7] Ramjee Prasad, Marina Ruggieri, "Technology Trends in Wireless Communications", Artech House, 2003

[8] IEEE standard definitions of terms for antennas, IEEE Std 145-1983, June 1983.

[9] Christos G. Christodoulou, Parveen F. Wahid, "Fundamentals of Antennas: Concepts and Applications," SPIE Press, 2001

[10] Sterling, Christopher and George Shiers (Eds). History of Telecommunications Technology: An Annotated Bibliography (Lanham, MD: Scarecrow, 2000).

[11] V. H. Rumsey, Frequency Independent Antennas, 1957 IRE National Convention Record, Part 1, pp. 114-118.

[12] G. A. Deschamps, Microstrip microwave Antennas, presented at the Third USAF symposium on Antennas, 1953.

[13] Tapan K. Sarkar, History of Wireless, Wiley-IEEE Press, 2006.

[14] Sheng-Bing Chen, Yong-Chang Jiao, Wei Wang, and Fu-Shun Zhang, "Modified T-Shaped Planar Monopole Antennas for Multiband Operation," IEEE Trans. Antennas and Propagat., vol.54, pp. 3267-3270,2006

[15] Shaoqiu Xiao, Bing-Zhong Wang, Wei Shao, and Yan Zhang, "Bandwidth-Enhancing Ultralow-Profile Compact Patch Antenna," IEEE Trans. Antennas and Propagat., vol.53, pp. 3443-3447,2005

[16] Z. N. Chen and M. Y. W. Chia, Broadband Planar Antennas: Design and Applications(New York: John Wiley & sons, Inc. 2006).

[17] Ramesh Garg, Prakash Bhartia, Inder Bahl, A. Ittipiboon, "Microstrip Antenna Design Handbook," Artech House, 2001

[18] John L. Volakis, Richard C. Johnson, Henry Jasik, "Antenna Engineering Handbook," McGraw-Hill Professional, 2007

[19] Z.D. Liu, P.S. Hall, and D. Wake, "Dual-frequency planar inverted-F antenna". IEEE Trans Antennas Propagat AP-45, pp.1451–1458, 1997.

[20] C.R. Rowell and R.D. Murch, "A compact PIFA suitable for dual- frequency 900/1800-MHz operation", IEEE Trans Antennas Propagat. AP-46, pp. 596–598, 1998.

[21] P. Salonen, M. Keskilammi, and M. Kivikoski, "New slot configurations for dual-band planar inverted-F antenna", Microwave Opt Technol Lett 28, pp. 293–298, 2001.

[22] M. Martı´nez-Va´zquez, M. Geissier, D. Heberling, A. Martı´nez-Gonza´- lez, and D. Sa´nchez-Herna´ndez, "Compact dual-band antenna for mobile handsets" , Microwave Opt Technol Lett 32,pp. 87–88, 2002.

[23] F.R. Hsiao, H.T. Chen, T.W. Chiou, G.Y. Lee, and K.L. Wong, "A dual-band planar inverted-F patch antenna with a branch-line slit", Microwave Opt Technol Lett 32, pp. 310–312, 2002.

[24] C.W. Chiu and F.L. Lin,"Compact dual-band PIFA with multiresonators", Electron Lett 38, pp. 538–540, 2002.

[25] C. P. Wen,"Coplanar Waveguide: A Surface Strip Transmission Line Suitable for Nonreciprocal Gyromagnetic Device Applications," IEEE Trans. Microwave Theory Tech.,Vol. 17, No. 12, pp. 1087—1090,Dec. 1969.

[26] J. Browne, "Broadband Amps Sport Coplanar Waveguide," Microwaves RF, Vol. 26, No. 2, pp. 131—134, Feb. 1987.

[27] Technology Close-Up, Microwaves RF, Vol. 27, No. 4, p. 79, April 1988.

[28] J. Browne, "Coplanar Waveguide Supports Integrated Multiplier Systems," Microwaves RF, Vol. 28, No. 3, pp.137—138, March 1989.

[29] J. Browne, "Coplanar Circuits Arm Limiting Amp with 100-dB Gain," Microwaves RF, Vol. 29, No. 4, pp. 213—220, April 1990.

[30] J. Browne, "Broadband Amp Drops through Noise Floor," Microwaves RF, Vol. 31, No. 2, pp. 141—144, Feb. 1992.

[31] J. Browne, "Coplanar MIC Amplifier Bridges 0.5 To 18.0 GHz," Microwaves RF, Vol. 26, No. 6, pp. 194—195, June 1987.

[32] T. M. Weller, L. P. B. Katehi, and G. M. Rebeiz, "High Performance Microshield Line Components," IEEE Trans. Microwave T heory Tech., Vol. 43, No. 3, pp.534—543, March 1995.

[33] V. Milanovic, M. Gaitan, E. D. Bowen, and M. E. Zaghloul, Micromachined Microwave Transmission Lines in CMOSTechnology," IEEE Trans. Microwave T heory Tech., Vol. 45, No. 5, pp. 630—635, May 1997.

Review of Literature

This chapter serves to review the important developments in the design and modeling of printed antennas since its origin. Developments in Multiband and broadband antennas around the world are also reviewed. Recent works in planar monopole and CPW antennas along with the developments in FDTD based numerical analysis is presented at the end of this chapter.

2.1 Printed Antenna design

There is a strong interest in the printed antennas for millimeter- wave applications. Due to the attractive features like ease of integration with the final RF stage of the communication system, many researchers around the world are attracted by the printed antenna technology.

The foundation of printed antenna was originally started in 1953 [1] when Deschamps proposed the use of microstip feed lines to feed an array of printed antenna elements. Shortly thereafter, Lewin investigated [2] radiation from strip line discontinuities. In the late 1960's Kaloi did some additional studies over basic rectangular and square configurations. However the microstrip element was first patented by Muson [3] and data on basic rectangular and circular microstrip patches were published by Howell in the 1970's [4].

Later Weinschel [5] developed some microstrip geometries for use with cylindrical S-band arrays on rockets. The application of microstip element as an array was showed by Sanford [6]. The early work by Munson on the development of microstrip antennas for use as low-profile flush-mounted antennas on rockets and missiles showed that this was a practical concept for use in many antenna system problems, and thereby gave birth to a new antenna industry.

Soon after the introduction of microstrip antenna, papers appeared describing methods of analysis for these antennas, including the transmission line model [7], the cavity model [8] and the spectral- domain method [9].

C. L. Mak et al. [10] proposed an Experimental Study of a Microstrip Patch Antenna with an L-Shaped Probe. The antenna provides 36% impedance bandwidth (SWR 2) as well as about 7-dBi average gain. A two-element array fed by-probes is used to substantially suppress the cross polarization of the proposed antenna. Both the antennas have stable radiation patterns across the pass band.

A novel shorted dual spiral printed antenna is presented by H.K. Kan et al. [11]. The antenna consists of two inter leaved shorted spiral radiators and a feed network etched on a high dielectric material below the ground plane. The antenna provides a 10dB return loss bandwidth of 9.2% with an omni-directional radiation pattern.

A novel single-layer rectangular patch antenna using a coupled line feed is described by M.D. van Wyk et al. [12]. This coupled line matching technique increases the bandwidth of the patch antenna by a factor of more than 2.5 as compared to the normal edge-fed patch with the same geometrical dimension.

J.S. Baligar et al. [13] designed a Broadband two-layer shorted patch antenna with low cross-polarization. The antenna has a bandwidth of 11% centered around 1.975 GHz with a gain of 8.6 dB, and exhibits better than -13dB cross-polarisation levels in the H-plane.

Kevin M. K. H. Leong et al. [14] proposed a surface wave enhanced broadband planar antenna for wireless applications. The antenna proposed utilizes the truncated microstrip ground plane as a surface-wave reflector element rather than an additional metal sheet to achieve unidirectional radiation results in a significant savings in overall antenna size and weight.

Cross-polarization reduction for a broad-band probe-fed patch antenna with a novel U-shaped ground plane is demonstrated by Wen-Hsiu Hsu et al. [15]. Owing to the two conducting flanges of the U-shaped ground plane, gain enhancement of the proposed antenna, compared to a corresponding conventional antenna with a same ground-plane size, is observed.

Ban-Leong Ooi et al. [16] proposed a novel design of broad-band stacked patch antenna. The proposed antenna has the input impedance bandwidth of about 38.41%, better than the conventional E-shaped microstrip patch antenna, which has an input impedance bandwidth of 33.8%. Through the use of the

washer on the probe of the stacked patch antenna, the input impedance bandwidth is improved further to 44.9%.

A new design of a broad-band probe-fed patch antenna with a W-shaped ground plane is presented by Kin-Lu Wong et al. [17]. With the use of the proposed W-shaped ground plane, the required probe-pin length in the substrate remains to be small, resulting in a much wider operating bandwidth. Also, by choosing proper dimensions of the W-shaped ground plane, the antenna gain for frequencies over the obtained wide bandwidth is enhanced, compared to the conventional patch antenna with a planar ground plane.

A novel kind of planar monopole broadband antenna with a parasitic radiator is proposed by Xing Jiang et al. [18]. The bandwidth of the monopole antenna is considerably improved with a parasitic element earthed with a matching inductor.

C.L. Mak et al. [19] presented a half-sized U-slot quarter-wave patch antenna. Employing the same parameters as the U-slot quarter-wave patch except with half the area, similar performances are maintained such as a broad bandwidth of 28% (SWR < 2), stable far-field radiation patterns and gain.

Chi Yuk Chiu et al. [20] proposed a novel technique that improves the performance of a conventional quarter-wave patch antenna. Two different geometries (U-slot and L-slit) are being investigated experimentally. With the inclusion of a folded inner small patch, they achieved impedance bandwidths of 53% and 45% for the U-slot and L-slit, respectively.

Y. J. Sung et al. [21] proposed a microstrip patch antenna using the defected ground structure (DGS) to suppress higher order harmonics. An H-shaped defect on the ground plane with only one or more unit lattices has been utilized and yielded band stop characteristics.

A microstrip antenna incorporating a V-shape slot on its patch is introduced and studied for its impedance bandwidth and radiation characteristics by Gh. Rafi et al. [22]. The antenna is inherently broadband, and by optimizing the V-

parameters its performance is improved considerably over that of a U-slotted patch.

W.-C. Liu et al. [23] designed a dual-polarised single-layer slotted patch antenna. The antenna has two highly decoupled orthogonal input ports and is capable of generating dual-polarised radiation.

Y. Qin et al. [24] proposed a broadband patch antenna with ring slot coupling. The broad band is achieved using an H-shaped patch coupled to a microstrip feed line via a ring slot in the ground plane. The antenna provides a wide impedance bandwidth of 54% (2.3–3.845 GHz), together with a broadband gain of 6.6 dB and low levels of cross polarization.

H.K. Kan et al. [25] presented a compact dual concentric ring printed antennas. The configuration consists of concentric shorted annular ring printed antennas. Each ring is loaded by a localized dielectric layer and can therefore be optimized to operate at a certain frequency, thus enhancing the overall bandwidth of the antenna.

H.K. Kan et al. [26] designed a simple dual-resonance printed antenna based on a spiral-like shorted patch configuration with an additional shorting pin to generate the second resonance. The antenna allows for relatively independent control of the two resonant frequencies. The 10 dB return loss bandwidth is greater than 1.4% across each of the resonant frequencies.

Wayne S. T. Rowe et al. [27] proposed a technique to reduce the spurious feed radiation from edge-fed patch antennas by using a dual thickness substrate. A thin microwave substrate is employed for the feed network, and then a transition is made to a thick substrate for the patch antenna element.

A novel folded monopole antenna is investigated numerically and experimentally by G. Ruvio et al. [28]. The proposed antenna comprises a short folded monopole suitably shaped at the base with two vertical grounding probes.

This small antenna occupies impedance bandwidth up to 125%(1.6GHz to 7.5GHz) for a 10dB return loss.

Ki-Hak Kim et al. [29] presented a novel band-rejected ultrawideband antenna with one parasitic strip. It is designed to operate from 3 to 17 GHz. The proposed antenna is fed by microstrip line and utilizes the parasitic strip to reject the frequency band (5.15–5.825 GHz) limited by IEEE 802.11a and HIPERLAN/2.

The design of a compact planar antenna featuring ultra wideband performance and simultaneous signal rejection in the 4–6 GHz band, assigned for IEEE802.11a and HIPERLAN/2,is presented by A. M. Abbosh et al. [30]. The antenna features near omnidirectional characteristics and good radiation efficiency.

A compact multiband planar inverted-F antenna (PIFA) suitable for distributed radio-over-fiber repeater networks is modified into a planar structure by Benito Sanz-Izquierdo et al. [31]. The parasitic element in the ground plane adds a new mode making the 2 GHz band much wider and incorporates all systems between 1690 and 2210 MHz. Additional tuning allows coverage to be extended across GSM, DECT, UMTS, Bluetooth and HiperLAN bands.

Bahadır S. Yıldırım [32] proposed a low-profile and planar antenna suitable for WLAN/Bluetooth and UWB applications. The antenna exhibits dual-band operation at 2400–2484 MHz (Bluetooth) and 5150–5825 MHz (IEEE 802.11a and HiperLAN/2) bands with satisfactory radiation properties.

A new low-profile planar antenna with a non-uniform meander-line and a fork-type ground is proposed for triple-band wireless local-area network (WLAN) applications in IEEE 802.11b/g/a systems by Chin-Ming Wu et al. [33].The top patch in the proposed antenna is a non-uniform meander-line and is responsible for generating two resonant modes.

Shaoqiu Xiao et al. [34] designed a Low-profile microstrip antenna with enhanced bandwidth and reduced size. In the proposed design loading of multi-

couple staggered slots on the patch and inset feed structure is used to excite two modes at two close frequencies.

Kin-Lu Wong et al. [35] presented an internal patch antenna with a thin air-layer substrate for GSM/DCS operation. The antenna generates two wide resonant modes for GSM (890–960 MHz) and DCS (1710–1880 MHz) operation. The antenna's top patch comprises a resonant narrow strip supporting a longer resonant path for GSM operation and a resonant sub patch supporting a shorter resonant path for DCS operation.

A method to improve the cutoff capability of an ultra wideband (UWB) planar antenna at the out-of-band frequencies using a meandered slot is proposed by Marek E. Bialkowski et al. [36] . In the presented UWB design, the antenna is formed by a planar monopole and a ground plane both of half circle shape, with a meandered-shape slot made in the monopole.

Yi-Fang Lin et al. [37] developed a novel coupling technique for circularly polarized annular-ring patch antenna. Proper positioning of the coupling fan-shaped patch excites two orthogonal resonant modes with 90 phase difference, and a pure circular polarization is obtained.

Yazid Yusuf et al. [38] presented a low-cost patch antenna phased array with analog beam steering without using phase shifters. This novel technique greatly reduces the cost of a phased-array system and will enable the wide-scale deployment of phased arrays in low-end commercial products.

C.-W. Su et al. [39] proposed a CP microstrip antenna with wide beam width for GPS band application. With a pyramidal ground structure and a partially enclosed flat conducting wall adopted, the designed CP patch antenna has a height of about 0.12λ only and exhibits a 3 dB axial-ratio beam width of more than 130 degree.

2.2 Multiband antenna

The integration of modern wireless protocols like GPS, WLAN, WiBree etc made drastic developments in the field of multiband antenna research. The recent works in the 20th century made communication between any two points around the world as easy affair. The following section illustrates major developments in the antenna design which resulted multiband, handheld communication systems.

J. George et al. [40] proposed a dual frequency miniature microstrip antenna with a shorting pin. Without increasing the overall size of the antenna the proposed antenna gives a large variation in frequency ratio of the two operating frequencies.

Mohammod Ali et al. [41] presented the design of a multiband internal antenna for third generation mobile phone handsets. The antenna consists of a driven meander-line element and two parasitic elements. The proposed antenna operates effectively in the AMPS 800 (824–894 MHz), GSM 900 (880–960 MHz), and GSM 1900 (1850–1990 MHz) bands within 2.5:1 (voltage standing wave ratio (VSWR).

A multiband conical monopole antenna derived from a modified sierpinski gasket is presented by Steven R. Best in [42].the multiband conical monopole offers improved radiation pattern performance in terms of omni-directionality and better pattern symmetry between each operating band.

The multiband behavior of a series of perturbed fractal Sierpinski gasket antennas is proposed in [43] by C. T. P. Song et al. Two methods of overcoming the matching difficulties of a perturbed fractal Sierpinski gasket antenna is addressed. These techniques enable multiband match to a conventional 50 Ω SMA connector, without matching circuits.

The design of a new fractal multiband antenna based on the hexagon is presented by P. W. Tang et al. [44].This new fractal antenna allows flexibility in matching multiband operations in which a larger frequency separation is required.

Pascal Ciais et al. [45] presented the design of a compact Planar Inverted-F Antenna (PIFA) suitable for cellular telephone applications. The quarter-wavelength antenna combines the use of a slot, shorted parasitic patches and capacitive loads to achieve multiband operation.

Raj et al. [46] proposed a compact planar multiband antennas for GPS, DCS, 2.4/5.8 GHz WLAN applications. A reflector at the backside of the substrate was used to get the desired multiband operations.

Wen-Chung Liu et al. [47] proposed a multiband CPW-fed monopole antenna using a particle swarm optimization approach. By embedding appropriate slits into the 50 feeding line, good impedance matching for multi resonant mode is obtained.

A novel compact single feed quad-band planar inverted F-antenna (PIFA) is presented by Dalia Mohammed Nashaat et al. [48]. Two techniques such as inserting a U-shaped slit and loading a capacitive plate between the radiating surface and the ground plane are used to reduce the physical size.

P. Nepa et al. [49] presented a novel compact planar inverted-F antenna (PIFA) to be mounted on laptop computers. The proposed multiband single-feed PIFA simultaneously operates in the IEEE 802.11a, IEEE 802.11b/g, and HIPERLAN2 frequency bands. The multiband behavior is obtained by combining a trapezoidal feed plate with two different resonance paths in the radiating structure.

Marta Martínez-Vázquez et al. [50] proposed an integrated planar multiband antennas for personal communication handsets. Triple band operation was achieved by combining spur-line techniques with parasitic patches, while the use of an additional slot introduces a fourth resonance with acceptable performance without increasing antenna volume so that a quad-band antenna is obtained.

Benito Sanz-Izquierdo et al. [51] presented a single and double layer planar multiband PIFA for WLAN applications. The antenna size was reduced by removing metallization in areas of low current density.

Angus C. K et al. [52] proposed a reconfigurable multiband antenna designs for wireless communication devices. The uniqueness of the antenna designs are that they allow various groups of their operating frequency bands to be selected electronically.

APIFA-type antenna is proposed by Hyeong-Sik Yoon et al. [53]. It can serve as a hexaband internal antenna for DCS/PCS/IMT-2000/UMTS/ISM/WLAN mobile handset applications. The two folded feed lines of the proposed antenna play important roles in achieving an increased impedance bandwidth and size reduction.

2.3 Wide band antenna

Modern wireless communication systems have significantly increased the demand for wideband antennas in order to support large number of users and to provide more information with high data speed. Recent research in the area of wideband antennas are as follows.

A broadband gap coupled microstrip antenna for broadband operation using parasitic elements is proposed by C.K. Anandan et al. [54]. The proposed antenna produce an impedance bandwidth, eight times that of a conventional patch antenna of the same size. M. Deepu kumar et al. [55] presented a new dual port microstrip antenna geometry for broad band dual frequency operation. The structure consists of the intersection of two circles of the same radius with their centers displaced by a small fraction of the wavelength. This antenna provides wide impedance bandwidth and excellent isolation between its ports.

W.-C. Liu et al. [56] presented a novel and simple printed wideband and multiband monopole antenna. The proposed antenna consists of two parallel S-shaped meandered lines of different sizes, capable of generating a number of separate resonant modes for multiband operations. By introducing a protrudent strip to a two-arm S-like monopole antenna, much wider impedance matching concealing multi-frequency resonant modes at the higher band is produced.

M. Joseph et al. [57] proposed a novel compact wideband antenna for wireless local area network (WLAN) applications in the 2.4 GHz band. The proposed antenna offers 18.6% bandwidth and a gain of 5dBi in the operating band.

A small microstrip-fed monopole antenna is designed by Jihak Jung et al. [58].The proposed antenna is designed to operate over 3.1 to 11 GHz. To achieve the maximum impedance bandwidth, a pair of notches is placed at the two lower corners of the patch and the notch structure is embedded in the truncated ground plane.

Kyungho Chung et al. [59] proposed a wideband microstrip-fed monopole antenna having frequency band-notch function. To increase the impedance bandwidth of an antenna, a narrow slit is used. By inserting a modified inverted U-slot on the proposed antenna, the frequency band notch characteristic is obtained.

The design of a monopole square-ring patch antenna with wideband operation is presented by Jeen-Sheen Row et al. [60]. The proposed antenna provide the impedance bandwidth of 30% at least when the antenna height is varied between 0.06 and $0.11\lambda_0$.The impedance bandwidth is further improved to the extent of more than 50% by using a smaller inner slot size in the square-ring patch.

A novel wideband hybrid dielectric resonator antenna structure comprises a rectangular dielectric resonator (DR) and a coplanar waveguide (CPW) inductive slot is proposed by Yuan Gao et al. in [61]. In this configuration, the CPW

inductive slot simultaneously acts as an effective radiator and the feeding structure of the DR. Dual resonances of the two radiators are merged to extend the antenna's bandwidth.

Hoon Park et al. [62] presented the design of a PIFA with very wide impedance bandwidth. The proposed antenna consists of a main patch with a pair of slant slits and L-shaped patch. A very wide impedance bandwidth characteristic is achieved by optimizing not only the length and height of a L-shaped patch between the main patch and ground plane but also the length and width of a pair of slits on the main patch which is excited by the modified coplanar waveguide-feed.

A compact wideband modified planar inverted antenna (PIFA) with two shorting strips for 2.4/5.2-GHz wireless local area network (WLAN) operations is presented by Dong-Uk Sim et al. [63].A wideband characteristic is optimized by tuning the parts of two shorted patches and size of each strip line segment.

J.-Y. Jan et al. [64] proposed a CPW-fed wide planar slot antenna with an asymmetrical slot. By choosing suitable lengths of the asymmetrical slot, broadband operation is obtained. The proposed antenna has good slot-like radiations for all operating bands including DCS, PCS, 3G, and Bluetooth bands.

Y.-F. Ruan et al. [65] presented a compact wideband antenna for wireless communications. An additional shorted parasitic element to the F-shaped wire antenna is introduced to achieve a dual-band operation. The antenna operates in the 2.4 and 5.2/5.8 GHz bands.

Q. Wu et al. [66] proposed a new CPW-fed quasi-circular monopole antenna, which is composed of a triangle and its tangent circle. This smooth monopole structure reduces the dimensions and improves impedance bandwidth dramatically. The measured bandwidth defined by VSWR< 2 is from 2.55 to 18.5 GHz.

2.4 Planar monopole antennas

The development in the planar antenna design, resulted compact communication gadgets. The planar antennas provide ease of integration to the handheld communication devices while maintaining the radiation characteristics. Recent works in the planar antenna field are described below,

S. Honda et al. [67] presented a circular disk monopole antenna with 1:18 impedance band width and omni-directional radiation characteristics. M. Hammoud et al. [68] proposed a circular disc monopole antenna having a large band width. The antenna provides a broad band width of 2.25-17.25 GHz for VSWR<2.

A.P Agrawall et al. [69] proposed a new configurations of wide band monopole antennas such as elliptical (with different ellipticity ratios), square, rectangular, and hexagonal disc monopole antennas. A simple formula is also proposed to predict the frequency corresponding to the lower edge of the bandwidth for each of these configurations.

Lee et al. [70] developed a simple compact wideband planar antenna which is capable of covering the DECT/DCS1800/PHS/WLAN and UMTS bands. A simple shoring pin is added to the planar monopole antenna to generate an additional mode below the fundamental mode.

Z. N. Chen presented [71] a new planar monopole antenna for broad band application. The antenna consists of a square parasitic planar radiator and a probe-fed strip, which are separated by a thin dielectric slab. The electromagnetic coupling of the planar radiator improves the impedance characteristics of a conventional monopole antenna.

A broadband triangular planar monopole is presented by Z. N. Chen et al. in [72]. The equilateral triangular radiating sheet electromagnetically coupled with a probe-driven strip forms the EMC planar monopole. The antenna has the

advantage of about half area reduction and ease of installation over elliptical or rectangular planar monopoles, especially in lower- frequency applications.

A type of annular planar monopole antenna is presented by Z. N. Chen et al. in [73]. He demonstrated that the proposed antennas are still capable of offering dramatically broad impedance bandwidths and acceptable radiation patterns even when more than half of the circular element has been removed.

Kin-Lu Wong et al. [74] developed a novel planar monopole antenna with a very low profile and capable of multiband operation. The proposed antenna is operated with the inner sub patch resonating as a quarter-wavelength structure and the outer one resonating as both a quarter-wavelength and a half-wavelength structure.

M. J. Ammann et al. [75] proposed a wide-band shorted planar monopole with bevel. A combination of beveling and shorting technique is used to increase the impedance bandwidth of the antenna.

A novel shorted, folded planar monopole antenna for application in GSM/DCS dual-band mobile phones is proposed by C.Y. Chiu in [76]. In which the antenna is shorted to the system ground plane, to improve impedance matching.

A square planar monopole antenna including two feed points and a beveled variant is developed by E. A. Daviu et al. [77]. Double feed is used in order to generate a pure and intense vertical current distribution in the whole structure and to avoid horizontal currents, which degrade the polarization properties and the impedance bandwidth performance of the antenna.

Jen-Yea Jan et al. [78] proposed a small planar monopole antenna with a shorted parasitic Inverted-L wire for wireless communications in the 2.4-5.2 and 5.8-GHz Bands. The driven monopole element and shorted parasitic wire can separately control the operating frequencies of two excited resonant modes.

The application of genetic algorithm (GA) optimization to the design and analysis of planar monopole antennas is presented by Aaron J. Kerkhoff et al. [79].Through analysis of the GA generated designs, it was shown that the wideness of the radiating element base and its close proximity to the ground plane cause the RBT to achieve a wider matching bandwidth with a reduced size compared with the BT.

Shun-Yun Lin [80] introduced a folded planar monopole antenna, which has a very low profile of about one twentieth of the wavelength of the lowest operating frequency. The effect is achieved by using a bended rectangular radiating patch and an inverted L-shape ground plane.

A square planar metal-plate monopole antenna fed by using a novel trident-shaped feeding strip is presented by Kin-Lu Wong et al. in [81].With the use of the proposed feeding strip, the square planar monopole antenna studied shows a very wide impedance bandwidth of about 10 GHz which is larger than three times the bandwidth obtained using a simple feeding strip (about 1.5–3.3 GHz, bandwidth ratio about 1:2.3).

Rong Lin Li et al. [82] developed a new excitation technique to improve the impedance bandwidth and to lower the manufacturing cost of a short backfire antenna (SBA). The new excitation structure consists of a planar monopole and a microstrip feed line, both of which are printed on the same dielectric substrate. The wide-band performance is achieved by splitting the printed monopole with a slot.

Wang-Sang Lee et al. [83] proposed a Multiple Band-Notched Planar Monopole Antenna for Multiband Wireless Systems. The proposed antenna consists of a wideband planar monopole antenna and the multiple U-shape slots, producing band-notched characteristics.

W.-C. Liu et al. [84] developed a rectangular notch is introduced to expand the impedance bandwidth of a dual-band planar monopole antenna for application

in PCS/WLAN systems. The antenna is fed by a CPW line and resembles the shape of the letter 'Y'. By properly cutting a notch on a tapered patch, good radiation characteristics and sufficient impedance bandwidths suitable for the personal communication system (PCS) 1800 and 5.2/5.8 GHz wireless local area network (WLAN) operations is achieved.

A novel CPW-fed wideband planar monopole antenna with asymmetrically slope ground plane is proposed by J.-Y. Jan et al.in [85]. In this proposed antenna asymmetric slop angle technique is used to obtain wideband performance.

W.-C. Liu [86] designed a CPW-fed notched planar monopole antenna for multiband operations using a genetic algorithm (GA) in conjunction with the method of moments (MoM). A suitable notch to a rectangular CPW-fed patch is used in the proposed antenna to get multi-frequency resonant modes and broad impedance bandwidths.

A novel type of ultrawide-band (UWB)antenna, which has a low voltage standing wave ratio (VSWR) while excepting from interference with existing wireless system with band notched characteristics is designed by Jianming Qiu et al. in [87]. The bandwidth and central frequency of the notched band can be adjusted with ease by proper selection of antenna parameters. The proposed band-notched antenna provides an impedance bandwidth of 3.1–10.6 GHz with VSWR 2, except the bandwidth of 5.15–5.825 GHz for IEEE802.11.

Wang-Sang Lee et al. [88] presented a wideband planar monopole antennas with dual band-notched characteristics. In order to generate dual band-notched characteristic, they proposed nine types of planar monopole antennas, which have two or three (or inverted L)-shaped slots in the radiator. This technique is suitable for creating ultra-wideband antenna with narrow frequency notches or for creating multiband antennas.

Sheng-Bing Chen et al. [89] proposed a modified T-shaped planar monopole antennas for multiband operation. In the proposed antenna two asymmetric

horizontal strips are used as additional resonators to produce the lower and upper resonant modes.

J.-S. Kuo et al. [90] designed a Triple-frequency planar monopole antenna for side-feed communication device on GSM/DCS/PCS operation. The planar monopole antenna is side-fed and mounted perpendicularly to the main circuit board of a communication device so that it offers a novel design with a free degree of feed point so as to save device space, resulting in a low profile to the system ground plane.

A planar monopole antenna with an extremely wide bandwidth is introduced by X.-L. Liang et al. in [91]. The antenna composed of an elliptical monopole patch and a trapeze form ground plane; both printed on the same side of a substrate, and are fed by a tapered CPW feeder in the middle of the ground plane. The antenna achieves a ratio impedance bandwidth of 21.6:1 for VSWR_2, and exhibits a nearly omni-directional radiation pattern

Giuseppe Ruvio et al. [92] proposed a novel Wideband Semi-Planar Miniaturized Antenna. The antenna combines the attractive features of PCB and PIFA technologies with those of asymmetry and beveling. Besides compactness and low cost manufacturability, the proposed antenna provides high efficiency and good omni-directional radiation patterns which do not show heavy dependence on the presence of a large ground plane when mounted on it, in various arrangements.

An ultra-wideband (UWB) planar monopole antenna with a tunable band-notched response is proposed by E. Antonino-Daviu et al. in [93]. Tuning of the rejected frequency is realized by loading an embedded resonant slot with a varactor.

A novel modified microstrip-fed ultrawideband (UWB) planar monopole antenna with variable frequency band-notch characteristic is presented by Reza Zaker et al. [94]. By inserting two slots in the both sides of microstrip feed line on the ground plane, much wider impedance bandwidth is produced. A modified H-

shaped conductor-backed plane with variable dimensions is used in order to generate the frequency band-stop performance and control its characteristics such as band-notch frequency and its bandwidth.

Tzyh-Ghuang Ma et al. [95] presented a new multi-resonator loaded band-rejected planar monopole antenna for ultrawideband applications. The proposed microstrip-fed antenna is composed of a flared metal plate, a truncated ground plane, and two pairs of folded strips. By applying the resonance nature of the folded strips and the associated cross coupling effects, the proposed antenna demonstrates band stop-filter-like response with bandwidth controllability at the targeted rejection band.

A printed monopole antenna with two steps and a circular slot for ultrawide band (UWB) applications is presented by Osama Ahmed et al. [96]. The proposed antenna has a wide frequency bandwidth of 8.4 GHz starting from 3 GHz up to 11.4 GHz for a return loss of less than -10dB and gain flatness over the frequency range. By introducing a simple and proper narrow slot in the radiating element, frequency-notched characteristics can be obtained and a good band-notched performance in the 5–6 GHz band is achieved.

2.5 CPW Fed Antennas

A Coplanar patch antenna consists of a patch surrounded by closely spaced ground conductor on a dielectric substrate. CPW antennas have many attractive features, such as no soldering points, easy fabrication and integration with monolithic microwave integrated circuits, and a simplified configuration with a single metallic layer. Thus, the designs of the CPW-fed antennas have recently received much attention. Relevant papers in this area are summarized in the following section.

A CPW-fed dual frequency monopole antenna has been presented by Horng-Dean Chen et al. [97]. The proposed antenna utilizes the advantages of the CPW line to simplify the structure of the antenna into a single metallic level, thereby making easier the integration with the microwave integrated circuits. The antenna consists of a combination of two monopoles connected in parallel at the feed point, each operating at a specified frequency mode.

K. Chung et al. [98] presented a Wideband CPW-fed monopole antenna with parasitic elements and slots. The wide bandwidth is achieved by adding two parasitic elements along the length of the monopole and three narrow slots.

W.-C. Liu [99] presented a new design of a planar monopole antenna consisting of a rectangular microstrip patch with a rectangular notch. The antenna is fed by a coplanar waveguide (CPW) line such that only a single-layer substrate is required for this antenna. To produce dual frequency wide impedance band behavior a notch is introduced to the radiating patch. He is also presented a paper on Broadband dual-frequency meandered CPW-fed monopole antenna [100]. The antennas were developed to widen the narrow bandwidth of the coplanar patch antenna. This was achieved by inserting a meandered line between the 50 ohm CPW lines and radiating patch.

A novel wideband dual-frequency design of a coplanar waveguide (CPW)-fed monopole antenna is proposed by W.-C. Liu [101]. The antenna comprises a planar patch element with a sided L-shaped slit to become a double inverted-L monopole and is capable of generating two separate resonant modes with good impedance matching conditions.

J. Liang et al. [102] presented a study of coplanar waveguide (CPW) fed circular disc monopole antenna for ultra-wideband (UWB) applications. It has been shown that the feed gap, the width of the ground plane, and the dimension of the CPW-fed circular disc monopole antenna are the most important parameters that determine the performance of the antenna.

A miniature dielectric loaded monopole antenna fed by coplanar waveguide is proposed by Yi-Fang Lin et al. in [103] for WLAN applications in the 2.4/5-GHz bands. The proposed antenna has a small size, effective feeding structure and adequate operational bandwidth, such that it is suitable for use in WLAN applications.

The analysis of a new printed antenna is presented by V. Zachou et al. [104]. This antenna consists of a printed monopole, with one or two sleeves on each side, fed by a coplanar waveguide (CPW) line. Switches are used to control the length of the monopole and the sleeves and to tune the resonant frequencies of the antenna.

A simple and compact ultrawideband (UWB) aperture antenna with extended band-notched designs was presented by Yi-Cheng Lin et al. [105]. The antenna consists of a rectangular aperture on a printed circuit board ground plane and a T-shaped exciting stub. The proposed planar coplanar waveguide fed antenna is easy to be integrated with radio-frequency/microwave circuitry for low manufacturing cost.

M.-T. Zhang et al. [106] developed a Dual-band CPW-fed folded-slot monopole antenna for RFID application. The open end and the balance shaped strip fed by the CPW connecting to an SMA produces the dual band performance.

A coplanar waveguide (CPW)-fed monopole antenna for 5 GHz wireless communication is proposed by W.-C. Liu in [107].The proposed antenna consisting of a hook strip and a CPW feeding structure with a rectangular ground and an inverted L-shaped ground. The antenna has a compact antenna size, good impedance bandwidth, and good radiation characteristics suitable for the 5.2 (5.15–5.35 GHz) or 5.8 GHz (5.725–5.825 GHz) WLAN=RFID operation.

Joon Il Kim developed [108] an ultra wideband (UWB) coplanar waveguide (CPW)-fed LI-shape planar monopole antenna. The proposed antenna consists of

an L-shaped monopole and an I-shaped open stub monopole connected at the end of a CPW feed line.

A novel dual-band design of a coplanar waveguide (CPW)-fed monopole antenna with a cross slot was proposed by C.-M. Wu [109]. The antenna, comprising a planar patch element embedded with a cross slot, is capable of generating two separate resonant modes with good impedance matching conditions. The CPW-feed technology is applied to the design, such that only a single-layer substrate is required for this antenna, and thus fabrication is easy.

A. Djaiz developed [110] a CPW-feed miniaturized antenna with bandwidth enhancement for Biomedical Localization applications. A meander arm is used as the radiating element and an additional layer as superstrate to reduce the antenna area dimension and improve the performance in terms of bandwidth.To achieve dual-band antenna performance with less interdependency of the two operation bands, a dual-band CPW-fed slot monopole hybrid antenna with orthogonal polarizations operation was proposed by Xian-Chang Lin [111].Guorui Han presented [112] a novel compact dual-band coplanar waveguide (CPW)-fed antenna with a microstrip stub. The proposed dual-band antenna works at the bands of 2.4 GHz and 5.8 GHz simultaneously.

2.6 FDTD for antenna analysis

In 1966 Yee [113] proposed the technique to solve Maxwell's curl equations using the finite-difference time-domain (FDTD) technique. Yee's method has been used to solve numerous scattering problems on microwave circuits, dielectrics, and electromagnetic absorption in biological tissue at microwave frequencies. Yee used an electric-field *(E)* grid, which was offset both spatially and temporally from a magnetic-field *(H)* grid, to obtain update equations that yield the present fields throughout the computational domain, in terms of the past fields. The update

equations are used in a leap frog scheme, to incrementally march the E and $\boldsymbol{H}$ fields forward in time.

The original Yee FDTD algorithm is second-order accurate in both space and time. Numerical-dispersion and grid-anisotropy errors can be kept small by having a sufficient number of grid spaces per wavelength. Taflove was among the first to rigorously analyze these errors [114]. The correct stability criteria for the original orthogonal-grid Yee algorithm was also first introduced by Taflove [115].

The analysis of microstrip antennas were first introduced by Reineix et al. [116] . Sheen et al. [117] presented FDTD results for various microstrip structures, including a rectangular-patch antenna, a lowpass filter, and a branch-line coupler. Leveque et al. [118] modeled frequency-dispersive microstrip antennas. The FDTD method to accurately measure the reflection coefficient of various microstrip-patch configurations is presented by Wu et al. [119]. Uehara et al. [120] presented an analysis of the mutual coupling between two microstrip antennas.

The conformal FDTD approaches to analyze microstrip antennas on a curved surface is presented by Oonishi et al. [121] and Kashiwa et al. [122]. Berenger [123] put forward the most relevant advances in material –based ABCs .His ABC, termed the perfectly-matched-layer (PML) absorbing boundary condition, appears to yield a major improvement in the reduction of boundary reflections, compared to any ABC proposed previously. Qian et al. [124] used the FDTD method to design twin-slot antennas.

Reineix et al. [125,126,127] has expanded their FDTD analysis to include the input impedance of micro strips with slots, to obtain the radar cross section of microstrip-patch antennas, and to model the radiation from microstrip patches with a ferrite substrate.

Luebbers et al. [128] and Chen et al. [129] analyzed hand-held on a monopole antenna on a conducting or dielectric box using FDTD in 1992. The input impedance and gain of monopole, PIFA, and loop antennas on hand-held

transceivers is proposed by Jensen and Rahmat-Samii [130]. They are also studied the interaction of a hand held antenna and a human [131].

The FDTD analysis of dual-feed microstrip patch antennas are described by M. Kar et al. [132] . FDTD analysis of radiation pattern of antenna on truncated ground plane was investigated by Yamamoto et al. [133].

Huey-Ru Chuang et al. [134] described t**he** 3-D FDTD design analysis of a 2.4-GHz polarization-diversity printed dipole antenna with integrated balun and polarization-switching circuit for WLAN and wireless communication applications. Pattern reconfigurable leaky-wave antenna analysis using FDTD method was introduced by Shaoqiu Xiao et al. [135]**.**

References:

[1] G. A. Deschamps, "Microstrip Microwave Antennas," 3rd USAF Symposium on Antennas, 1953

[2] L. Lewin, " Radiation from Discountinuities in Stripline, Proceedings of Institution of Electronic Engineers, vol. 107, pp. 163-170, 1960.

[3] R. E. Muson, "Single Slot Cavity Antennas," US patent no-3713162, jan, 1973

[4] J. Q. Howell," Microstrip Antenna," IEEE International Symposium Digest on Antennas and Propagation, Williamsburge Virginia, pp. 177-180, 1972

[5] H. D. Weinschel, " Progress Report on Development of Microstrip Cylindrical Arrays for Soundings Rockets," Physic. And Sci. Lab., New Mexico State University, 1973

[6] G. G. Sanford, " Conformal Microstrip Phased Array for Aircraft tests with ATS-6," Proceedings of National Electronic Conference, vol. 29, pp. 252-257, 1974

[7] A. G. Derneryd, " Linear Polarized Microstrip Antennas," IEEE Trans. on Antennas and Propagat., vol. 30, pp. 846-850, 1976

[8] Y. T. Lo, D. Solomon and W. F. Richards, " Theory and Experiment on Microstrip Antennas," IEEE Trans. on Antennas and Propagat., vol. 27, pp. 137-145, 1979

[9] M. D. Deshpande and M. C. Bailey, "Input impedance of Microstrip antennas," IEEE Trans. on Antennas and Propagat., vol. 30, pp. 645-650, 1982

[10] C. L. Mak, K. M. Luk, K. F. Lee and Y. L. Chow, "Experimental Study of a Microstrip Patch Antenna with an L-Shaped Probe," IEEE Trans. on Antennas and Propagat., vol. 48, pp. 777-783, 2000

[11] H.K. Kan and R.B. Waterhouse, "Small square dual spiral printed antennas," Electronics Lett., vol. 37, pp. 478-479, 2001

[12] M.D. van Wyk and K.D. Palmer, "Bandwidth enhancement of microstrip patch antennas using coupled lines," Electronics Lett., vol. 37, pp. 806-807, 2001

[13] J.S. Baligar, U.K. Revankar and K.V. Acharya, "Broadband two-layer shorted patch antenna with low cross-polarisation," Electronics Lett., vol. 37, pp. 547-548, 2001

[14] Kevin M. K. H. Leong, Yongxi Qian and Tatsuo Itoh, "Surface Wave Enhanced Broadband Planar Antenna for Wireless Applications," IEEE Microwave and Wireless Comp. Lett., vol. 11, pp. 62-64, 2001

[15] Wen-Hsiu Hsu and Kin-Lu Wong, "Broad-Band Probe-Fed Patch Antenna With a U-Shaped Ground Plane for Cross-Polarization Reduction," IEEE Trans. on Antennas and Propagat., vol. 50, pp. 352-355, 2002

[16] Ban-Leong Ooi, Shen Qin, and Mook-Seng Leong, "Novel Design of Broad-Band Stacked Patch Antenna," IEEE Trans. on Antennas and Propagat., vol. 50, pp. 1391-1395, 2002

[17] Kin-Lu Wong Chia-Luan Tang, and Jyh-Ying Chiou, "Broad-Band Probe-Fed Patch Antenna With a W-Shaped Ground Plane," IEEE Trans. on Antennas and Propagat., vol. 50, pp. 827-831, 2002

[18] Xing Jiang, Simin Li and Guangjie Su, "Broadband planar antenna with parasitic radiator," Electronics Lett., vol. 39, no. 23, 2003

[19] C.L. Mak, R. Chair, K.F. Lee, K.M. Luk and A.A. Kishk, "Half U-slot patch antenna with shorting wall," Electronics Lett., vol. 39, no. 25, 2003

[20] Chi Yuk Chiu, Kam Man Shum, Chi Hou Chan and Kwai Man Luk, Bandwidth Enhancement Technique for Quarter-Wave Patch Antennas," IEEE Antennas and Wireless Propag. Lett., vol.2, pp. 130-132, 2003.

[21] Y. J. Sung, M. Kim, and Y.-S. Kim, "Harmonics Reduction With Defected Ground Structure for a Microstrip Patch Antenna," IEEE Trans. on Antennas and Propagat., vol. 2, pp. 111-113, 2003

[22] Gh. Rafi and L. Shafai, "Broadband microstrip patch antenna with V-slot," IEE Proc.-Microw. Antennas Propag., Vol. 151, pp. 435-440, 2004

[23] W.-C. Liu, C.-C. Huang and C.-M. Wu, "Dual-polarised single-layer slotted patch antenna," Electronics Lett., vol. 4, no. 12, 2004

[24] Y. Qin, S. Gao, A. Sambell, E. Korolkiewicz and M. Elsdon, "Broadband patch antenna with ring slot coupling," Electronics Lett., vol. 40, no. 1, 2004

[25] H.K. Kan, R.B. Waterhouse and D. Pavlickovski, "Compact dual concentric ring printed antennas," IEE Proc.-Microw. Antennas Propag., Vol. 151, pp. 37-42, 2004

[26] H.K. Kan, R.B. Waterhouse, A.Y.J. Lee and D. Pavlickovski "Dual-resonance spiral-like shorted patch Antenna," Electronics Lett., vol. 41, no. 10, 2005

[27] Wayne S. T. Rowe and Rod B. Waterhouse, "Edge-Fed Patch Antennas With Reduced SpuriousRadiation," IEEE Trans. on Antennas and Propagat., vol. 53, pp. 1785-1790, 2005

[28] G. Ruvio and M.J. Ammann, "From L-shaped planar monopoles to a novel folded antenna with wide bandwidth, "IEE Proc.-Microw. Antennas Propag., Vol. 153, pp. 456-460, 2006

[29] Ki-Hak Kim and Seong-Ook Park, "Analysis of the Small Band-Rejected Antenna with the Parasitic Strip for UWB," IEEE Trans. on Antennas and Propagat., vol. 54, pp. 1688-1692, 2006

[30] A. M. Abbosh, M. E. Bialkowski, J. Mazierska, and M. V. Jacob, "A Planar UWB Antenna With Signal Rejection Capability in the 4–6 GHz Band," IEEE Microwave and Wireless Comp. Lett., vol. 16, pp. 278-280, 2006

[31] Benito Sanz-Izquierdo, John C. Batchelor, Richard J. Langley, and Mohammed I. Sobhy, "Single and Double Layer Planar Multiband PIFAs," IEEE Trans. on Antennas and Propagat., vol. 54, pp. 1416-1422, 2006

[32] Bahadır S. Yıldırım, "Low-Profile and Planar Antenna Suitable for WLAN/Bluetooth and UWB Applications," IEEE Antennas and Wireless Propag. Lett., vol. 5, pp. 438-441, 2006

[33] Chin-Ming Wu, Cheng-Nan Chiu, and Cho-Kang Hsu, "A New Nonuniform Meandered and Fork-Type Grounded Antenna for Triple-Band WLAN Applications," IEEE Antennas and Wireless Propag. Lett., vol. 5, pp. 346-348, 2006

[34] Shaoqiu Xiao, Zhenhai Shao, Bing-Zhong Wang, Ming-Tuo Zhou, and Masayuki Fujise, "Design of Low-Profile Microstrip Antenna with Enhanced Bandwidth and Reduced Size," IEEE Trans. on Antennas and Propagat., vol. 54, pp. 1594-1599, 2006

[35] Kin-Lu Wong, Chih Lin, and Brian (Yen-Yu) Chen, "Internal Patch Antenna With a Thin Air-Layer Substrate for GSM/DCS Operation in a PDA Phone," IEEE Trans. on Antennas and Propagat., vol. 55, pp. 1165-1172, 2007

[36] Marek E. Bialkowski and Amin M. Abbosh , "Design of UWB Planar Antenna With Improved Cut-Off at the Out-of-Band Frequencies," ," IEEE Antennas and Wireless Propag. Lett., vol.7, pp. 408-410, 2008.

[37] Yi-Fang Lin, Hua-Ming Chen and Shih-Chieh Lin, "A New Coupling Mechanism for Circularly Polarized Annular-Ring Patch Antenna," IEEE Trans. on Antennas and Propagat., vol. 56, pp. 11-16, 2008

[38] Yazid Yusuf, and Xun Gong, "Low-Cost Patch Antenna Phased Array With Analog Beam Steering Using Mutual Coupling and Reactive Loading," IEEE Antennas and Wireless Propag. Lett., vol.7, pp. 81-84, 2008.

[39] C.-W. Su, S.-K. Huang and C.-H. Lee, "CP microstrip antenna with wide beamwidth for GPS band application," Electronics Lett., Vol. 43 No. 20

[40] J. George, K. Vasudevan, P. Mohanan and K. G. Nair, " Dual frequency miniature antenna," Electron. Lett, vol. 34, pp.1168-1170 , 1998

[41] Mohammod Ali, Gerard James Hayes, Huan-Sheng Hwang, and Robert A. Sadler, Design of a Multiband Internal Antenna for Third Generation Mobile Phone Handsets," IEEE Trans. Antennas Propagat., vol. 51, pp. 1452-1461, 2003

[42] Steven R. Best, "A Multiband Conical Monopole Antenna Derived From a Modified Sierpinski Gasket," IEEE Antennas and Wireless Pro. Lett., vol. 2, pp. 205-207, 2003

[43] C. T. P. Song, Member, S. Hall, and H. Ghafouri-Shiraz, "Perturbed Sierpinski Multiband Fractal Antenna With Improved Feeding Technique," ," IEEE Trans. Antennas Propagat., vol. 51, pp. 1011-1017, 2003

[44] P. W. Tang and P. F. Wahid, "Hexagonal Fractal Multiband Antenna," IEEE Antennas and Wireless Pro. Lett., vol. 3, pp. 111-112, 2004

[45] Pascal Ciais, Robert Staraj, Georges Kossiavas, and Cyril Luxey, "Design of an Internal Quad-Band Antenna for Mobile Phones," IEEE Microwave and Wireless Comp. Lett.,vol.14 , pp. 148-150, 2004.

[46] Raj R. K., Joseph M., Paul B., Mohanan P, " Compact planar multiband antenna for GPS, DCS, 2.4/5.8 GHz WLAN applications," Electron. Lett, vol. 41, pp.290-291 , 2005

[47] Wen-Chung Liu, "Design of a Multiband CPW-fed Monopole Antenna Using a Particle Swarm Optimization Approach," IEEE Trans. Antennas Propagat., vol. 53, pp. 3273-3279, 2005

[48] Dalia Mohammed Nashaat, Hala A. Elsadek and Hani Ghali, "Single Feed Compact Quad-Band PIFA Antenna for Wireless Communication Applications," IEEE Trans. Antennas Propagat., vol. 53, pp. 2631-2635, 2005

[49] P. Nepa, G. Manara, A. A. Serra, and G. Nenna, "Multiband PIFA for WLAN Mobile Terminals," IEEE Antennas and Wireless Pro. Lett., vol. 4, pp. 349-350, 2005

[50] Marta Martínez-Vázquez, Oliver Litschke, Matthias Geissler, Dirk Heberling, Antonio M. Martínez-González, and David Sánchez-Hernández, "Integrated Planar Multiband Antennas for Personal Communication Handsets," IEEE Trans. Antennas Propagat., vol. 54, pp. 384-391, 2006

[51] Benito Sanz-Izquierdo, John C. Batchelor, Richard J. Langley and Mohammed I. Sobhy, "Single and Double Layer Planar Multiband PIFAs," IEEE Trans. Antennas Propagat., vol. 54, pp. 1416-1422, 2006

[52] Angus C. K. Mak, Corbett R. Rowell, Ross D. Murch, and Chi-Lun Mak, "Reconfigurable Multiband Antenna Designs for Wireless Communication Devices," IEEE Trans. Antennas Propagat., vol. 55, pp. 1919-1928, 2007

[53] Hyeong-Sik Yoon and Seong-Ook Park, Member, "A New Compact Hexaband Internal Antenna of the Planar Inverted F-Type for Mobile Handsets," IEEE Antennas and Wireless Pro. Lett., vol. 6, pp. 336-339, 2007

[54] C. K. Aanandan, P. Mohanan and K. G. Nair, "Broad band gap coupled microstrip antenna," IEEE Transactionas on Antennas and Propagation, Vo. 38, pp. 1581-1586, 1990

[55] M. Deepukumar, J. George, C.K. Aanandan, P. Mohanan and K.G. Nair, "Broadband dual frequency microstrip antenna," Electronics Letters, Vol. 32, pp. 1531-1532, 1996

[56] W.-C. Liu, W.-R. Chen and C.-M.Wu, "Printed double S-shaped monopole antenna for wideband and multiband operation of wireless communications," IEE Proc.-Microw. Antennas Propag., Vol. 151, pp. 473-476, 2004

[57] M. Joseph, B. Paul, R.K. Raj and P. Mohanan, "Compact wideband antenna for 2.4 GHz WLAN applications," Electronics Lett., Vol. 40, no. 23, 2004

[58] Jihak Jung, Wooyoung Choi, and Jaehoon Choi, "A SmallWideband Microstrip-fed Monopole Antenna," IEEE Microwave and Wireless Comp. Lett., vol.15, pp. 703-705, 2005.

[59] Kyungho Chung, Jaemoung Kim and Jaehoon Choi, "Wideband Microstrip-Fed Monopole Antenna Having Frequency Band-Notch Function," IEEE Microwave and Wireless Comp. Lett., vol.15, pp. 766-768, 2005.

[60] Jeen-Sheen Row and Shing-Hau Chen, "Wideband Monopolar Square-Ring Patch Antenna," IEEE Trans. on Antennas and Propagat., vol. 54, pp. 1335-1339, 2006

[61] Yuan Gao, Ban-Leong Ooi, Wei-Bin Ewe and Alexandre P. Popov, "A Compact Wideband Hybrid Dielectric Resonator Antenna," IEEE Microwave and Wireless Comp. Lett., vol.16, pp. 227-229, 2006.

[62] Hoon Park, Kyungho Chung, and Jaehoon Choi, "Design of a Planar Inverted-F AntennaWith Very Wide Impedance Bandwidth," IEEE Microwave and Wireless Comp. Lett., vol.16, pp. 113-115, 2006.

[63] Dong-Uk Sim and Jae-Ick Choi, "A Compact Wideband Modified Planar Inverted F Antenna (PIFA) for 2.4/5-GHz WLAN Applications," IEEE Antennas and Wireless Propag. Lett., vol.5, pp. 391-394, 2006.

[64] J.-Y. Jan and C.-Y. Hsiang, "Wideband CPW-fed slot antenna for DCS, PCS, 3G and Bluetooth bands," Electronics Lett., vol. 42, pp. 1377 - 1378, 2006

[65] Y.-F. Ruan, Y.-X. Guo, K.-W. Khoo and X.-Q. Shi, "Compact wideband antenna for wireless Communications," IET Microw. Antennas Propag., pp. 556–560, 2007

[66] Q. Wu, R. Jin, J. Geng and M. Ding, "Compact CPW-fed quasi-circular monopolewith very wide bandwidth," Electronics Lett., vol. 43, no.2, 2007

[67] S. Honda, M. Ito and Y.Jinbo, " A Disk Monopole antenna with 1:18 Impedance Bandwidth and Omnidirectional Radiation pattern," Int. Symp. Antennas Propagat. Pp. 1145-1148, 1992

[68] M. Hammound, P. Poey and F. Colombel, " Matching the Input Impedance of a Broadband Disc Monopole," Electronics Lett., vol. 29, pp. 406-407, 1993

[69] Narayan Prasad Agrawall, Girish Kumar, and K. P. Ray, "Wide Band Planar Monopole Antennas," IEEE Trans. on Antennas and Propagat., vol. 46, pp. 292-295, 1998

[70] E. Lee, P.S. Hall and P. Gardner, "Compact wideband planar monopole antenna," Electronics Lett., vol. 35, pp. 2157-2158, 1999

[71] Z. N. Chen, "Broadband planar monopole antenna," IEE Proc.-Microw. Aniennus Propag., Vol. 147pp. 526-528, 2000

[72] Z. N. Chen and M. Y. W. Chia, "Impedance characteristics of triangular EMC planar monopole," Electronics Lett., vol. 37, pp. 1271-1272, 2001

[73] Z.N. Chen, M.J. Ammann, M.Y.W. Chia and T.S.P. See, "Annular planar monopole antennas," IEE Proc,-Microw. Antennas Propag., Vol. 149, pp. 200-203, 2002

[74] Kin-Lu Wong, Gwo-Yun Lee, and Tzung-Wern Chiou, "A Low-Profile Planar Monopole Antenna for Multiband Operation of Mobile Handsets," IEEE Trans. on Antennas and Propagat., vol. 51, pp. 121-125, 2003

[75] M. J. Ammann and Zhi Ning Chen, "A Wide-Band Shorted Planar Monopole With Bevel," IEEE Trans. on Antennas and Propagat., vol. 51, pp. 901-903, 2003

[76] Ching-Yuan Chiu, Pey-Ling Teng and Kin-Lu Wong, "Shorted, folded planar monopole antenna for dual-band mobile phone," Electronics Lett., vol. 39, pp. 1301 - 1302, 2003

[77] E. Antonino-Daviu, M. Cabedo-Fabre´s, M. Ferrando-Bataller and A. Valero-Nogueira, "Wideband double-fed planar monopole antennas," Electronics Lett., vol. 39, pp. 1635-1636, 2003

[78] Jen-Yea Jan andLiang-Chih Tseng, "Small Planar Monopole Antenna With a Shorted Parasitic Inverted-L Wire for Wireless Communications in the 2.4-5.2, and 5.8-GHz Bands," IEEE Trans. on Antennas and Propagat., vol. 52, pp. 1903-1905, 2004

[79] Aaron J. Kerkhoff, Member, Robert L. Rogers and Hao Ling, "Design and Analysis of Planar Monopole Antennas Using a Genetic Algorithm Approach," IEEE Trans. on Antennas and Propagat., vol. 52, pp. 2709-2718, 2004

[80] Shun-Yun Lin, "Multiband Folded Planar Monopole Antenna for Mobile Handset," IEEE Trans. on Antennas and Propagat., vol. 52, pp. 1790-1794, 2004

[81] Kin-Lu Wong, Chih-Hsien Wu, and Saou-Wen Su," Ultrawide-Band Square Planar Metal-Plate Monopole Antenna With a Trident-Shaped Feeding Strip," IEEE Trans. on Antennas and Propagat., vol. 53, pp. 1262-1269, 2005

[82] RongLin Li, Dane Thompson, John Papapolymerou, Joy Laskar, and Manos M. Tentzeris , "A New Excitation Technique for Wide-Band Short Backfire Antennas," IEEE Trans. on Antennas and Propagat., vol. 53, pp. 2313-2320, 2005

[83] Wang-Sang Lee, Won-Gyu Lim, and Jong-Won Yu, "Multiple Band-Notched Planar Monopole Antenna for Multiband Wireless Systems," IEEE Microwave and Wireless Comp. Lett., vol.15, pp. 576-578, 2005.

[84] W.-C. Liu and C.-F. Hsu, "Dual-band CPW-fed Y-shaped monopole antenna for PCS=WLAN application," Electronics Lett., vol. 41, pp. 390 - 391, 2005

[85] J.-Y. Jan and T.-M. Kuo, "CPW-fed wideband planar monopole antenna for operations in DCS, PCS, 3G, and Bluetooth bands," Electronics Lett., vol. 41, pp. 991 - 993, 2005

[86] W.-C. Liu, "Design of a CPW-fed notched planar monopole antenna for multiband operations using a genetic algorithm," IEE Proc.-Microw. Antennas Propag., Vol. 152, pp. 273-277 2005

[87] Jianming Qiu, Zhengwei Du, Jianhua Lu, and Ke Gong, "A Planar Monopole Antenna Design With Band-Notched Characteristic," ," IEEE Trans. on Antennas and Propagat., vol. 54, pp. 287-292, 2006

[88] Wang-Sang Lee, Dong-Zo Kim, Ki-Jin Kim, and Jong-Won Yu, Wideband Planar Monopole Antennas With Dual Band-Notched Characteristics," IEEE Trans. on Antennas and Propagat., vol. 54, pp. 2800-2806, 2006

[89] Sheng-Bing Chen, Yong-Chang Jiao, Wei Wang, and Fu-Shun Zhang, "Modified T-Shaped Planar Monopole Antennas for Multiband Operation," IEEE Trans. on Antennas and Propagat., vol. 54, pp. 3267-3270, 2006

[90] J.-S. Kuo and C.-Y. Huang, "Triple-frequency planar monopole antenna for side-feed communication device on GSM/ DCS/ PCS operation," Electronics Lett., vol. 42, pp. 268 - 270, 2006

[91] X.-L. Liang, S.-S. Zhong and W. Wang, " Elliptical planar monopole antenna with extremely wide bandwidth," Electronics Lett., vol. 42, pp. 441 - 442, 2006

[92] Giuseppe Ruvio and M. J. Ammann, "A Novel Wideband Semi-Planar Miniaturized Antenna," IEEE Trans. on Antennas and Propagat., vol. 55, pp. 2679-2685, 2007

[93] E. Antonino-Daviu, M. Cabedo-Fabre´s, M. Ferrando-Bataller and A. Vila-Jimenez, "Active UWB antenna with tunable band-notched behavior," Electronics Lett., vol. 43, pp. 959 - 960, 2007

[94] Reza Zaker, Changiz Ghobadi, and Javad Nourinia, "Novel Modified UWB Planar Monopole Antenna with Variable Frequency Band-Notch Function," IEEE Microwave and Wireless Comp. Lett., vol.7, pp. 112-114, 2008.

[95] Tzyh-Ghuang Ma, Ren-Ching Hua, and Chin-Feng Chou, "Design of a Multiresonator Loaded Band-Rejected Ultrawideband Planar Monopole Antenna With Controllable Notched Bandwidth," IEEE Trans. on Antennas and Propagat., vol. 56, pp. 2875-2883, 2008

[96] Osama Ahmed and Abdel-Razik Sebak, "A Printed Monopole Antenna with Two Steps and a Circular Slot for UWB Applications," IEEE Antennas and Wireless Propag. Lett., vol.7, pp. 411-413, 2008.

[97] Horng-Dean Chen and Hong-Twu Chen, "A CPW-Fed Dual-Frequency Monopole antenna," IEEE Trans. Antennas Propagat., vol. 52, pp. 978-982, 2004

[98] K. Chung, T. Yun and J. Choi, "Wideband CPW-fed monopole antenna with parasitic elements and slots," Electron. Lett, vol. 40 , pp. , 2008

[99] W.-C. Liu and C.-M. Wu, "Broadband dual-frequency CPW-fed planar monopole antenna with rectangular notch," Electron. Lett, vol. 40, pp. , 2004.

[100] W.-C. Liu, "Broadband dual-frequency meandered CPW-fed monopole antenna," Electron. Lett, vol. 40 , pp. , 2004

[101] W.-C. Liu, "Wideband dual-frequency double inverted-L CPW-fed monopole antenna for WLAN application,"IEE Proc.-Microw. Antennas Propag.,vol.152 , pp. 505-510, 2005

[102] J. Liang, L. Guo, C.C. Chiau, X. Chen and C.G. Parini, "Study of CPW-fed circular disc monopole antenna for ultra wideband applications," IEE Proc.-Microw. Antennas Propag., vol. 6, pp. 520-526 , 2005

[103] Yi-Fang Lin, Chia-Ho Lin, Hua-Ming Chen and P. S. Hall, "A Miniature Dielectric Loaded Monopole Antenna for 2.4/5 GHz WLAN Applications," IEEE Microwave and Wireless Comp. Lett.,vol.16 , pp. 591-593, 2006.

[104] V. Zachou, C. G. Christodoulou, M. T. Chryssomallis, D. Anagnostou, and S. Barbin, "Planar Monopole Antenna With Attached Sleeves," IEEE Antennas and Wireless Pro. Lett., vol. 5, pp. 286-289, 2006

[105] Yi-Cheng Lin and Kuan-Jung Hung, "Compact Ultrawideband Rectangular Aperture Antenna and Band-Notched Designs," IEEE Trans. Antennas Propagat., vol. 54, pp. 3075-3081, 2006

[106] M.-T. Zhang, Y.-C. Jiao and F.-S. Zhang, "Dual-band CPW-fed folded-slot monopole antenna for RFID application," Electron. Lett, vol. 42, pp. , 2006.

[107] W.-C. Liu and H.-J. Liu, "Compact CPW-fed monopole antenna for 5 GHz wireless application," Electron. Lett, vol. 42, pp. , 2006.

[108] Joon Il Kim and Yong Jee, "Design of Ultrawideband Coplanar Waveguide-Fed LI-Shape Planar Monopole Antennas," IEEE Antennas and Wireless Pro. Lett., vol. 6, pp. 383-387, 2007

[109] C.-M. Wu, "Dual-band CPW-fed cross-slot monopole antenna for WLAN operation," IET Microw. Antennas Propag., vol.1 , pp. 542-546, 2007

[110] A. Djaiz, T. A. Denidni and M. Nedil, "A new CPW-feed miniaturized antenna with Bandwidth Enhancement for Biomedical Localization applications," vol. , pp. 539-542, 2007

[111] Xian-Chang Lin and Cheng-Chieh Yu, "A Dual-Band CPW-Fed Inductive Slot-Monopole Hybrid Antenna," IEEE Trans. Antennas Propagat., vol. 56, pp. 282-285, 2006

[112] Guorui Han, Wenwen Wang, Tingting An and Wenmei Zhang, "Compact Dual-Band CPW-Fed Antenna," 2008

[113] K. S. Yee, "Numerical solution of initial boundary value problems involving Maxwell's equations in isotropic media," IEEE Trans. Antennas Propagat., AP-14, 4, pp. 302-307, 1966

[114] Taflove, "Review of the formulation and applications of the finite-difference time-domain method for numerical modeling of electromagnetic wave interactions with arbitrary structures," Wave Motion, 10, 6, pp. 547-582, 1988.

[115] A. Taflove and M. E. Brodwin, "Numerical solution of steady state electromagnetic scattering problems using the time-dependent Maxwell's equations," IEEE Trans. on Microwave Theory Techniques, MTT-23, pp, 623-630, 1975

[116] Reineix and B. Jecko, "Analysis of microstrip patch antennas using finite difference time domain method," IEEE Trans. Antennas Propagat., AP-37, pp. 302-307, 1989

[117]D.M. Sheen, Sami. M. Ali, Mohamed D. Abouzahra and Jin Au Kong, "Application of the 3D FDTD method to the analysis of planar microstrip circuits", IEEE Transa. on Microwave Theory and Techniques, vol. 38, pp. 849-857, July 1990.

[118] P. Leveque, A. Reineix, and B. Jecko, "Modelling dielectriclosses in microstrip patch antennas: Application of FDTD method," Electron. Lett, vol. 28, pp.539-540, 1992.

[119] C. Wu, K.-L. Wu, Z.-Q. Bi, and J. Litva, "Accurate characterization of planar printed antennas using finite-difference time domain method," IEEE Trans. Antennas Propagat., AP-40, pp. 526-533, 1992.

[120] K. Uehara and K. Kagoshima, "FDTD method analysis of mutual coupling between microstrip antennas," IEICE Transactions on Commiinicatiotn, E76-B, 7, pp. 762-764, 1993.

[121] T. Oonishi, T. Kashiwa, and I. Fukai, "Analysis of microstrip antennas on a curved surface using the conformal grids FD-TD method," Electronics and Conimunications in Japan, Part 1, pp. 73-81, 1993

[122] T. Kashiwa, T. Onishi, and I. Fukai, "Analysis of microstrip antennas on a curved surface using the conformal grids FD-TD method," ," IEEE Trans. Antennas Propagat, AP-42,.pp. 423-427 1994

[123] J. P. Berenger, "A perfectly matched layer for the absorption of electromagnetics waves," Journal of Computational Physics, 1 14, 1, pp. 185-200, 1994

[124] Y. Qian, S. Iwata, and E. Yamashita, "Optimal design of an offset-fed, twin-slot antenna element for millimeter-wave imaging arrays," IEEE Microumv aiid Guided Wave Letters, 4, 7, pp. 232-234, 1994.

[125] A. Reineix and B. Jecko, "A time domain theoretical method for the analysis of microstrip antennas composed by slots," Annales des Telecommunications, 48, 112, pp. 29-34, 1993

[126] A. Reineix, J. Paillol, and B. Jecko, "FDTD method applied to the study of radar cross section of microstrip patch antennas," Annales des Telecommunications, 48, 11/12, pp. 589-593, 1993.

[127] A. Reineix, C. Melon, T. Monediere, and F. Jecko, "The FDTD method applied to the study of microstrip patch antennas with a biased ferrite substrate," Annales des Telecommunications, 49, 314, pp. 137-142, 1994.

[128] R. Luebbers, L. Chen, T. Uno, and S. Adachi, "FDTD calculation of radiation patterns, impedance, and gain for a monopole antenna on a conducting box," IEEE Trans. Antennas Propagat, AP-40, pp, 1577-1583, 1992.

[129] L. Chen, T. Uno, S. Adachi, and R. J. Luebbers, "FDTD analysis of a monopole antenna mounted on a conducting box covered with a layer of dielectric," IEICE Transactions on Communications, E76-B, 12, pp. 1583-1586, 1993.

[130] M. A. Jensen and Y. Rahmat-Samii, "Performance analysis of antennas for hand-held transceivers using FDTD," IEEE Trans. Antennas Propagat,, vol. 42, , pp. 1106-1 113, 1994.

[131] M. A. Jensen and Y. Rahmat-Samii, "EM interaction of handset antennas and a human in personal communications," Proceedingsof the IEEE, 83, 1, pp, 7-17, 1995.

[132] M. Kar and P.F Wahid, " The FDTD analysis of a microstrip patch antenna with dual feed lines, "Proc. IEEE southeast conference, April 24-26, 1988.

66

[133] Yamamoto D and Arai H, "FDTD analysis of radiation pattern of antenna on truncated ground plane,", Microwave Conference, Asia-Pacific, 3-6 Dec. 2000 pp. 378 – 381

[134] Huey-Ru Chuang and Liang-Chen Kuo, "3-D FDTD design analysis of a 2.4-GHz polarization-diversity printed dipole antenna with integrated balun and polarization-switching circuit for WLAN and wireless communication applications," IEEE Trans. on Microwave Theory and Techniques, , Vol. 51, , pp. 374 – 381, 2003

[135] Shaoqiu Xiao, Zhenhai Shao;, Fujise M, Bing-Zhong Wang, "Pattern reconfigurable leaky-wave antenna design by FDTD method and Floquet's Theorem," IEEE Trans. Antennas Propagat., Vol. 53, pp. 1845 – 1848, 2005

Chapter Three

METHODOLOGY

The experimental and simulation methodology utilized for the analysis of the proposed antennas are described in this chapter. Photolithographic process is used to fabricate different antenna geometries, while the antenna characterization is done with the help of Vector Network Analyzer in the Anechoic chamber. The FEM based Ansoft HFSS is used to perform the parametric analysis of the antenna geometry.

3.1 Fabrication of the antenna geometry

The choice of dielectric substrate plays an important role in the design of transmission lines as well as antennas at microwave frequencies. The dielectric constant and loss tangent are two important characteristics of a material which affects the efficiency of the antenna. The power handling capability is also determined by the substrate material. Using thin substrates with high dielectric constant would result in smaller antenna size. But this also results negative impact over the antenna efficiency and bandwidth. Therefore, there must be a design trade-off between antenna size and good antenna performance. The FR4 substrate material with dielectric constant 4.4 and loss tangent of 0.005 was chosen for initial studies. However, the final design is tested with commercially available substrate.

At microwave frequencies the precise fabrication of prototype plays a vital role. Therefore photolithographic process is used to fabricate the antenna geometries. Photolithography is the process of transferring geometrical shapes from a photo mask to the surface of a substrate which results optical accuracy.

The computer aided design of the antenna is printed on a high quality butter paper with a high resolution laser printer. The copper clad of suitable dimension is cleaned with a suitable solvent like acetone to remove any chemical impurities and dried. Now a very thin layer of the negative photo resist material is applied over the copper clad using a high speed spinner. The copper clad is then exposed to UV light through the carefully aligned mask. Extreme care must be taken to ensure that no dust or impurities are present in between the mask and copper clad. The layer of photo resist material in the exposed portions hardens. Now the clad is immersed in a developer solution, to remove the photo resist material from the unexposed region. The unwanted copper is then removed by rinsing the copper clad in a ferric chloride solution. The laminate is then cleaned to remove the

hardened photo resist using acetone solution. The various steps involved in the photolithographic technique are illustrated in Fg.3.1.
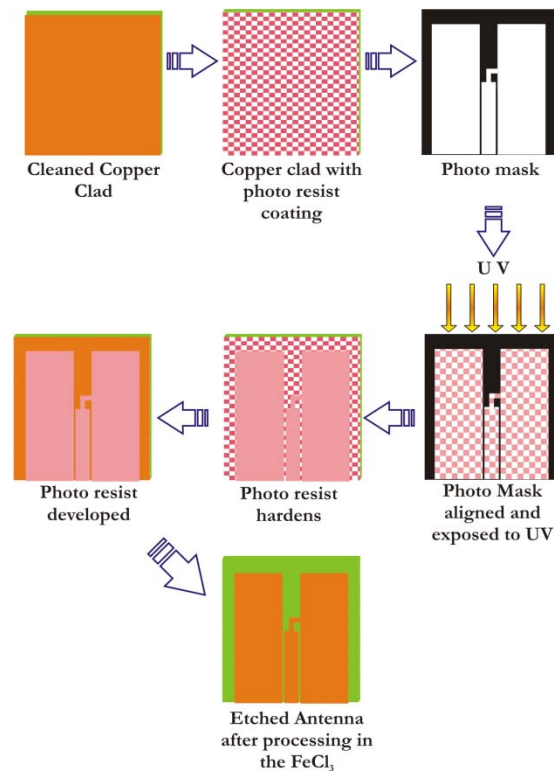
Fig.1.3. Various steps involved in the photolithographic process

3.2 Facilities used

A short depiction of equipments and facilities used for the measurements of antenna characteristics is presented in this section.

3.2.1   HP 8510c Vector Network Analyzer

The HP 8510C series microwave vector network analyzers provide a complete solution for characterizing the linear behavior of either active or passive networks over the 45 MHz to 50 GHz frequency range [1]. The network analyzer measures the magnitude, phase, and group delay of two-port networks to

characterize their linear behavior. The analyzer is also capable of displaying a network's time domain response to an impulse or a step waveform by computing the inverse Fourier transform of the frequency domain response.
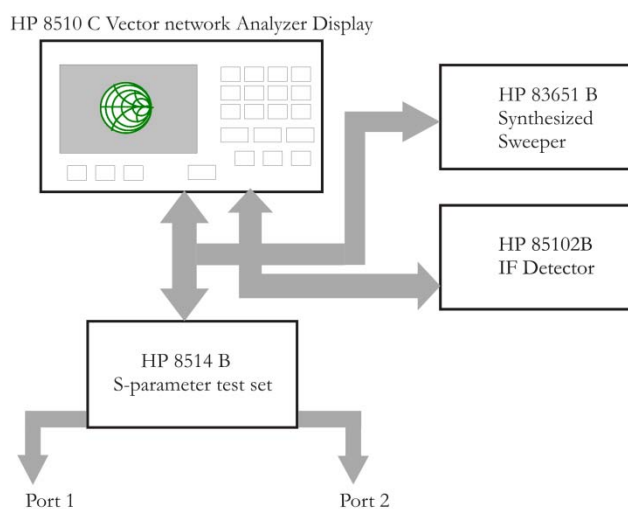
Fig.3.2 Block diagram of HP8510C Vector Network Analyzer

The HP 8510C network analyzer consists of a microwave source, S-parameter test set, signal processor and display unit as shown in Fig. 3.2. The synthesized sweep generator HP 83651B uses an open loop YIG tuned element to generate the RF stimulus. Frequencies from 10 MHz to 50 GHz can be synthesized either in step mode or ramp mode depending on the required measurement accuracy. The antenna under test (AUT) is connected to any one of the port of the S-parameter test set HP8514B. The frequency down converter unit separates the forward and reflected power at the measurement point and down converted it to 20MHz. It is again down converted to lower frequency and

processed in the HP8510C processing unit with Motorola 68000 processor. All the above systems are interconnected with HPIB bus and RF cables. The Matlab based data acquisition software in IBM pc coordinates the measurements and records the data in csv format.

3.2.2   E8362B Precision Network Analyzer (PNA)

Precision Network Analyzer is the recent series from Agilent Vector Network Analyzer family which provides the combination of speed and precision for the demanding needs of today's high frequency, high-performance component test requirements. The modern measurement system meets these testing challenges by providing the right combination of fast sweep speeds, wide dynamic range, low trace noise and flexible connectivity. The Analyzer is capable for performing measurements from 10 MHz to 20 GHz and it has 16, 001 points per channel with < 26 µsec/point measurement speed. The photograph of the PNA E8362B used for the antenna measurements is shown in Fig. 3.3 below.

Fig. 3.3 PNA E8362B Network Analyzer

3.2.3   Anechoic Chamber

The Echo free measurement facility which is used to accurately measure the antenna characteristics is termed as Anechoic Chamber. It is an acoustic free

room which consists of microwave absorbers [2] fixed on the walls, roof and floor to avoid EM reflections. The photograph of the anechoic chamber used for the antenna measurements is shown in Fig. 3.4 below.

Fig.3.4. Anechoic chamber

Microwave absorbers are high quality, low foam, impregnated with dielectrically / magnetically lossy medium such as poly urethane. The tapered shapes of the absorber provide good impedance matching for the microwave power impinges upon it and it results high absorption by total internal reflection. Aluminium shielding reduces electromagnetic interference from surroundings.

3.2.4 Radiation pattern measurement setup

A high precision turntable assembly interfaced to an IBM PC through a microcontroller is utilized to measure the radiation pattern. The antenna under test is mounted on the turntable and a linearly polarized wideband standard horn antenna is used as the transmitter. The main lobe tracking for gain measurement as well as the polarization measurement are carried out through this setup (Fig. 3.4). The antenna characterization is carried out using a Matlab based Graphical User Interface- CREMA Soft.
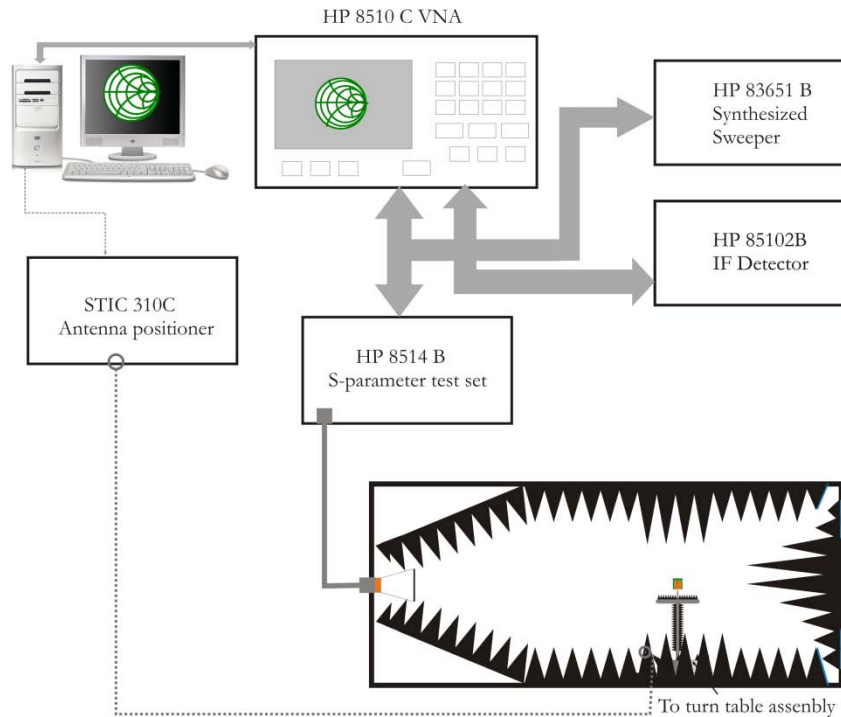
Fig.3.4 Radiation characteristic measurement setup

3.3   Antenna Characterization

The major antenna characterization procedures are depicted in the following sessions,

3.3.1 Reflection Measurement and Impedance Bandwidth

The reflection measurement of the antenna under test is carried out by connecting it to any one of the network analyzer port and operating the PNA in S_{11}/S_{22} mode. The specific port of the analyzer should be calibrated prior to the measurement in the frequency range of interest using the standard open, short and matched load. The returnloss values of the antenna in the entire frequency band

are then stored on a computer in '.csv' format with the help of 'CREMA SOFT'. The frequency at which the returnloss value is minimum is taken as the resonant frequency of the antenna. The range of frequency for which the returnloss value is within the -10dB points is usually treated as the band width of the antenna and is usually expressed in percentage.

3.3.2 Radiation Characteristics

The radiation characteristics of the antenna are carried out in the anechoic chamber in order to avoid the reflections from the surrounding objects. The antenna under test is mounted over the turntable and connected to one port of the HP 8510C network analyzer configured in the receiver mode, while the other port of the network analyzer is connected to a wideband horn which act as the transmitter. The network analyzer and the turntable controller are interfaced to a computer which runs the measurement automation software "CREMA SOFT". The measurement automation software requires *the band under measurement*, *angular step size* and *file name* as input data. The system automatically undergoes through calibration prior to the measurement and performs the S_{21} measurement for each step angle and saves the angular transmission characteristics in a file specified by the *file name*.

3.3.3 Gain Measurement

Gain of the Antenna is measured using the gain transfer method. The experimental setup for determining the gain is similar to the radiation pattern measurement setup. The gain of the antenna under test (AUT) is measured relative to the power levels detected by a standard gain antenna [3,4]. In order to measure the gain, the standard gain antenna is mounted on the turntable and a through calibration is performed at the bore sight direction. The antenna under test is carefully mounted on the turntable and extreme care is taken for the exact

alignment. The relative power level is obtained from the network analyzer and this provides the gain with respect to the standard antenna. The gain of the standard antenna is added to the relative gain to plot the actual gain of the antenna under test.

3.3.4 Antenna Efficiency

Wheeler cap method is utilized to measure the antenna efficiency, by making two impedance measurements [5]. The one is the input impedance before using the metallic cap over the antenna and the other one after putting the metallic cap. If the test antenna behaves like a series RLC circuit near its resonance, then the input resistance R should decrease after applying the cap, and the efficiency is calculated by the following expression.,

$$\eta = \frac{P_R}{P_R + P_L} = \frac{R_R}{R_R + R_L} = \frac{R_{nocap} - R_{cap}}{R_{nocap}}$$

3.4 Ansoft HFSS- The CAD tool

Ansoft HFSS is one of the globally accepted commercial Finite Element Method(FEM) solver for electromagnetic structures [6]. It is one of the most popular and powerful applications used for antenna design The optimization tool available with HFSS is very useful for antenna engineers to optimize the antenna parameters very accurately. There are many kinds of boundary schemes available in HFSS. Radiation and PEC boundaries are widely used in this work. The vector as well as scalar representation of E, H and J values of the device under simulation gives a good insight in to the problem under simulation.

78

References:

[1] HP 8510 C Network Analyzer operating and programming manual, Hewlett Packard , 1988.

[2] E. J. Zachariah, K. Vasudevan, P. A. Praveen kumar, P. Mohanan and K. G. Nair, "Design, Development and performance of an achechoic chamber for microwave antennas studies", Indian Journal of Radio and space Physices, vol 13, pp. 29-31, 1984

[3] C. A. Balanis, "Antenna Theory: Analysis and Design, second edition, John Wiely & Sons Inc. 1982

[4] John D. Kraus, Antennas Mc. Graw Hill International, second edition, 1988

[5] H. Choo, R. Rogers, and H. Ling, "On the wheeler cap measurement of the efficiency of microstrip antennas," *IEEE Transactionson Antennas and Propagation*, vol. 53, no. 7, pp. 2328–2332, 2005.

[6] HFSS user's manual, version 10, Ansoft Corporation, July 2005

NUMERICAL AND EXPERIMENTAL RESULTS

The wireless communication industry is integrating a number of services like Bluetooth, WLAN etc. to the hand held communication devices. Therefore the bandwidth requirement of the antenna while maintaining the compactness becomes more critical in the present scenario.

Wideband antennas are gaining prominence and becoming very attractive in modern wireless and mobile communication systems. These antennas avoid multiple band designs of narrow band elements and hence are simpler. One of the most popular antennas employed in wireless and mobile communication systems is the monopole antenna because of simple structure and powerful merits such as wide impedance bandwidth, omni-directional radiation pattern and moderate gain.

4.1 Development of a wideband Drum shaped antenna

Consider a simple strip monopole antenna printed on a substrate of relative permittivity ε_r and thickness h. A 50Ω microstip line of width Wm with ground plane dimensions W_Gx L_G is used to excite the strip monopole. For the present study the length of the strip monopole is selected as λg/4 [λg = λ/√(ε_r+1)/2] of the design frequency. The width of the radiating monopole is selected as the width of 50Ω microstrip line. The antenna is excited with a SMA (Sub Miniature Amphenol) connector. The top and side view of the printed strip monopole antenna geometry is illustrated in Fig. 4.1.
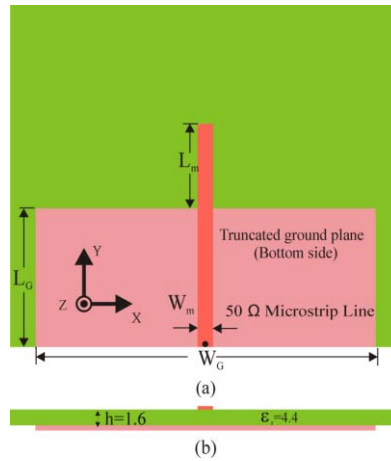
Fig. 4.1 Geometry of the Strip Monopole antenna (a) Top view (b)side view
L_G = 29mm, W_G = 67mm, L_m = 15mm, W_m = 3mm, h = 1.6mm and ε_r = 4.4

The measured return loss characteristic of the strip monopole antenna with design parameters L_G = 0.46λ_g (29mm), W_G = 1.06λ_g (67mm), L_m = 0.25λ_g (15mm), W_m = 3mm, h = 1.6mm and ε_r = 4.4 is shown in Fig. 4.2.(a) From the graph it is clear that the strip monopole provides a resonance at 2.9 GHz from 2.45 GHz to 3.48 GHz with a bandwidth of 1.03 GHz, 36%. The simulated return

loss characteristic of the strip monopole antenna is illustrated in the same graph for comparison. It is observed that the results are in good agreement.

(a)   (b)
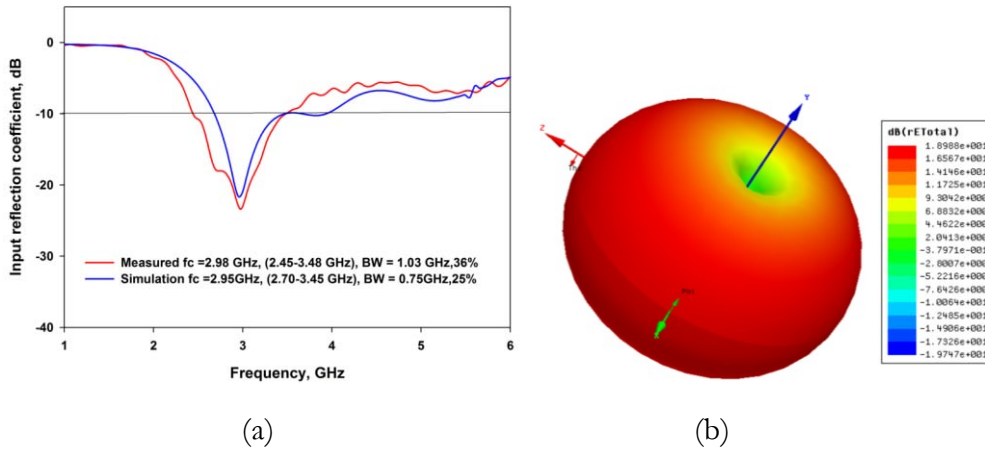
Fig. 4.2 Measured and simulated returnloss characteristics of the strip monopole. L_G = 29mm, W_G = 67mm, L_m = 15mm, W_m = 3mm, h = 1.6mm and ε_r = 4.4

It is clear from the simulated 3D radiation pattern that the strip monopole exhibit almost omni-directional radiation characteristics. Investigations on simple strip monopole antenna show that the antenna provides a 2:1 VSWR bandwidth of 36% with omni-directional radiation characteristics. But this bandwidth is not sufficient for the modern wireless communication systems. The methodology adopted to increase the bandwidth of the monopole antenna is discussed.

It is found that a bowtie antenna is offering very large impedance bandwidth. In [1] Jacob et al. has proposed a drum shaped compact microstrip antenna for large impedance bandwidth. So a drum shaped antenna is selected to top load the monopole for further enhance the bandwidth. By suitably selecting the resonant frequency of the monopole and drum shaped patch the bandwidth can be improved.

The parametric analysis of the proposed drum shaped monopole antenna is carried out using Finite Element Method (FEM) based Ansoft High Frequency Structure Simulator. The proposed antenna is fabricated using photolithographic technique and the simulation results are experimentally verified using Vector Network Analyzer. The analysis carried out in this section is summarized in Table 4.1

Parameter	Measurements conducted
o finite ground dimensions (L_G, W_G)	Returnloss, Radiation Pattern, Current density plots, and Gain
o Substrate parameters (ε_r, h)	
o Length of the drum shaped patch, L	
o Width of the drum shaped patch, W	
o Central width of the drum shaped patch, B	

Table 4.1 Summary of the analysis

4.1.1 Antenna Geometry:

The geometry of the wideband drum shaped antenna is illustrated in Fig. 4.3
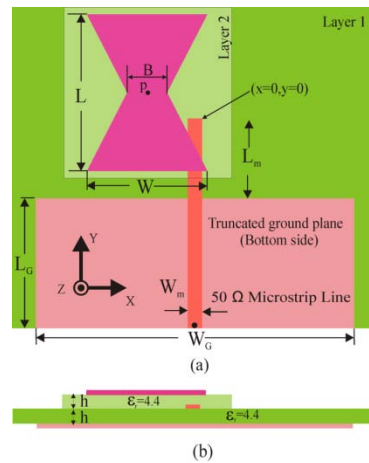
Fig. 4.3 Geometry of the Drum shaped wideband antenna (a) Top view (b)side view[L_G = 29mm, W_G = 67mm, L_m = 15mm, L = 33mm, W = 24mm, B = 8mm, P=(x = -10mm, y = 5.5mm), h = 1.6mm and ε_r = 4.4]

The geometry consists of a strip monopole of length, L_1 with truncated ground plane of dimension L_G x W_G on dielectric Layer 1. The strip monopole is loaded with a drum shaped patch on dielectric Layer 2 with dimensions of length L, width W and central width B. Both the strip monopole and the patch are fabricated on a substrate with relative permittivity, ε_r =4.4 and thickness, h =1.6mm.The drum shaped patch is placed at the optimum position and electromagnetically excited with the strip monopole.

4.1.2 Return loss Characteristics

The measured return loss characteristics of the electromagnetically excited drum shaped optimum antenna for the design having design parameters L_G = 0.0.37λ_g (29mm), W_G = 0.85λ_g (67mm), L_m = 0.19λ_g (15mm), L = 0.42λ_g (33mm), W

= 0.30λ_g (24mm), B = 0.10λ_g (8mm), P=(x = -0.13λ_g (-10mm), y = 0.07λ_g (5.5mm)), is illustrated in Fig. 4.4.
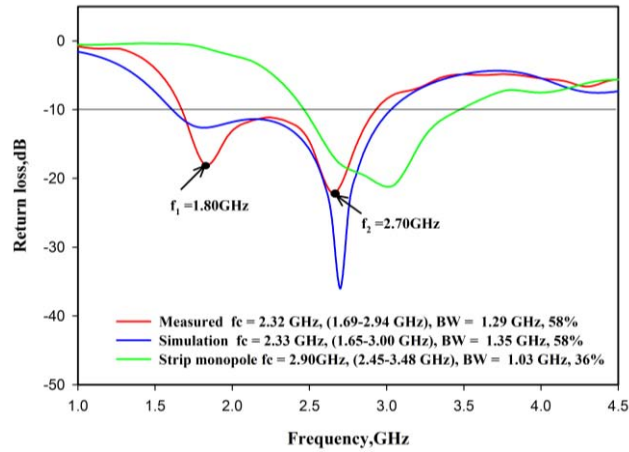
Fig.4.4Measured and simulated returnloss characteristics of the electromagnetically excited drum shaped monopole antenna and strip monopole. [L_G = 29mm, W_G = 67mm, L_m = 15mm, L = 33mm, W = 24mm, B = 8mm, P =(x = -10mm, y = 5.5mm), h = 1.6mm and ε_r = 4.4]

It is observed from the plot that the strip monopole alone provides a resonance at 2.9 GHz from 2.45 GHz to 3.48 GHz with a bandwidth of 1.03 GHz, 36%. By loading the drum shaped patch vertically, at the optimum position, it is observed that the antenna offers a 2:1 VSWR band from 1.69 GHz- 2.94 GHz with 58% bandwidth centered at 2.32 GHz. An improvement of 22% bandwidth is observed. The simulation result is in good agreement with the measured values.

4.1.3 Resonance behavior:

A better understanding about the resonance and radiation behavior of the proposed antenna can be obtained by analyzing the computed current density plots at the resonant frequencies. The current density plots at 1.8 GHz are shown in Fig.4.5
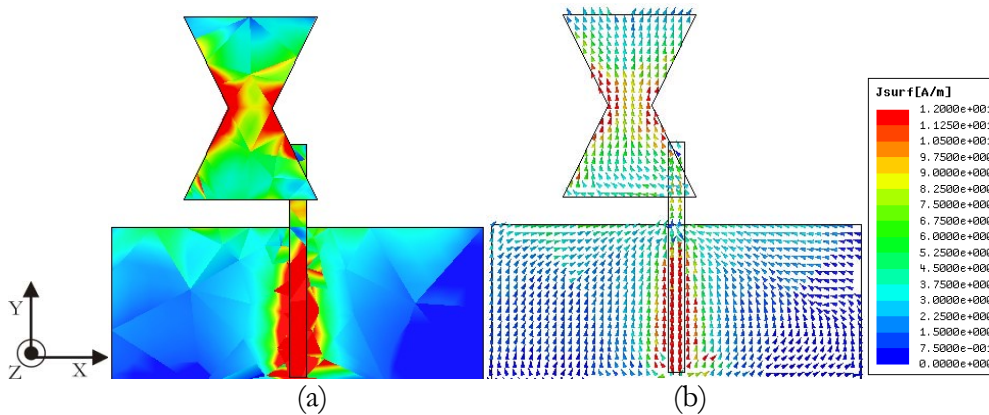
Fig. 4.5 Simulated surface current density plots of the drum shaped antenna at 1.8 GHz (a) magnitude (b) vector[L_G = 29mm, W_G = 67mm, L_m = 15mm, L = 33mm, W = 24mm, B = 8mm, P=(x = -10mm, y = 5.5mm), h = 1.6mm and ε_r = 4.4]

It is observed from the current density plot that the drum shaped patch is strongly excited at the first resonance. A half wave current variation is also found along the length of the patch which corresponds to the first resonant length. It is also worth to note that only a feeble current density variation is observed in the ground plane.

The current distribution on the antenna is shown in Fig.4.5 (b). It is found that the current on the monopole is along the Y direction. That means the monopole is Y polarized. It is also noted that with respect to the centre of the drum, the X polarized currents are equal and opposite. These currents will cancel at the far field. So X polarized currents will not contribute for far field radiation. But the Y polarized currents are same in all parts of the structure. This Y polarized currents are responsible for the far field radiation for the drum. So the drum is also radiates Y polarized waves.

<center>(a)   (b)</center>
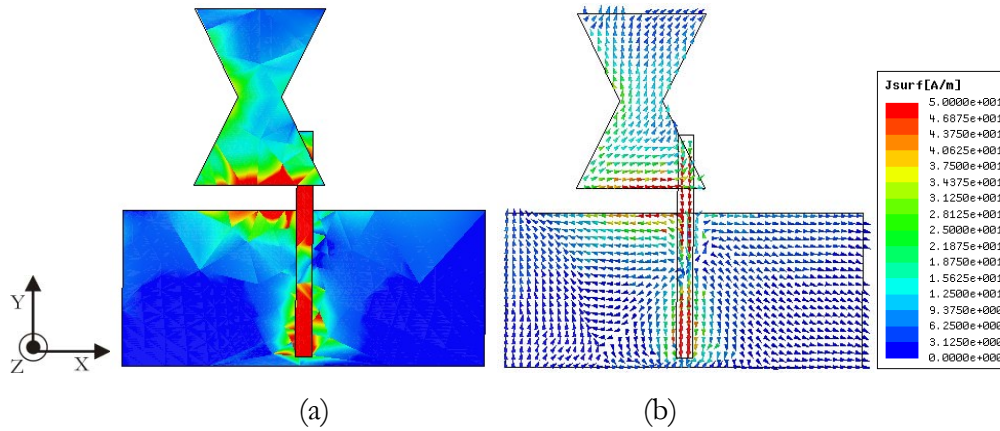
Fig. 4.6 Simulated surface current density plots of the drum shaped antenna at 2.7 GHz (a) magnitude (b) vector [L_G = 29mm, W_G = 67mm, L_m = 15mm, L = 33mm, W = 24mm, B = 8mm, P=(x = -10mm, y = 5.5mm), h = 1.6mm and ε_r = 4.4]

Fig.4.6 illustrates the surface current at the second resonance. It is seen from the plot that the lower side of the drum shaped patch and strip monopole are excited strongly.

It is seen from the vector form of surface current depicted in Fig.4.6 (b) that the current at the lower side of the patch along W and the neighboring ground plane are almost equal in magnitude and opposite in direction. Therefore the X directed E-field will cancel each other in the far field and does not contribute for radiation. So that second mode of the monopole is Y polarized.

Therefore it can be concluded that the antenna provides a wideband resonance by merging two resonances one belongs to the drum shaped patch and other to the strip monopole.

4.1.4 Polarization

The variation of received power from a highly linearly polarized horn antenna throughout the resonant band at both the polarization plane is depicted in the Fig.4.7
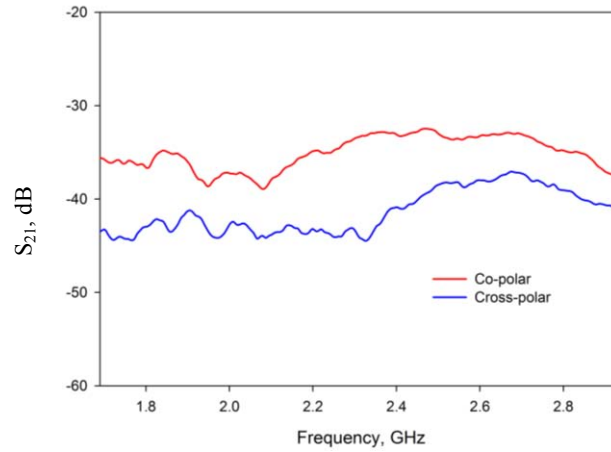
Fig. 4.7 S_{21} characteristics of the wideband antenna along the bore sight direction [L_G = 29mm, W_G = 67mm, L_m = 15mm, L = 33mm, W = 24mm, B = 8mm, P=(x = -10mm, y = 5.5mm), h = 1.6mm and ε_r = 4.4]

As predicted from the current density plot described earlier, the measurement results reveals that the radiated electromagnetic signal is linearly polarized along Y direction throughout the entire operating band. A cross polarization level of better than 5dB is observed throughout the band.

4.1.5 Radiation pattern

The measured radiation patterns in the principle planes at 1.8 GHz and 2.4GHz are depicted in Fig.4.8
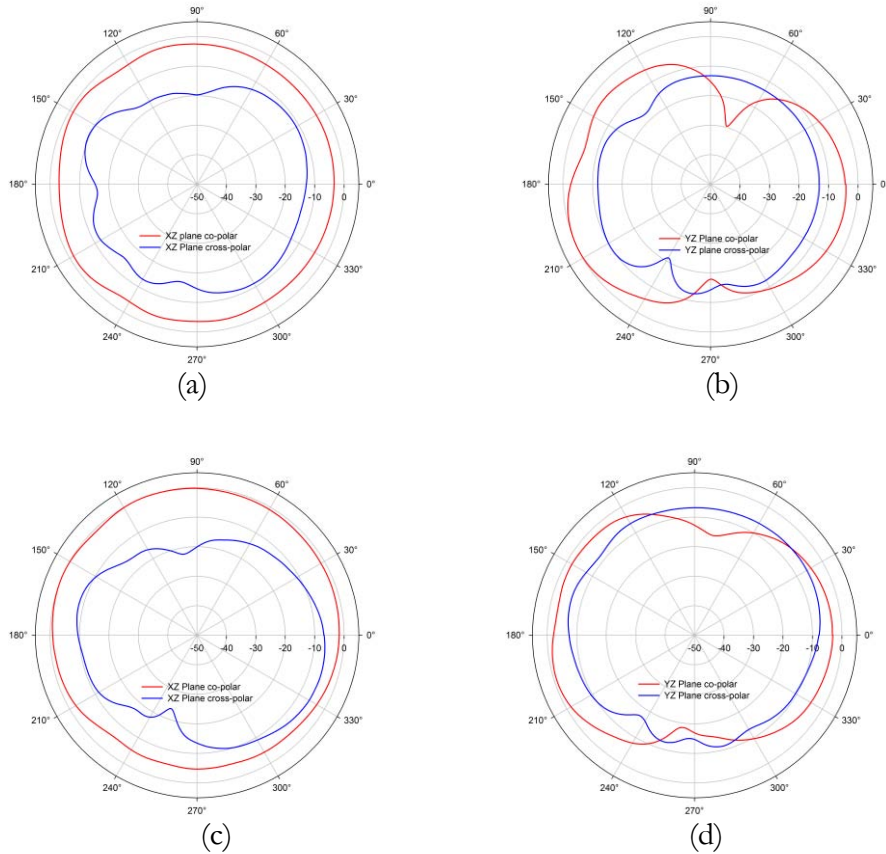
Fig.4.8 Measured radiation patterns in the two orthogonal planes at 1.8GHz [Fig. (a)-(b)] and at 2.4GHz [Fig.(c)-(d)]. [L_G = 29mm, W_G = 67mm, L_m = 15mm, L = 33mm, W = 24mm, B = 8mm, P=(x = -10mm, y = 5.5mm), h = 1.6mm and ε_r = 4.4]

It is observed that the hybrid antenna provides nearly omni-directional radiation characteristics with linear polarization along Y direction in the entire operating band. The antenna radiation in XZ plane is non-directional while that of the orthogonal plane is directional, which in turn provide nearly omnidiretionality suitable for wireless communication devices.

4.1.6 Gain

The measured gain in the bore sight direction is depicted in Fig. 4.9.
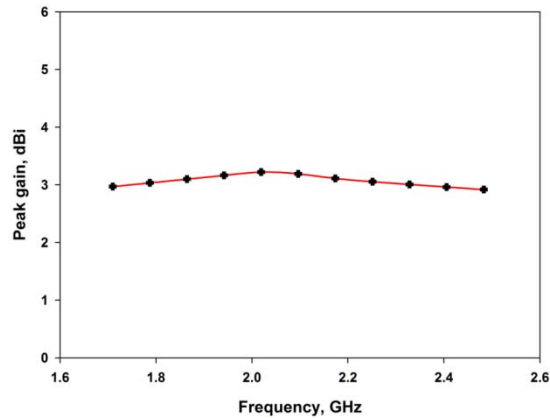
Fig. 4.9 Gain of the wideband coplanar antenna[L_G = 29mm, W_G = 67mm, L_m = 15mm, L = 33mm, W = 24mm, B = 8mm, P=(x = -10mm, y = 5.5mm), h = 1.6mm and ε_r = 4.4]

The antenna provides a moderate gain greater than 3dBi throughout the operating band. The maximum gain observed is 3.25dBi at 2GHz. It is also clear from the plot that the maximum variation of the gain is only 0.25dBi over the entire application band.

4.1.7 Parametric analysis

The parametric analysis of the proposed antenna is conducted and effects of various antenna parameters over the antenna characteristics are studied. The results and discussion on various parametric studies are provided in this session.

4.1.7.1 Position of the Patch.

It is found that the location of the patch over the monopole is very important. The bandwidth and impedance of the antenna is highly depending on the offset location of the patch 'P'. The dependence of the bandwidth of the

antenna on the offset position 'P' is shown Fig. 4.10 It is observed that when the 'y' offset is small the bandwidth is virtually independent of 'x'. However, when 'y' offset is greater than 4.5mm ($0.06\lambda_g$) and it is highly dependent of 'x'. Maximum bandwidth for minimum x offset is observed when y offset is 5.5mm ($0.07\lambda_g$).
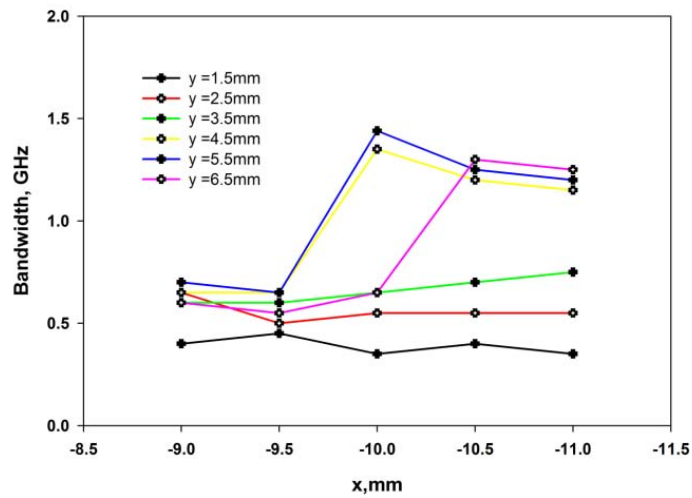
Fig. 4.10 Effect of position of the drum shaped patch on the feed line (a) bandwidth [L_G = 29mm, W_G = 67mm, L_m = 15mm, L = 33mm, W = 24mm, B = 8mm, h = 1.6mm and ε_r = 4.4]

93

4.1.7.2 Effect of Length (L) of the patch:

The influence of length of the patch over the returnloss characteristics is depicted in Fig.4.11.
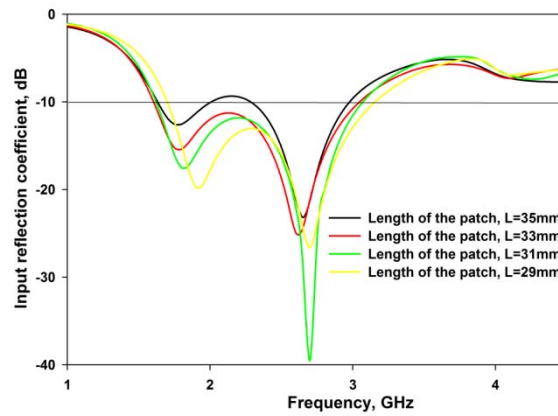
(a)
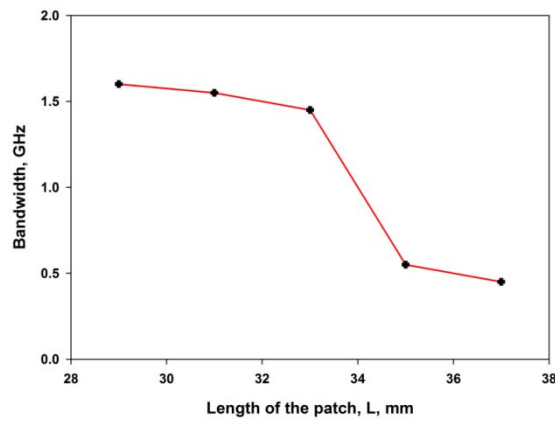
(b)

Fig. 4.11 Effect of patch length 'L' over the antenna characteristics[L_G = 29mm, W_G = 67mm, L_m = 15mm, W = 24mm, B = 8mm, P=(x = -10mm, y = 5.5mm), h = 1.6mm and ε_r = 4.4]

In the present study the length of the patch is varied from 29mm to 37mm ($0.37\lambda_g$ to $0.47\lambda_g$) by maintaining other parameters constant. It is observed

from the return loss characteristics of the antenna provided in Fig.4.11 (a) that the first resonance shifts to a lower value with the increase in L, as predicted from the surface current density plots in the previous session. It is also worth to note that the second resonance remains almost unaltered.

The efficient merging of these two resonant modes provides maximum bandwidth. It is observed that the increase of L beyond 33mm $(0.42\lambda_g)$ results sudden decrease in the bandwidth because of the drastic shift in the first resonance to a lower frequency region.

4.1.7.3 Effect of width (W) of the patch

The influence of the patch dimension 'W' over the return loss characteristics is depicted in Fig.4.12.
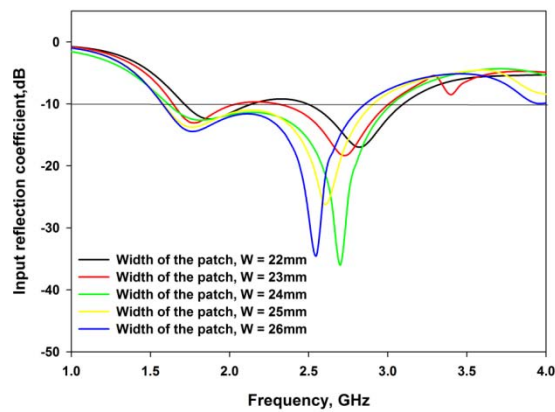
Fig.4.12(a) Effect of patch width 'W' over the returnloss characteristics
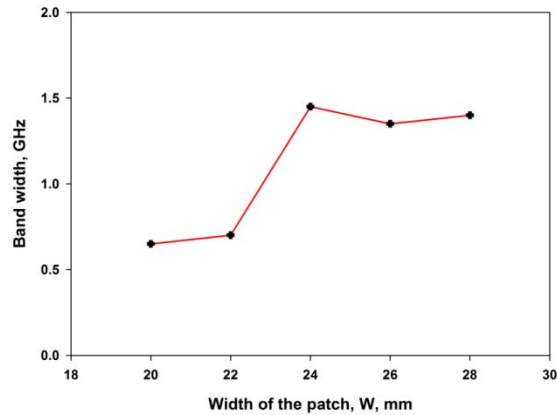
(b)

Fig.4.12(*contd*) Effect of patch width 'W' over the Bandwidth[L_G = 29mm, W_G = 67mm, L_m = 15mm, L = 33mm, B = 8mm, P=(x = -10mm, y = 5.5mm), h = 1.6mm and ε_r = 4.4]

It is very clear from Fig.4.12 that the width of the patch is responsible for the second resonance. When the width of the patch is 22mm ($0.28\lambda_g$) the second resonance occurs at 2.8 GHz. When the width is increased to 26mm ($0.33\lambda_g$) it is shifted to lower side that is 2.52 GHz. This conform that the width is responsible for the second resonance. It is also interesting to note that the first resonant frequency remains almost unaltered by the variation of width (W) of the patch. It reveals that the width of the patch provides a tuning effect for the second resonance as predicted through current density plots.

The effective merging of two resonances results optimum bandwidth. It is clear from the bandwidth variations shown in Fig.4.12 (b) that at W =24mm ($0.30\lambda_g$) the two resonant bands merge efficiently which results higher bandwidth.

4.1.7.4 Effect of Central width B of the patch:

The influence of central width B over the returnloss characteristics are depicted in Fig.4.13.
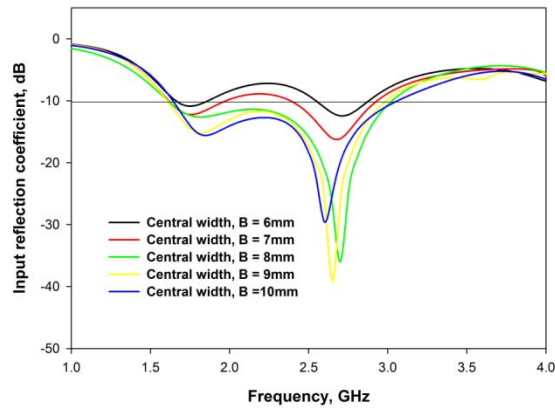
(a)
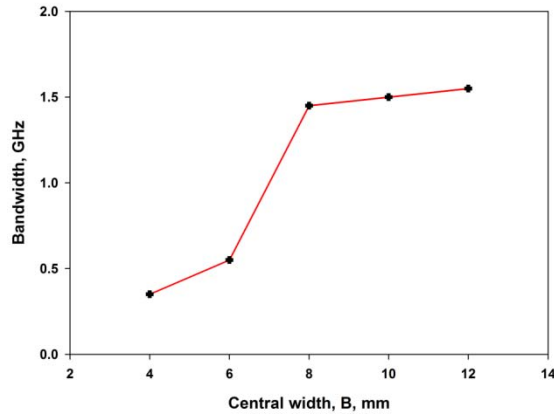
(b)

Fig.4.13 Effect of patch central width 'B' over the antenna characteristics
[L_G = 29mm, W_G = 67mm, L_m = 15mm, L = 33mm, W = 24mm, P=(x = -10mm, y = 5.5mm), h = 1.6mm and ε_r = 4.4]

It is found that with the central width 'B', the effective length of the patch is changing. When B is minimum the effective length is maximum. When

97

the width is equal to 'W' the effective length is minimum. So the first resonance is shifted towards the lower side with decrease of 'B'. It is also found that when the centre width is large the size of the drum is increased. This will apparently increase the overlapping area between the patch and monopole and more coupling between the two is observed. This will effectively change the resonant frequency of the second resonance.

The bandwidth is also get affected by the variation in B. It is found that two bands merge together to form a wideband characteristics for B greater than 8mm $(0.10\lambda_g)$.

4.1.8 Horizontal Orientation of the patch.

It is found that when the patch length L is vertically oriented we obtained some good result. Next section deals with the horizontal orientation of the patch.

The drum shaped patch loaded horizontally is shown in Fig.4.14.
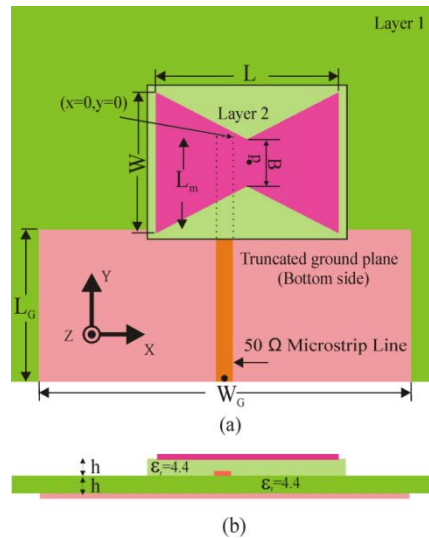
Fig. 4.14 Geometry of the horizontally oriented drum loaded monopole antenna. [L_G = 29mm, W_G = 67mm, L_m = 15mm, L = 33mm, W = 24mm, B = 8mm, P=(x = -2.5mm, y = -4.0mm), h = 1.6mm and ε_r = 4.4]

The drum shaped patch is loaded horizontally and placed at the optimum position. The return loss characteristics of the antenna is plotted in Fig.4.15
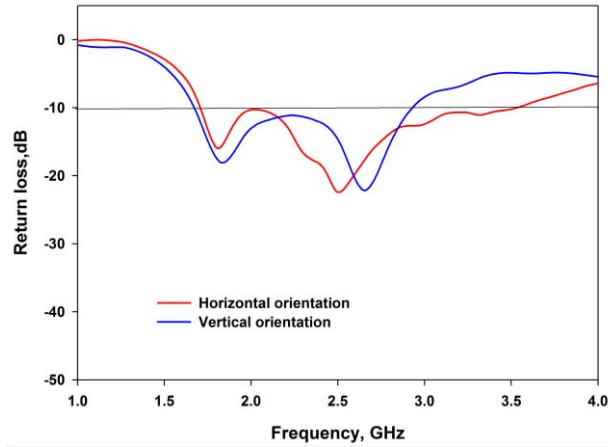
(a)
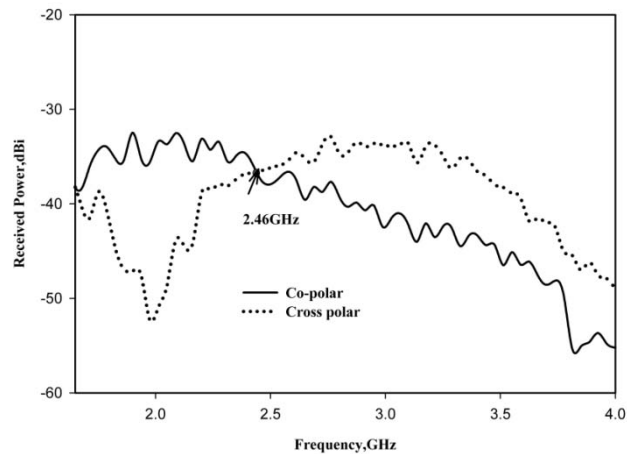
(b)

Fig. 4.15 Reflection and transmission characteristics of the horizontally oriented drum shaped monopole antenna [L_G = 29mm, W_G = 67mm, L_m = 15mm, L = 33mm, W = 24mm, B = 8mm, P=(x = -2.5mm, y = -4.0mm), h = 1.6mm and ε_r = 4.4]

It is seen from the plot that the antenna exhibits a 2:1 VSWR band from 1.71GHz – 3.50 GHz with 68% bandwidth centered at 2.61 GHz. The measurement results reveal that the horizontal loading results an improvement in

bandwidth by 10%. It is also evident from the transmission characteristics that the polarization of the antenna in the resonant band crosses at 2.46GHz.

Thus it can be concluded that even though the horizontal orientation provides an improvement of bandwidth by 10% the polarization purity becomes poor. So the two bands are polarized orthogonal to each other.

So dual band single polarized vertical loading is the best solution. Alternatively for dual band dual polarization application horizontal loading can be employed.

4.1.9 Comparison with circular and rectangular patch

The proposed antenna is compared with a rectangular and circular patch. It is observed that the drum shaped antenna is more compact than a rectangular or circular patch. A typical comparison is provided in Table 4.2.

Shape	Band, GHz	Bandwidth, GHz	Area, mm^2
Rectangle	1.60-3.20	1.60	792
Circle	1.65-3.70	2.05	855
Drum	1.60-3.05	1.45	528

Table.4.2. Comparison of proposed antenna with circular and rectangular patch

It is found that the drum shaped geometry offers 33% and 38% area reduction compared to the rectangular and circular geometry respectively.

4.2 Single layer-direct fed drum shaped monopole antenna

In the previous section we had discussed about a broad band antenna. Even though the antenna is offering very large bandwidth the structure is bulky and mechanically not robust due to the multiband structure. In this section, development of a broad band antenna in a single layer is discussed.

Development and analysis of a Single layer microstrip fed monopole is presented in this session. From the previous studies, it is clear that the drum shaped antenna can provide a broad bandwidth when it is placed at the optimum position over the strip monopole. Broad bandwidth is due to the merging of the two resonant frequencies corresponding to the strip monopole and the drum shaped patch. From the studies it is also clear that the horizontal orientation provides dual polarization characteristics while the vertical orientation of the patch provides linear polarization throughout the operation band which is highly suitable for modern wireless communication devices.

Considering all these points a single layer microstrip fed antenna for broad band application is developed from the previous design. The antenna characteristics and a parametric analysis are discussed in this module.

4.2.1 Antenna geometry

Fig.4.16 presents the geometry of the proposed drum shaped monopole antenna for wide band operation.
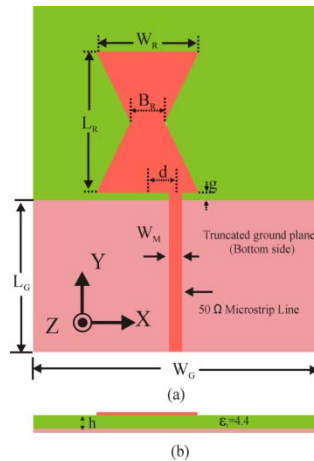
Fig.4.16 Geometry of the drum shaped strip monopole.[W_G = 67mm, L_G =35.5mm, W_M =3mm, W_R = 24mm, L_R =33mm, B_R = 8mm, d = 6.5mm, g =1.5mm h=1.6mm and ε_r =4.4]

The antenna geometry consists of a drum shaped monopole of Length L_R = $0.45\lambda_g$ (33mm), Width, W_R = $0.33\lambda_g$ (24mm) and central width B_R = $0.11\lambda_g$ (8mm). The monopole is excited with a 50Ω microstrip feed line of width 3mm. The antenna is etched on a substrate with a thickness 1.6mm and relative permittivity 4.4. The antenna is characterized by a truncated ground plane of length L_G =$0.49\lambda_g$ (35.5mm) and width W_G = $0.92\lambda_g$ (67mm) below the microstrip feed line. The offset distance (d) of the patch and the feed gap (g) are optimized for wideband operation.

4.2.2. Return loss characteristics

The experimental and simulated return loss characteristic of the drum shaped monopole antenna is illustrated in Fig.4.17.
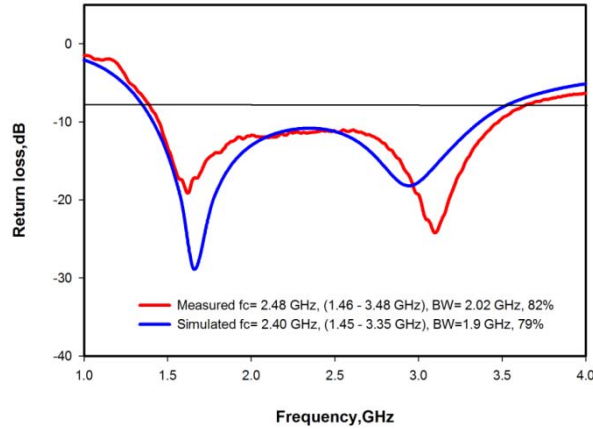
Fig. 4.17 Experimental and simulated returnloss characteristics of the drum shaped monopole antenna. [W_G = 67mm, L_G =35.5mm, W_M =3mm, W_R = 24mm, L_R =33mm, B_R = 8mm, d = 6.5mm, g =1.5mm h=1.6mm and ε_r =4.4]

It is seen from the returnloss characteristics that the antenna operates from 1.46GHz to 3.48GHz with a fractional bandwidth of 82% centered at 2.48GHz. The plot has two resonant dip which form the wideband characteristics as in the case of electromagnetically excited monopole antenna discussed in the previous session. Compared to the electromagnetically excited drum shaped patch loaded antenna discussed in the previous session, the present design holds merits including improvement of bandwidth by 24 percentage and more ease of fabrication.

4.2.3 Surface current density at the two resonances

A better understanding about the resonance and radiation behavior of the monopole can be obtained by analyzing the current at the metallic patch surface of the antenna. Fig. 4.18 illustrates the magnitude and direction of surface current at the first resonant dip at 1.6GHz.
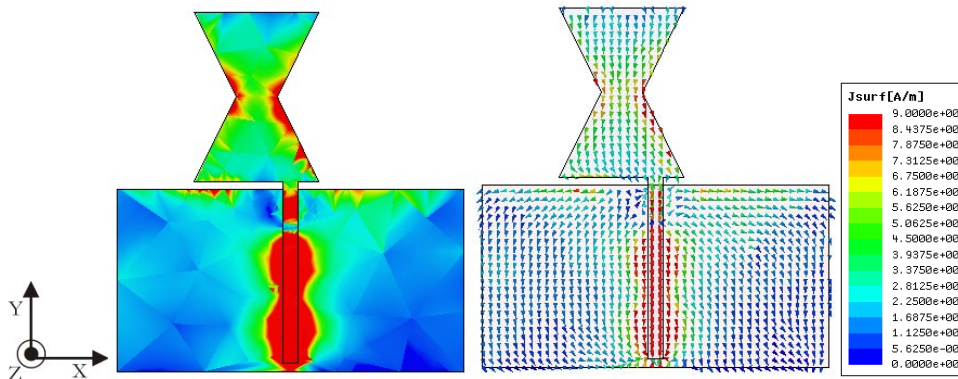
Fig.4.18 current density plot of the monopole antenna at 1.6GHz[W_G = 67mm, L_G =35.5mm, W_M =3mm, W_R = 24mm, L_R =33mm, B_R = 8mm, d = 6.5mm, g =1.5mm h=1.6mm and ε_r =4.4]

It is clear from the current density plot in Fig.4.18 (a) that the lateral dimensions of the drum are strongly excited at the first resonance. It is also observed that both sides of the drum in the Y-direction are strongly excited. The vector plot shows the direction of the current at the resonance. It is found that the current in the oblique regions are of same direction and the resultant vector is Y-directed. Therefore the polarization of the antenna will be in Y-direction.

The surface current at the second dip in the resonant band is depicted in Fig.4.19.
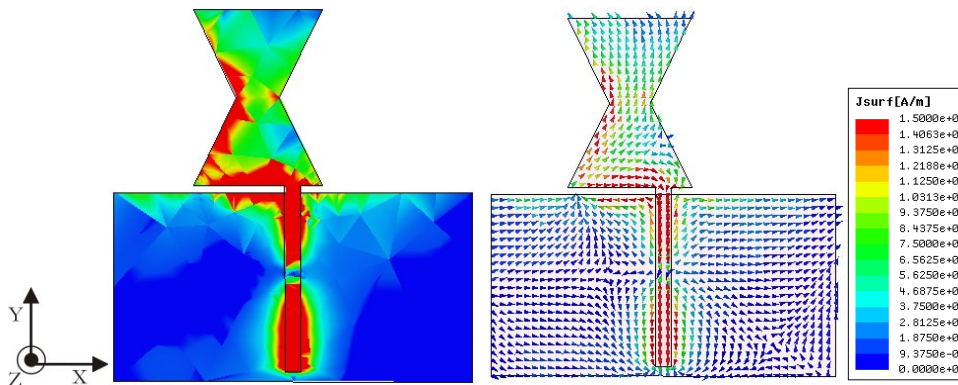
Fig. 4.19 current density plot of the monopole antenna at 3.1 GHz[W_G = 67mm, L_G =35.5mm, W_M =3mm, W_R = 24mm, L_R =33mm, B_R = 8mm, d = 6.5mm, g =1.5mm h=1.6mm and ε_r =4.4]

It is seen from the magnitude plot in Fig.4.19 (a) that both the lateral dimensions, width and length, are strongly excited at the second resonance. It is also worth to note that the neighboring side of the drum in the ground plane is also slightly excited. The vector plot provided in Fig.4.19 (b) reveals that the direction of current in the drum along the width and the neighboring ground plane are equal and opposite. Therefore they will cancel each other in the far field and do not contribute for radiation. Meanwhile the resultant current vector along the length of the drum is Y-directed and results Y-polarized radiation.

4.2.4 Polarization

The transmission characteristics of the proposed antenna is measured and depicted in Fig.4.20
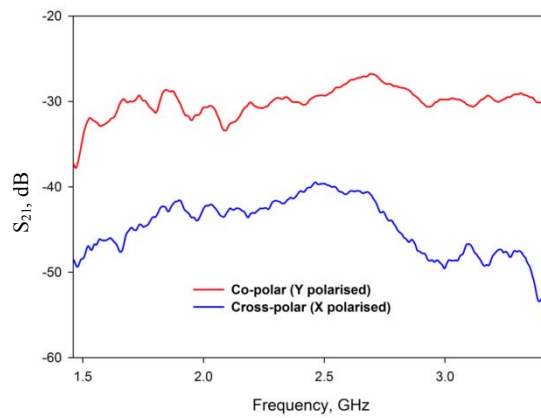
Fig. 4.20 Received power of the antenna [W_G = 67mm, L_G =35.5mm, W_M =3mm, W_R = 24mm, L_R =33mm, B_R = 8mm, d = 6.5mm, g =1.5mm h=1.6mm and ε_r =4.4]

It is evident from the measured results that the antenna exhibits y-polarized radiation throughout the resonant band with a cross polarization level of better than 10dB.

4.2.5 Radiation pattern

The measured radiation patterns in the XZ and YZ planes at different frequency points are illustrated in Fig. 4.21.

(a)   (b)

(c)   (d)

(e)   (f)
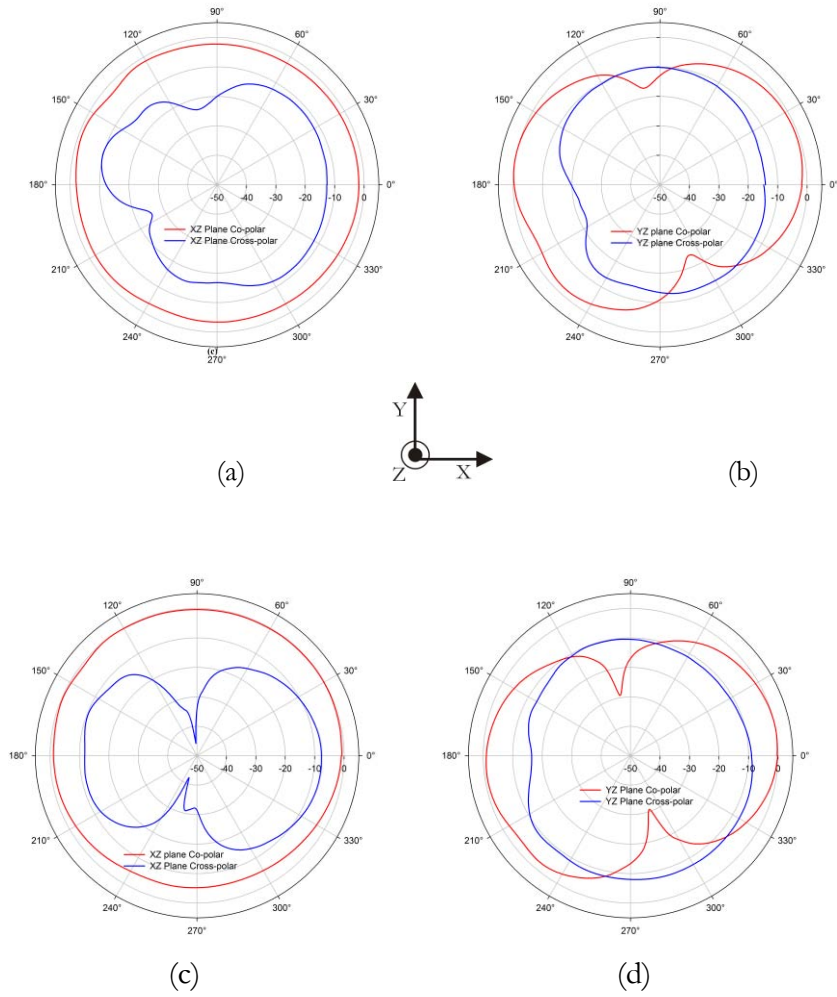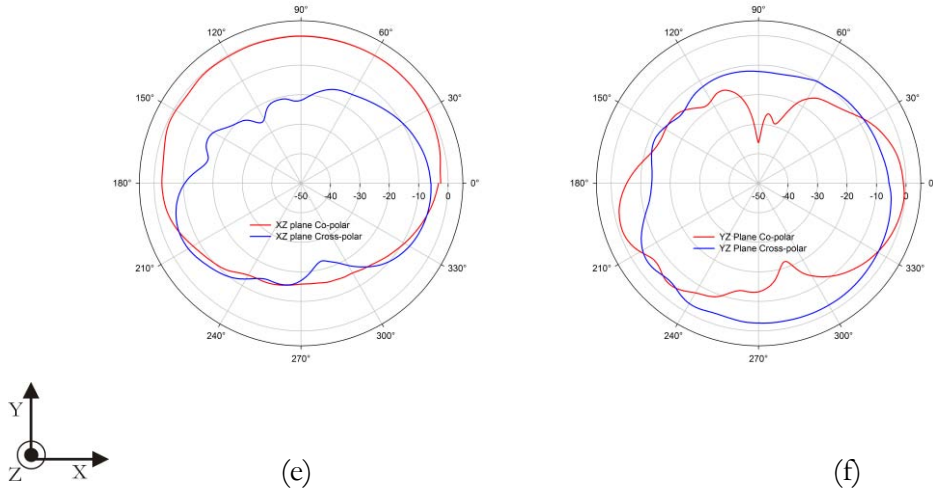
Fig. 4.21 Measured radiation pattern of the proposed antenna. (a)-(b)1.45GHz (c)-(d)2.4GHz(e)-(f)3.4GHz[W_G = 67mm, L_G =35.5mm, W_M =3mm, W_R = 24mm, L_R =33mm, B_R = 8mm, d = 6.5mm, g =1.5mm h=1.6mm and ε_r =4.4]

It is observed from the measured results that the antenna provides wide radiation coverage in the XZ-plane while behaves directional in the orthogonal plane.

4.2.6 Antenna Gain

The peak gain of the antenna measured at each frequency points by gain comparison method is illustrated in Fig. 4.22. The antenna offers moderate gain in the desired frequency band. It shows a peak gain of 5.5dBi at 3 GHz. It is also worth to note that the gain variation of the antenna in the entire operating band is only 0.5dBi.
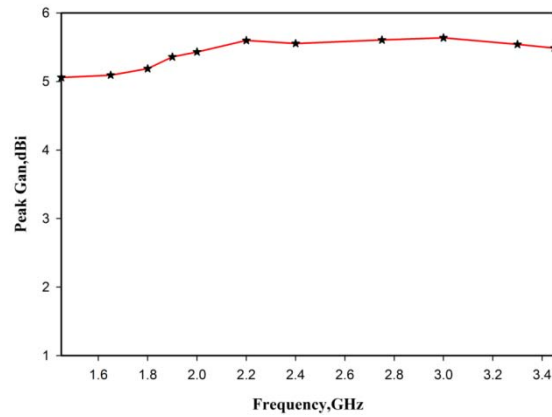
Fig. 4.22 Measured peak gain of the monopole antenna[W_G = 67mm, L_G =35.5mm, W_M =3mm, W_R = 24mm, L_R =33mm, B_R = 8mm, d = 6.5mm, g =1.5mm h=1.6mm and ε_r =4.4]

4.2.7 Parametric Analysis:

A parametric analysis is performed for the drum shaped monopole antenna in order to investigate the effect of various antenna parameters over the antenna characteristics. The studies conducted are the effect of dielectric properties (relative permittivity of the material and thickness of the substrate) and effect of structural parameters (various geometrical parameters). The following sessions provides discussions on the effect of each parametric analysis and conclusions derived from the analysis.

4.2.7.1 Ground plane parameters

The ground dimensions of any radiator, especially the monopole devices, play an important role in the antenna characteristics. The following session provides the effect of finite ground dimensions of the drum shaped geometry (L_G and W_G) over the antenna characteristics.

4.2.7.1.1 Ground plane width W_G

It is seen form the returnloss characteristics that the shifts in the resonant frequencies are almost nil but the matching gets affected with the variation in W_G. This in turn result bandwidth variations as depicted in Fig. 4.21 (b). The antenna offers optimum bandwidth for W_G = 67mm ($0.92\lambda_g$).
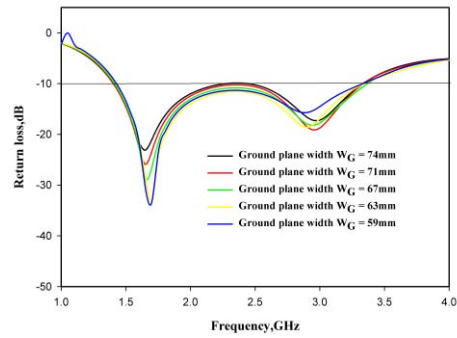
(a)
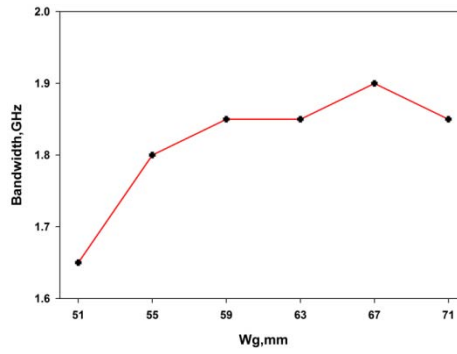
(b)

Fig. 4.23 Variation in return loss characteristics with ground plane width[L_G =35.5mm, W_M =3mm, W_R = 24mm, L_R =33mm, B_R = 8mm, d = 6.5mm, g =1.5mm h=1.6mm and ε_r =4.4]

4.2.7.1.2 Ground plane length, L_G

The length of the ground plane is varied from 25mm to 37.5 mm to investigate its effect over the returnloss characteristics. The variation in returnloss characteristics are depicted in Fig. 4.24
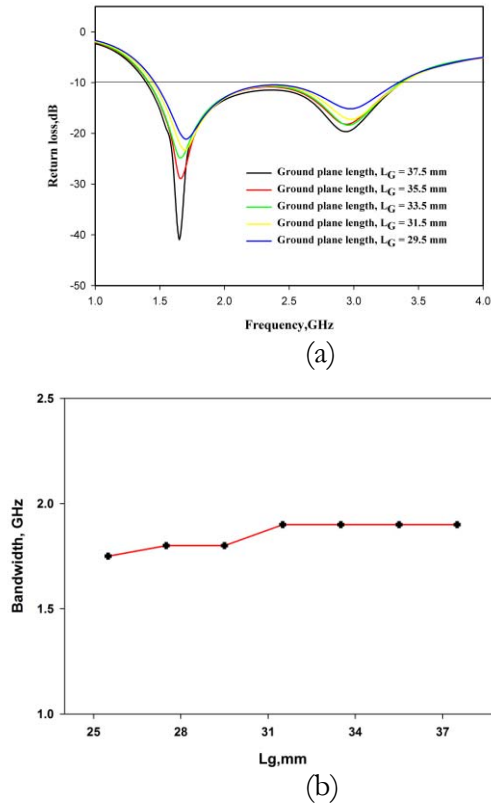
Fig. 4.24 Influence of ground plane length over the return loss characteristics[W_G = 67mm, W_M =3mm, W_R = 24mm, L_R =33mm, B_R = 8mm, d = 6.5mm, g =1.5mm h=1.6mm and ε_r =4.4]

As in the case of ground plane width, length of the ground plane is also not affecting the resonant frequency. It is evident from Fig. 4.24 (b) that the bandwidth of the antenna is slightly increasing for as L_G increases and remains almost stable for L_G variations greater than 31mm $(0.42\lambda_g)$.

4.2.7.2 Effect of gap, g:

The influence of gap between drum and neighboring ground plane is studied and depicted in Fig. 4.25
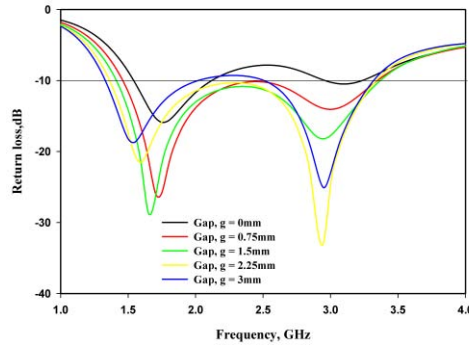
Fig. 4.25 Return loss variations with gap, g. [W_G = 67mm, L_G =35.5mm, W_M =3mm, W_R = 24mm, L_R =33mm, B_R = 8mm, d = 6.5mm, h=1.6mm and ε_r =4.4]

It is found from the analysis that the gap g is very crucial for the proposed antenna. The optimum value of 1.5mm (0.02λ_g) is selected for maximum bandwidth and effective merging of two resonances. Without gap the antenna is resonating at two frequencies. At the optimum coupling the two resonant frequencies can be merged to form a single band.

4.2.7.3 Influence of offset parameter (d):

The drum is placed at an offset position determined by the parameter d for maximum bandwidth. The effect of 'd' over the returnloss characteristics is depicted in Fig. 4.26.
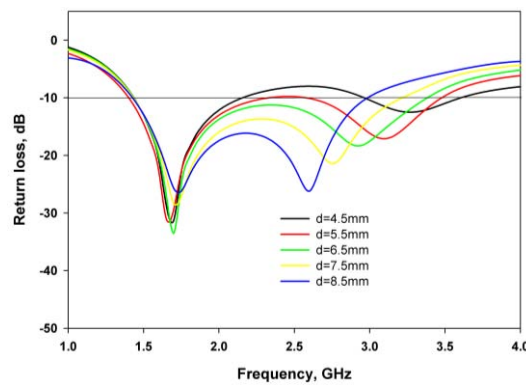
Fig. 4.26 Effect of offset parameter 'd' over the returnloss characteristics. [W_G = 67mm, L_G =35.5mm, W_M =3mm, W_R = 24mm, L_R =33mm, B_R = 8mm, g =1.5mm h=1.6mm and ε_r =4.4]

111

It is found from the plot that as the position of the patch varies from 0 (Feed point is at the center of the drum) to 9.75mm ($0.13\lambda_g$) the bandwidth varies drastically. The optimum position is found to be d =6.5mm ($0.09\lambda_g$) for maximum bandwidth.

4.2.7.4 Influence of drum length 'L_R'

The influence of length L_R of the drum is studied and depicted in Fig. 4.27
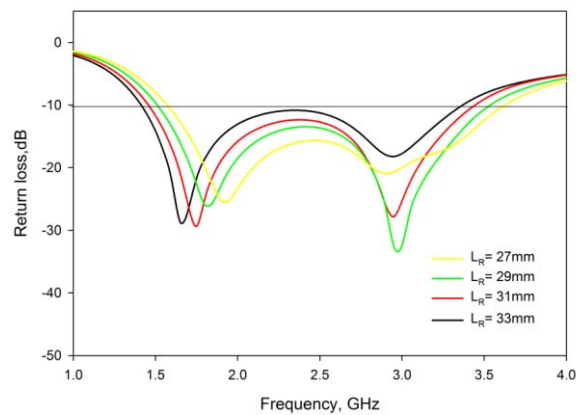
(a)
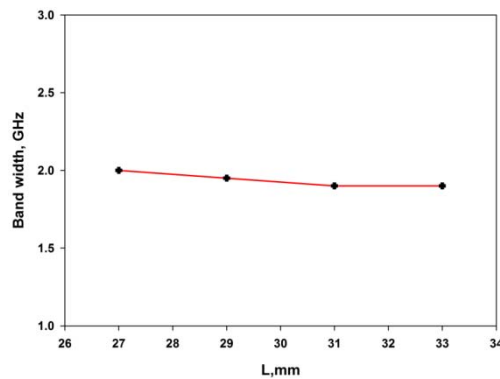
(b)

Fig. 4.27 Variations on return loss characteristics with drum dimension 'L_R'. [W_G = 67mm, L_G =35.5mm, W_M =3mm, W_R = 24mm, B_R = 8mm, d = 6.5mm, g =1.5mm h=1.6mm and ε_r =4.4]

It is found from the analysis that the first resonance is affected much more than the second resonance with the L_R variation. As L_R increases from 27 to 33 mm ($0.37\lambda_g$ to $0.45\lambda_g$) the first resonance shifts from 1.9GHz to 1.6GHz while the second resonance 3.0GHz to 2.9GHz. This is because the resonant length corresponds to the first resonance highly depends on L_R. The bandwidth found to be almost stable with the length variation.

4.2.7.5 Influence of drum width 'W_R'

The effect of W_R over the returnloss characteristics are shown in Fig. 4.28.
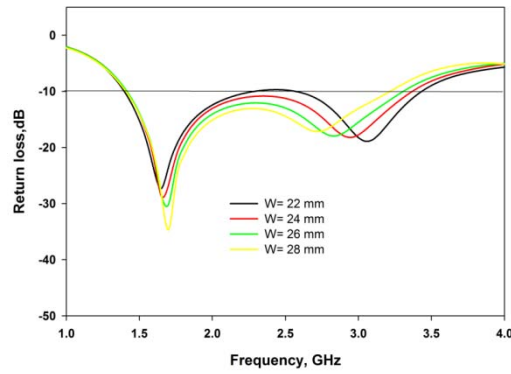
(a)
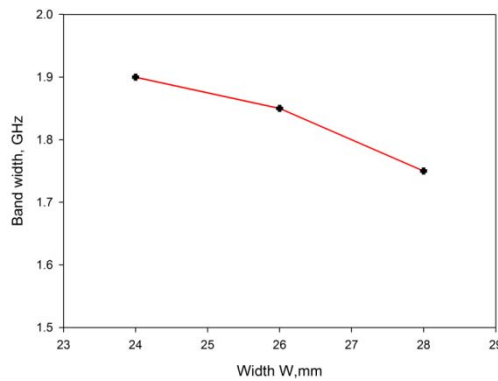
(b)

Fig. 4.28 The effect of returnloss characteristics with drum dimension W_R [W_G = 67mm, L_G =35.5mm, W_M =3mm, L_R =33mm, B_R = 8mm, d = 6.5mm, g =1.5mm h=1.6mm and ε_r =4.4]

It is observed from the plot that the second resonance is affected by the W_R variation as predicted by the surface current analysis in the previous section. As W_R increases the second resonant frequency shifts to a lower frequency region. The drift in the first resonance is almost negligible compared to the second resonance. The band width found to be decreasing with increase in W_R.

4.2.7.6 Variations with central width 'B_R' of the patch:

The influence of central strip width is studied and plotted in Fig. 4.29
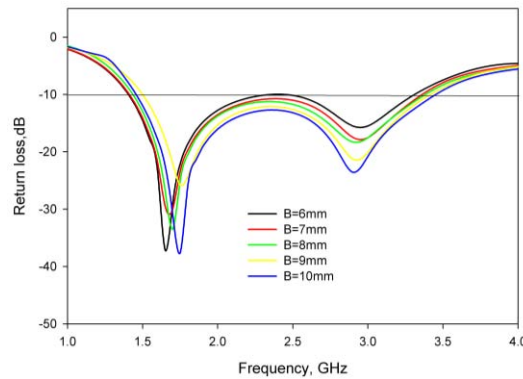
(a)
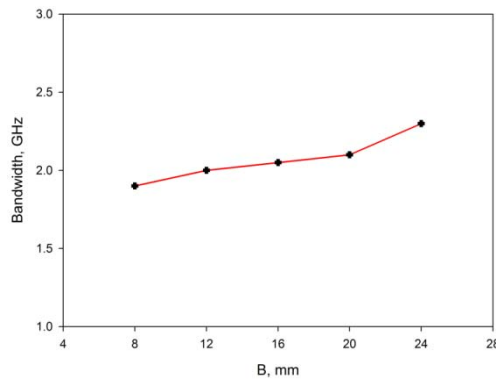
(b)

Fig. 4.29 Influence of central width 'B_R' of the antenna[W_G = 67mm, L_G =35.5mm, W_M =3mm, W_R = 24mm, L_R =33mm, d = 6.5mm, g =1.5mm, h=1.6mm and ε_r =4.4]

It is observed that the central width 'B$_R$' has a small influence on the first resonant frequency. Because as B$_R$ increases the first resonant length decreases and hence the first resonance shift to a higher frequency region. Compared to the first resonant frequency the second resonance is almost unaltered. The bandwidth of the antenna found to be increased as B$_R$ increases. For values of 'B$_R$' less than 7mm (0.01λ$_g$) the impedance matching at the center portion of the wide resonant band becomes poor.

4.2.7.7 Effect of substrate parameters

Parametric analysis of the substrate parameters – dielectric constant, ε$_r$ and height of the substrate, h are conducted and the results are extracted. The effect of relative permittivity over the antenna characteristics are studied and depicted in Fig. 4.30.
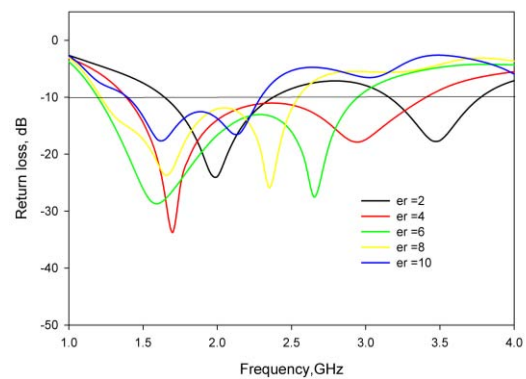
Fig. 4.30 (a)
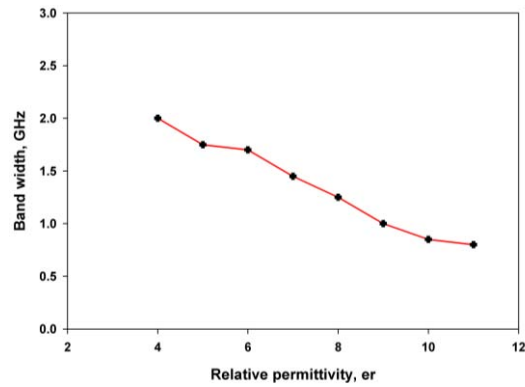
(b)

Fig. 4.30(Contd) Effect of relative permittivity over the return loss characteristics. [W_G = 67mm, L_G =35.5mm, W_M =3mm, W_R = 24mm, L_R =33mm, B_R = 8mm, d = 6.5mm, g =1.5mm, h=1.6mm]

The relative permittivity (ε_r) of the substrate material is varied from 2 to 11. It is found from the plot that the band width of the antenna decreases rapidly as ε_r increases. This is because of the increase of Q with dielectric constant. It is also found from the analysis that for the values of ε_r less than 4 the bandwidth of both the resonances decreases drastically and results in narrow band performance. The influence on substrate thickness is plotted in Fig. 4.31.
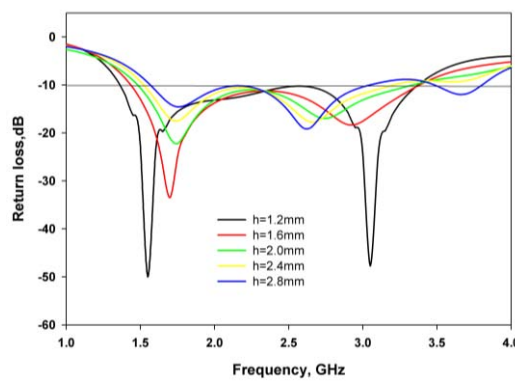
Fig.4.31 Effect of substrate height over the return loss characteristics [W_G = 67mm, L_G =35.5mm, W_M =3mm, W_R = 24mm, L_R =33mm, B_R = 8mm, d = 6.5mm, g =1.5mm and ε_r =4.4]

It is seen from the plot that the substrate height h has influence over the returnloss characteristics. As substrate height increases the device bandwidth will be less. It is noticed that the impedance matching at the centre portion becomes poor for higher values of substrate thickness.

4.2.8 Conclusions

A novel planar drum shaped monopole antenna is designed and experimentally verified. The current density analysis has made an insight into the resonance and radiation phenomena of the monopole antenna. Wide impedance bandwidth and omni-directional patterns with moderate gain are the striking features of the design. The characteristics of drum shaped antenna configurations are summarized in Table.4.3

Antenna Parameters	Electromagnetic excitation		Single layer
	Vertical orientation	Horizontal orientation	W_G = 67mm, L_G =35.5mm, W_M =3mm, W_R = 24mm, L_R =33mm, B_R = 8mm, d = 6.5mm, g =1.5mm and ε_r =4.4, h = 1.6mm
Antenna Geometry	L_G = 29mm, W_G = 67mm, L_m = 15mm, L = 33mm, W = 24mm, B = 8mm, P=(x = -10mm, y = 5.5mm), h = 1.6mm and ε_r = 4.4	L_G = 29mm, W_G = 67mm, L_m = 15mm, L = 33mm, W = 24mm, B = 8mm, P=(x = -2.5mm, y = -4.0mm), h = 1.6mm and ε_r = 4.4	
Band	1.69GHz-2.94GHz	1.71GHz-3.50GHz	1.46GHz-3.48GHz
Bandwidth	58%	68%	82%
Radiation	Nearly Omni-directional	Nearly Omni-directional	Nearly Omni-directional
Polarization	Linear Polaziation	Orthoganal polarization	Linear Polaziation
Peak Gain	3.25 dBi	4.9dBi	5.8dBi
Application Bands	AWS,DCS,PCS/DECT,PHS,3G,UMTS,DSR,Wi-Bro,Blue Tooth/ WLAN/WiBree/ZigBee, DMB	AWS,DCS,PCS/DECT,PHS,3G ,UMTS,DSR,Wi-Bro, BlueTooth /WLAN/WiBree/ZigBee, DMB	AWS,DCS,PCS/DECT,PHS,3G,UMTS,DSR,Wi-Bro, BlueTooth/WLAN/ WiBree/ZigBee, DMB

Table.4.3: Summary of drum shaped antenna configurations.

4.3 Development of a wideband funnel shaped antenna

This module of the chapter discusses the development and analysis of a funnel shaped monopole antenna that operates from 1.68 GHz to 4.9 GHz, covering major wireless communication bands like AWS, DCS, DECT, PCS, PHS, 3G, UMTS, DSR, Wi.Bro, ISM and DMB.

4.3.1   Antenna geometry

The geometry and dimension of the funnel shaped monopole antenna is illustrated in Fig. 4.32.
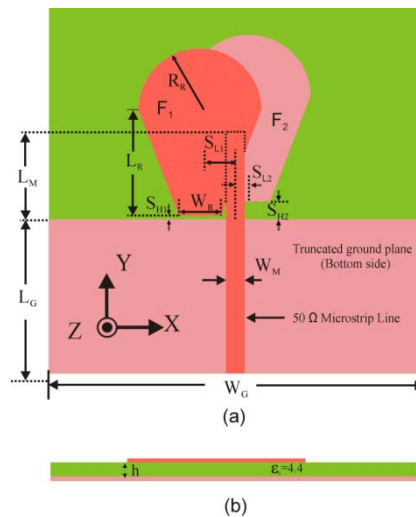
Fig. 4.32 Geometry and optimized dimensions of the proposed antenna [W_G = 67, L_G = 29, L_M = 15, W_M = 3, W_R = 7.5, L_R = 19, R_R = 11, S_{H1} = 0.3, S_{L1} = 6.5, S_{H2} = 3, S_{L2} = 5.25, h = 1.6 (Units in mm), ε_r = 4.4]

The proposed antenna comprises of a 50Ω microstrip line feed, strip monopole of length L_M = 0.164λ (15mm) and width W_M = 3mm (same as the width of 50Ω microstrip line) with a funnel shaped patch F_1 and a similar patch F_2

118

electromagnetically coupled to the monopole on other side of the substrate. The antenna is etched on a substrate of relative permittivity $\varepsilon_r = 4.4$ and thickness h = 1.6mm. The radiating patches have a base width $W_R = 0.082\lambda$ (7.5mm), length $L_R = 0.208\lambda$ (19mm) and the radius of curvature $R_R = 0.121\lambda$ (11mm), where λ is the free space wave length corresponding to the mean frequency (f_c) in the band.

4.3.2   Return loss Characteristics

Fig. 4.33 shows the simulated and measured return loss characteristics of the strip monopole, strip monopole with patch F_1 and the strip monopole with patch F_1 and F_2 respectively. The measurement confirms the wideband characteristic of the proposed antenna, as predicted in the simulation.
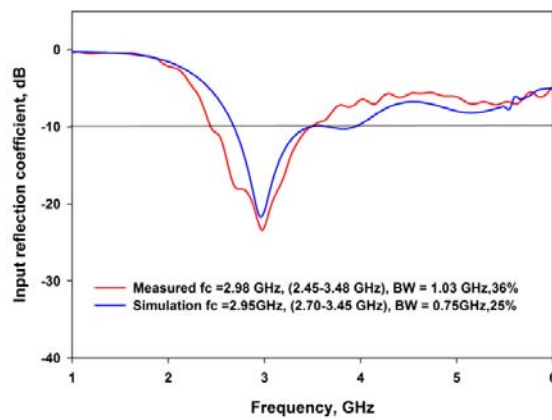
Fig. 4.33(a)
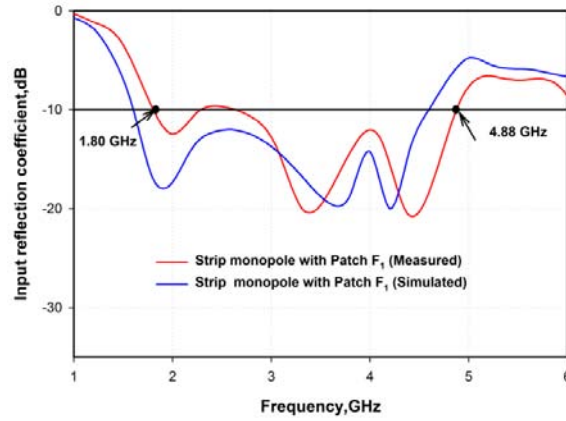
(b)
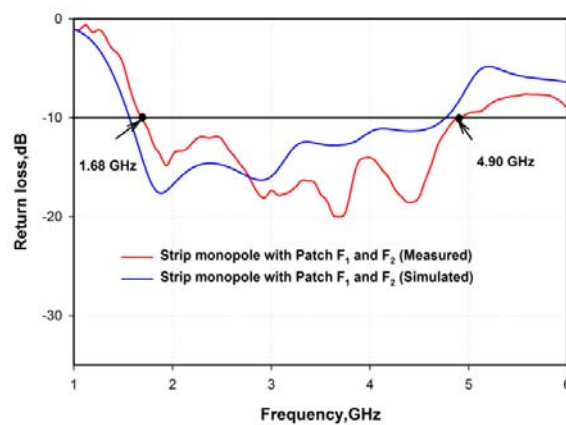
(c)

Fig. 4.33(contd): Measured and simulated return loss characteristics of the proposed antenna a) Strip monopole alone [W_G = 67, L_G = 29, L_M = 15, W_M = 3, h = 1.6 (Units in mm), ε_r = 4.4] b) Strip monopole with Patch F_1 [W_R = 7.5, L_R = 19, R_R = 11, S_{H1} = 0.3, S_{L1} = 6.5, (Units in mm)] c) Strip monopole with patch F_1 and F_2 [S_{H2} = 3, S_{L2} = 5.25(Units in mm)]

The strip monopole with the truncated ground plane resonates at 2.9 GHz with a 2: 1 VSWR band width of 34.8%. It is clear from Fig. 4.33 (b) and 2(c) that the influence of the patch F_2 is predominant at the low frequency region (around 2.5 GHz). The lower cutoff frequency is also lowered by the introduction of the

patch F$_2$. It can be seen that the proposed structure exhibits a 2:1 VSWR band from 1.68 GHz - 4.9 GHz with 98% bandwidth at mean frequency (f$_c$) of 3.29 GHz, satisfying the present day requirements of communication channels.

4.3.3 Current distribution

A more insightful understanding of the proposed antenna behavior can be obtained by analyzing the current distributions at different frequencies depicted in Fig. 4.34

(a)   (b)

(c)   (d)

121

(e)   (f)
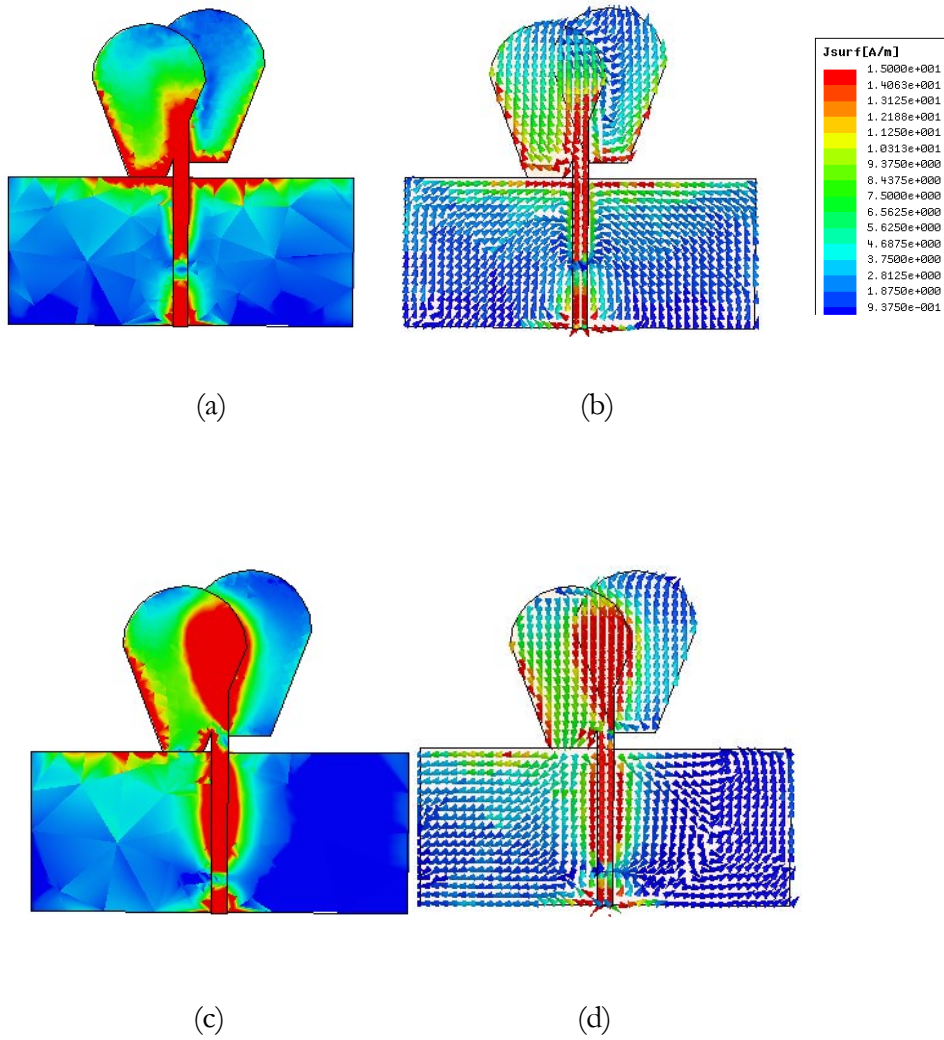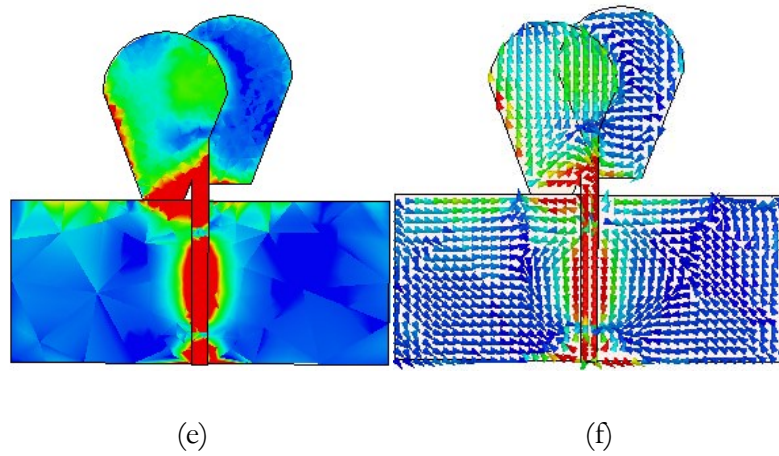
Fig. 4.34 Simulated current distributions of the proposed antenna at (a) 1.7 GHz magnitude (b) 1.7 GHz vector (c)3.2 GHz magnitude (d) 3.2 GHz vector (e) 4.5 GHz magnitude (f)4.5GHz vector [W_G = 67, L_G = 29, L_M = 15, W_M = 3, W_R = 7.5, L_R = 19, R_R = 11, S_{H1} = 0.3, S_{L1} = 6.5, S_{H2} = 3, S_{L2} = 5.25, h = 1.6 (Units in mm), ε_r = 4.4]

It is evident from Fig. 4.34 (a)-(b) that at lower frequencies all the antenna elements are contributing for the radiation. In the middle frequency region (around 3.2 GHz, Fig. 4.34 c- d) strip monopole and patch F_1 contribute strongly to the radiation, while patch F_2 improves the overall impedance matching. At the higher frequency second harmonic on the strip (Fig. 4.34 e- f) is responsible for the radiation.

4.3.4 Radiation pattern:

The measured radiation patterns of the funnel shaped antenna in the X-Z and Y-Z planes at 1.7 GHz, 1.8 GHz, 2.4 GHz and 4.9 GHz are illustrated in Fig. 4.35

(a)

(b)

(c)

(d)

(e)   (f)

(g)   (h)
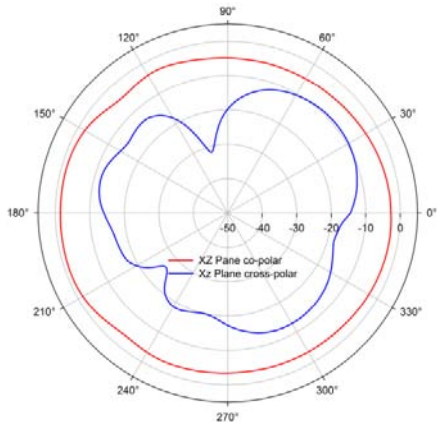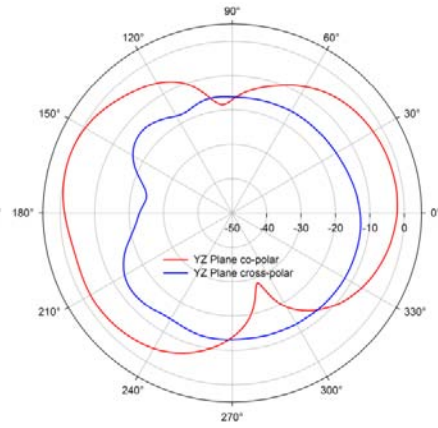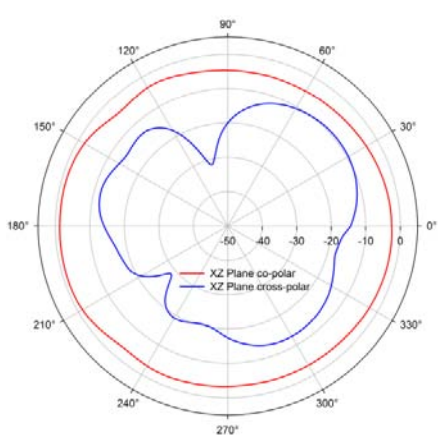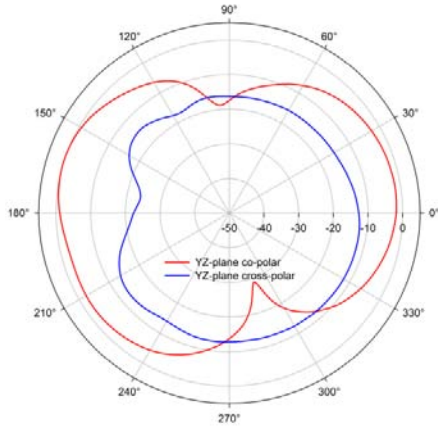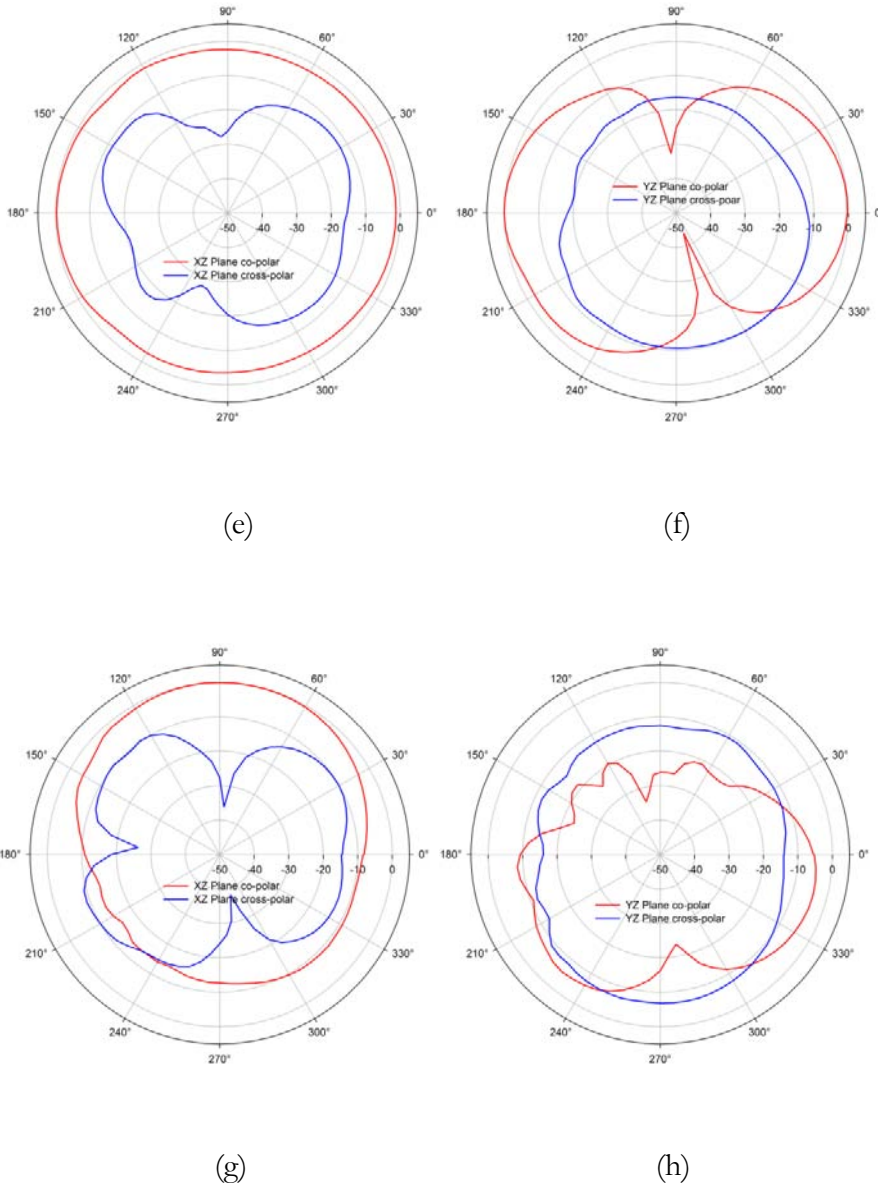
Fig. 4.35 Measured radiation patterns of the proposed antenna (a)-(b) 1.7 GHz (c) –(d)1.8 GHz (e) –(f)2.4 GHz (g)-(h) 4.9 GHz [W_G = 67, L_G = 29, L_M = 15, W_M = 3, W_R = 7.5, L_R = 19, R_R = 11, S_{H1} = 0.3, S_{L1} = 6.5, S_{H2} = 3, S_{L2} = 5.25, h = 1.6 (Units in mm), ε_r = 4.4]

It is seen from the plot that the antenna offers nearly similar radiation patterns throughout the band, except at the higher band edge. The pattern is

124

found to be nearly circular along the X–Z plane and figure-of-eight shape in the Y–Z plane. Thus the presence of funnel shaped patches has resulted in enhancing the impedance bandwidth of single monopole antenna, without deteriorating its radiation performance.

4.3.5 Polarization:

The far field transmission characteristic of the wideband antenna is illustrated in Fig. 4.36.
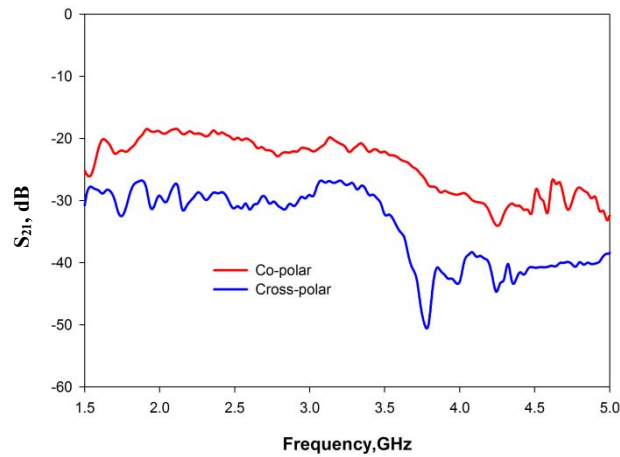
Fig. 4.36 Transmission characteristics of the funnel shaped monopole antenna[W_G = 67, L_G = 29, L_M = 15, W_M = 3, W_R = 7.5, L_R = 19, R_R = 11, S_{H1} = 0.3, S_{L1} = 6.5, S_{H2} = 3, S_{L2} = 5.25, h = 1.6 (Units in mm), ε_r = 4.4].

It is found from the transmission characteristics that the antenna provides linear polarization throughout the operating band

4.3.6 Gain and efficiency:

The gain measurements are carried out using Vector Network Analyzer HP 8510c by gain transfer method with standard antenna. Measured antenna gains in different bands are listed in Table 4.4

Band	Measured Gain at the center frequency of the band, dBi (Gain Transfer Method)
AWS (1710-1755 MHz)	2.7
AWS (2110-2115 MHz)	3.7
DCS (1710-1880 MHz)	4.0
DECT(1880-1900 MHz)	4.6
PCS (1850-1990 MHz)	5.3
PHS (1905-1920 MHz)	5.0
3G (1920-2170 MHz)	4.0
UMTS (1920-2180 MHz)	3.5
DSR (2290-2300 MHz)	3.1
Wi.Bro (2300-2390 MHz)	3.6
ISM (2400-2485 MHz)	4.5
DMB (2605-2655 MHz)	4.6

Table.4.4. Measured Gain of the proposed antenna in different bands
[$W_G = 67$, $L_G = 29$, $L_M = 15$, $W_M = 3$, $W_R = 7.5$, $L_R = 19$, $R_R = 11$, $S_{H1} = 0.3$, $S_{L1} = 6.5$, $S_{H2} = 3$, $S_{L2} = 5.25$, $h = 1.6$ (Units in mm), $\varepsilon_r = 4.4$]

It is seen from the table that the antenna offers reasonable gain over the entire band of operation. High gain in PCS and PHS band is due to monopole radiation aided by current distribution on funnel shaped geometry.

The radiation efficiency of the proposed monopole antenna is determined using Wheeler Cap method. The average efficiency of the antenna is found to be around 85 %.

4.3.7 Parametric Analysis:

A parametric analysis, investigating the effect of each antenna elements over the antenna characteristics is conducted and the results are as follows,

4.3.7.1 Effect of the position of the funnel patches

The effects of the position of the patch F1 is depicted in Fig. 4.37

(a)

(b)
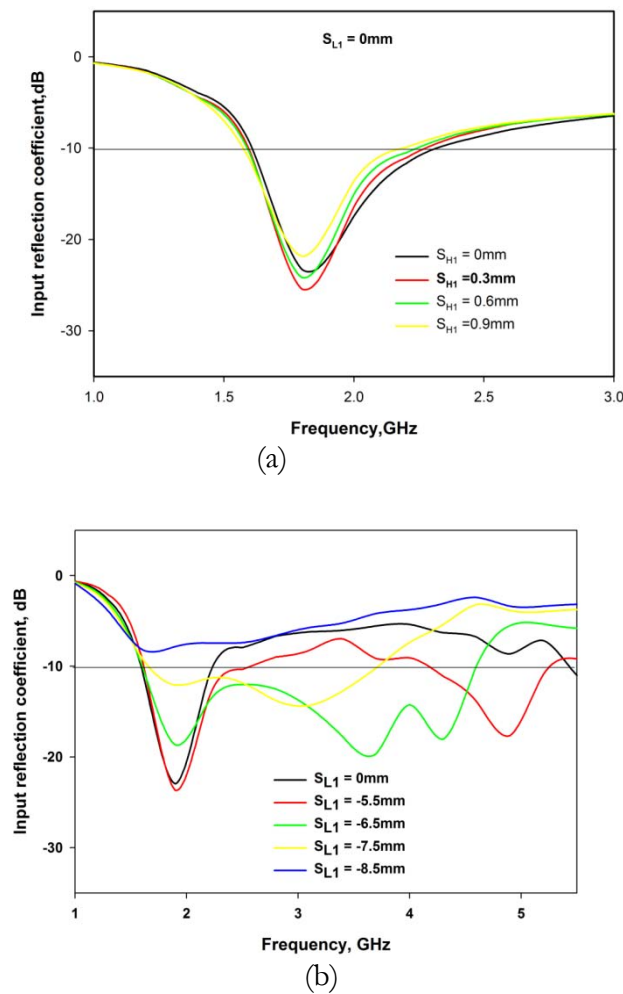
Fig. 4.37 Effect of position of patch F_1 on return loss characteristics [W_G = 67, L_G = 29, L_M = 15, W_M = 3, W_R = 7.5, L_R = 19, R_R = 11, S_{H1} = 0.3, h = 1.6 (Units in mm), ε_r = 4.4]

It is found from the analysis that, slight offset of patch F_1 is required for the optimum bandwidth. Patch F_1 placed symmetrically over the strip monopole offered low impedance bandwidth. From the exhaustive simulations of the offset parameters S_{H1} and S_{L1}, the optimum position of F_1 was identified. In the present design, the optimum offset parameters are $S_{H1} = 0.003\lambda$ and $S_{L1} = 0.071\lambda$.
The effect of patch position F2 is studied by placing the patch F1 in the optimized location and is illustrated in Fig. 4.38
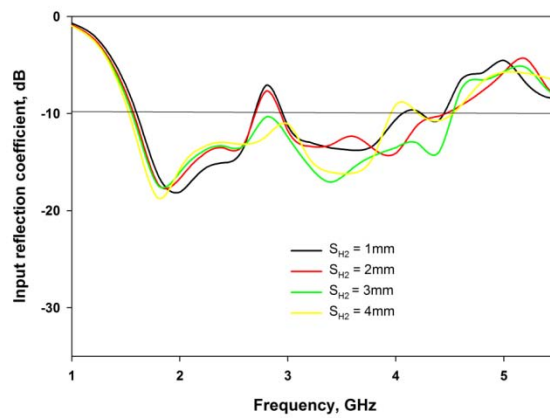
(a)   Effect of S_{H2}
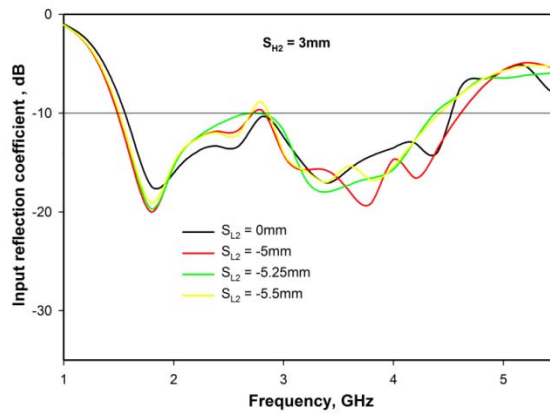
(b) F2 in the same direction as F1
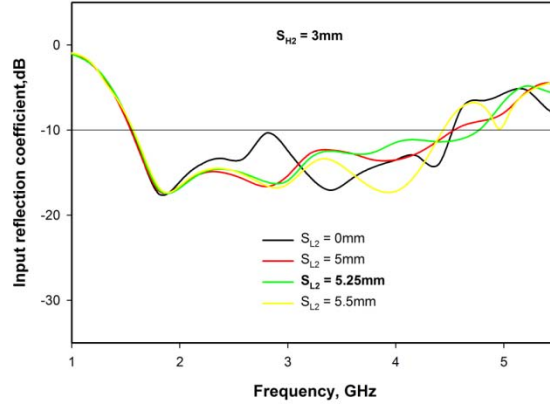
(c)F2 offset in the opposite direction to F1

Fig. 4.38 Effect of position of patch F_2 on return loss characteristics [$W_G = 67$, $L_G = 29$, $L_M = 15$, $W_M = 3$, $W_R = 7.5$, $L_R = 19$, $R_R = 11$, $S_{H1} = 0.3$, $S_{L1} = 6.5$, $S_{H2} = 3$, h = 1.6 (Units in mm), $\varepsilon_r = 4.4$]

It is clear from Fig. 4.38 that the optimum bandwidth is obtained when S_{H2} = 0.033λ and $S_{L2} = 0.057\lambda$, with F_2 offset in the direction opposite to that of F_1.

Moreover, under this condition the excited field distribution is in such a way that more fringing electric field is available on the periphery of the geometry and hence the radiation efficiency is more. On the other hand, if the patch F_2 is moved along the same direction as patch F_1, the electric field becomes weak along the periphery. Thus reducing the fringing effect and resulting in low radiation efficiency. This is clearly demonstrated in Fig. 4.39 (a) and (b).
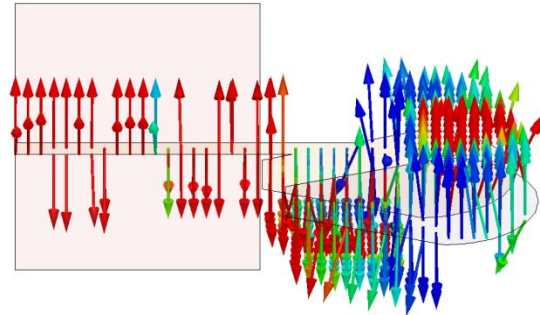
(a)
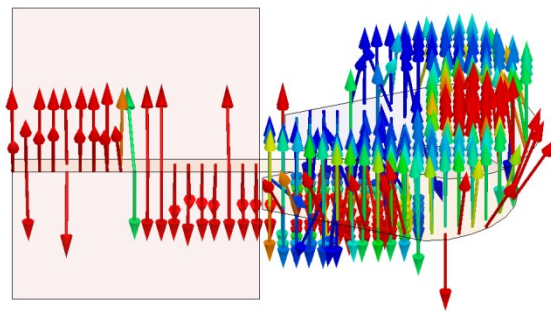
(b)

Fig. 4.39 Electric field distribution in the antenna at center frequency (a) patch F_2 in the same direction as patch F1, (b) patch F_2 in the opposite direction.

4.3.7.2 Effect of ground plane dimensions:

The effect of ground plane dimensions L_g and W_g are illustrated in Fig. 4.40.
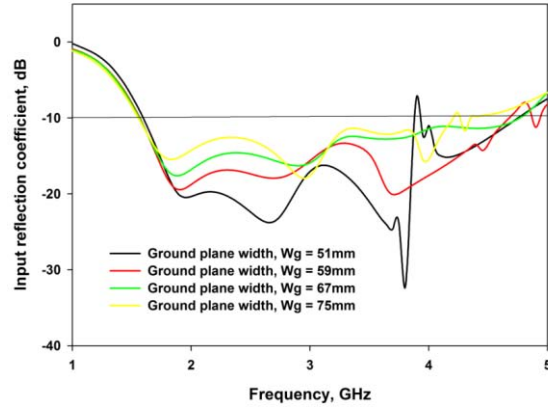
(a)
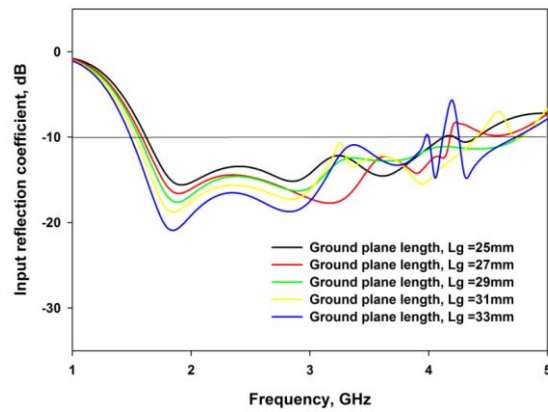
(b)

Fig. 4.40 Effect of ground plane dimensions on the return loss characteristics) W_G variation b) L_G variation [L = 67, L_M = 15, W_M = 3, W_R = 7.5, L_R = 19, R_R = 11, S_{H1} = 0.3, S_{L1} = 6.5, S_{H2} = 3, S_{L2} = 5.25, h = 1.6 (Units in mm), ε_r = 4.4]

The analysis reveals that the ground plane has only a feeble effect on return loss characteristics. However, it is clear from the analysis that the antenna offers maximum bandwidth performance for ground plane with a width of W_G = 0.735λ and length L_G = 0.318λ.

4.3.7.3 Effect of patch parameters:

The reflection characteristics of the antenna for different base width (W_R), radius of curvature (R_R), and length (L_R), are studied and the observations are listed in Table. 4.5, 4.6 & 4.7 respectively.

W_R (mm)	f_L- f_H (GHz)	Bandwidth (GHz)
5.5	1.45-4.1	2.65
6.5	1.45-4.2	2.75
7.5	1.5-4.5	3
8.5	1.55-4.85	3.3
9.5	1.55-3.15	1.6
	3.55-4.85	1.3
10.5	1.55-3.2	1.65
	3.45-4.95	1.5

Table. 4.5 Influence of patch parameter W_R over the antenna L = 67mm, W_G = 67mm, L_G = 29mm, L_M = 15mm, W_M = 3mm, S_{H1} = 0.3mm, S_{L1} = -6.5mm, S_{H2} = 3mm, S_{L2} = 5.25mm, ε_r = 4.4, h= 1.6mm, L_R = 19mm, R_R = 11mm, f_L- lower cut-off frequency and f_H – upper cut-off frequency

R_R (mm)	f_L- f_H (GHz)	Bandwidth (GHz)
7	1.75-3.25	1.5
	3.6-3.8	0.2
9	1.6-4.2	2.6
11	1.5-4.5	3
13	1.45-4.55	3.1
15	1.35-5.7	4.35
17	1.3-5.4	4.1
19	1.25-5.15	3.9

Table. 4.6 Influence of patch parameter W_R over the antenna[L = 67mm, W_G = 67mm, L_G = 29mm, L_M = 15mm, W_M = 3mm, S_{H1} = 0.3mm, S_{L1} = -6.5mm, S_{H2} = 3mm, S_{L2} = 5.25mm, ε_r = 4.4, h= 1.6mm, L_R = 19mm, W_R = 7.5 mm, f_L- lower cut-off frequency and f_H – upper cut-off frequency]

L_R (mm)	f_L- f_H (GHz)	Bandwidth (GHz)
15	1.65-5.35	3.7
17	1.55-4.6	3.1
	4.75-4.95	0.2
19	1.5-4.5	3
21	1.45-4.25	2.8

Table. 4.7 Influence of patch parameter W_R over the antenna[L = 67mm, W_G = 67mm, L_G = 29mm, L_M = 15mm, W_M = 3mm, S_{H1} = 0.3mm, S_{L1} = -6.5mm, S_{H2} = 3mm, S_{L2} = 5.25mm, ε_r = 4.4, h= 1.6mm, R_R = 11mm, W_R = 7.5 mm, f_L- lower cut-off frequency and f_H – upper cut-off frequency

It has been found that by increasing the base width W_R, the operating band can be shifted to higher frequency region with considerable increase in bandwidth up to W_R = 8.5mm (0.093λ). There after exhibiting dual band behavior. Improvement in impedance bandwidth is observed while increasing the radius of curvature R_R, till 15mm (0.165λ). The increase of R_R from 9mm to 15mm (0.099λ to 0.165λ) results an improvement in band width from 90% to 123%. Further increase in R_R, cause decrease in bandwidth. As the length L_R increases, the operating band is shifted to the lower frequency side. It is also found that increasing W_R and L_R results improvement in impedance matching of lower resonant frequency and lowers that of the upper resonant frequency.

4.3.7.4 Influence of Substrate parameters:

The influence of substrate parameters are illustrated in Table. 4.8.

h (mm)	ε_r	$W_{M(mm)}$	f_L- f_H (GHz)	Bandwidth (GHz)
0.159	2.2	0.47	1.35-1.7	0.35
0.3	2.2	0.9	1.4-2 3.2-3.6	0.6
0.5	2.2	1.5	1.5-2.35 2.8-4.1	0.85 1.3
0.8	2.2	2.45	1.5-5	3.5
1.6	2.2	4.9	1-3.79 4.87-6.58	2.79 1.71
0.159	4.4	0.3	1.3-1.55	0.25
0.3	4.4	0.55	1.3-1.65	0.35
0.5	4.4	0.94	1.35-1.9 2.35-3.2	0.55 0.85
0.8	4.4	1.5	1.4-3.8	2.4
1.6	4.4	3	1.5-4.5	3

Table. 4.8 Influence of patch parameter W_R over the antenna[L = 67mm, W_G = 67mm, L_G = 29mm, L_M = 15mm, W_M = 3mm, S_{H1} = 0.3mm, S_{L1} = -6.5mm, S_{H2} = 3mm, S_{L2} = 5.25mm, ε_r = 4.4, h= 1.6mm, R_R = 11mm, W_R = 7.5 mm, f_L- lower cut-off frequency and f_H – upper cut-off frequency]

It is observed from the analysis that as ε_r varies from 2.2 to 4.4 the band width of the antenna is found to be reduced to a lower value due to the high Q of the device. The substrate height variation indicate that the for higher substrate height the resonant band found to be broadened.

4.3.8 Conclusions:

A novel funnel shaped monopole antenna fed by microstrip line capable of serving the needs of new generation mobile applications is developed. It has been seen that the resonance behavior of the antenna is dependent on the antenna parameters such as the dimensions of the patch and the position of the patches relative to the monopole. Wide impedance bandwidth and omni-directional patterns with moderate gain are the striking features of the design.

4.4 Development of a Shorted Coplanar Antenna

Electronic devices have become an inevitable part of modern life. We are always surrounded by the electromagnetic waves emitted from a variety of fixed and mobile wireless devices. The development of a compact, uni-planar antenna with nearly good radiation coverage serves as an important candidate for present and future communication systems.

This module presents the outcome of the exhaustive investigations performed on the development of a compact coplanar antenna with nearly omni-directional radiation characteristics for wireless communication devices from a balanced coplanar transmission line. The conventional Coplanar Wave Guide(CPW) fabricated on a dielectric substrate consists of a center strip conductor with semi-infinite ground planes on either side. This structure supports a quasi-TEM mode of propagation and it offers several advantages including ease of fabrication, easy surface mounting of active and passive devices and the ground plane between two adjacent lines make CPW ideally suited for MIC as well as MMIC applications. In the present design of the compact antenna, Finite Ground CPW (FGCPW) is developed as an efficient radiator.

This module highlights the evaluation of a efficient broad band radiator from a coplanar waveguide(CPW). First part of this chapter includes results of investigations carried out to study the chance of radiation in the open ended, finite ground coplanar waveguide. The second part of the section provides the development and analysis of a shorted coplanar waveguide from a balanced open ended CPW. The results of these investigations explain the transition from a wave guiding device to an efficient radiator.

4.4.1 Resonance and radiation behavior of open ended FGCPW.

The conventional Finite Ground CPW(FGCPW) design with characteristics impedance of 50Ohm, printed on an FR4 substrate of $\varepsilon_r = 4.4$ and h = 1.6mm employed in the present study. The top and cross sectional view of the system is illustrated in Fig. 4.41
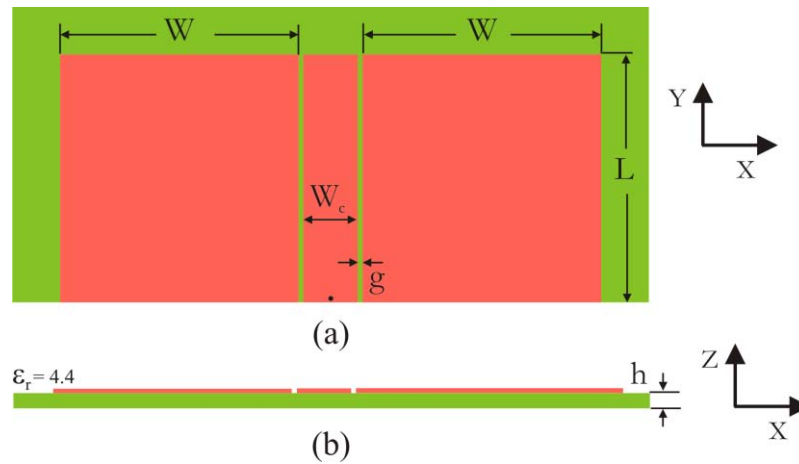
Fig. 4.41 Geometry of the open ended FGCPW.(a) Topview (b) Sideview[L = 26mm, W = 25mm, , W_c = 5.7mm, g = 0.5mm, h = 1.6mm and ε_r = 4.4]

The measured return loss curve of the above structure plotted in Fig. 4.42 reveals that the transmission line can transfer microwave energy efficiently in the lower frequency region. That is the open circuited transmission line is not resonating in the 1-6 GHz band. Most of the energy is reflected backwards.
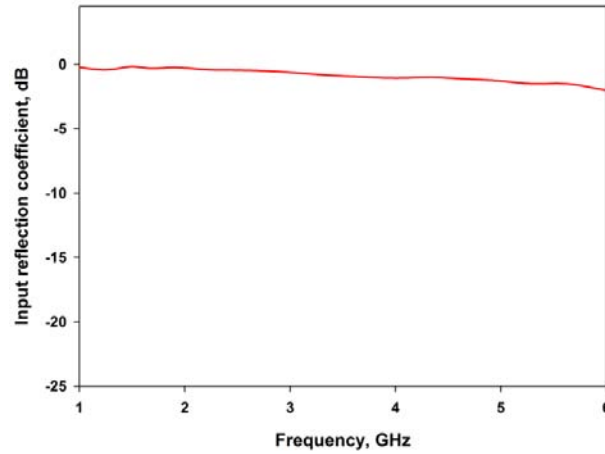
Fig. 4.42 Returnloss characteristics of the open ended FGCPW[L = 26mm, W = 25mm, W_c = 5.7mm, g = 0.5mm, h = 1.6mm and ε_r = 4.4]

4.4.2 Antenna Geometry

The geometry of the antenna consists of a Finite Ground Coplanar Waveguide fabricated on a substrate of thickness h and relative permittivity ε_r =4.4. The coplanar wave guide is designed with standard design equations for an impedance of 50Ω and the designed dimensions of the transmission line are Wc = 5.7mm and g = 0.5mm with finite ground dimensions are selected as L_g = 0.31λ_g (26mm) and W_g = 0.30 λ_g (25mm). The top and side view of the antenna geometry is illustrated in Fig. 4.43. Here one end of the signal line is shorted to one end of the ground plane and the signal is fed to the system at the other end.
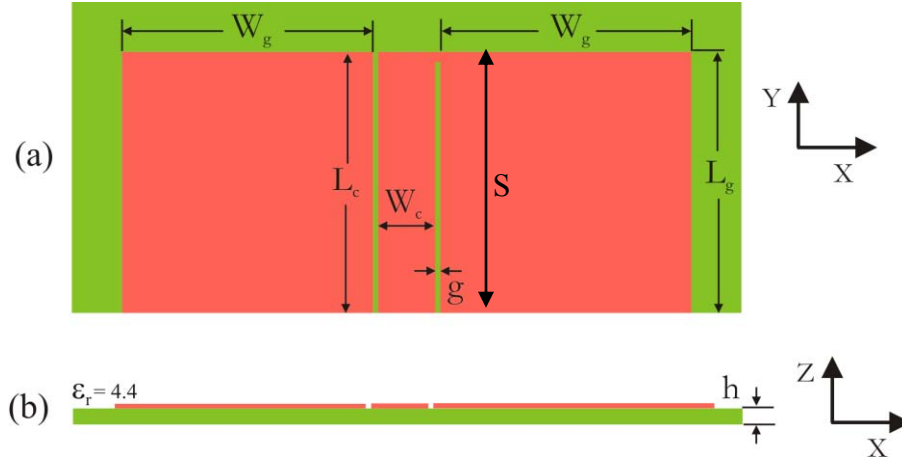
Fig.ure 4.43: Geometry of the proposed shorted FGCPW antenna.(a)Top view (b) Side view [L_g=26mm, W_g=25mm, L_c=26mm, W_c = 5.7mm, g =0.5mm, S =26mm, h = 1.6mm and ε_r = 4.4]

4.4.3 Returnloss Characterestics:

The returnloss characteristics (S_{11}) of the above described antenna configuration is shown in Fig. 4.44. The antenna exhibits resonance at 2.19 GHz, with the 2:1 VSWR band from 1.65 GHz to 2.80 GHz and a fractional bandwidth of 53%. The simulated S_{11} parameter of the antenna is illustrated in the same figure for comparison.
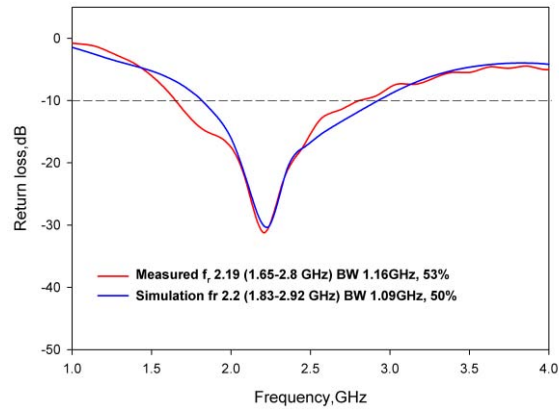
Fig. 4.44 Measured and simulated returnloss characteristics of the shorted FGCPW[L_g=26mm, W_g=25mm, L_c=26mm, W_c = 5.7mm, g =0.5mm,S =26mm, h = 1.6mm and ε_r = 4.4]

(a)   (b)
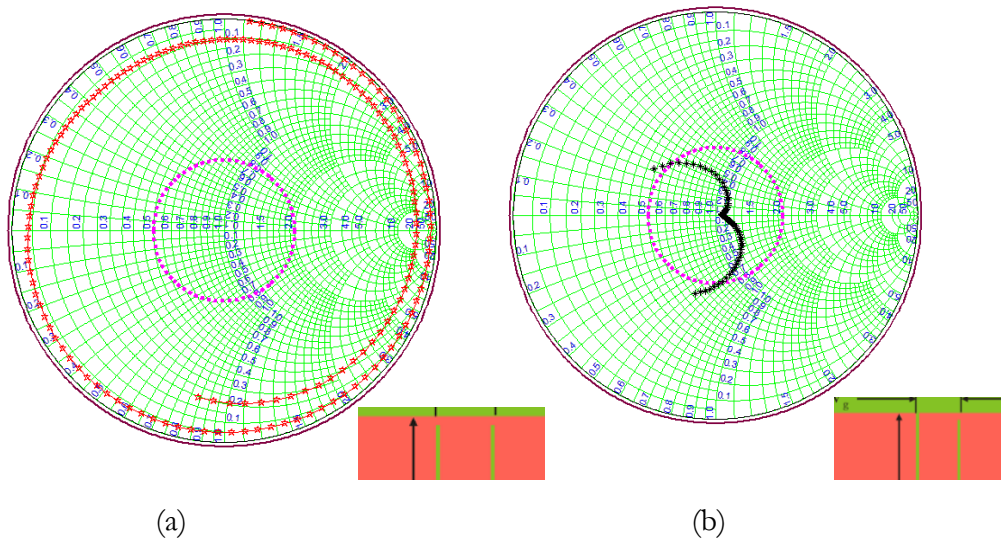
Fig. 4.45 Impedance plot of (a) symmetrically shorted FGCPW (b) Asymmetrically shorted FGCPW [L_g=26mm, W_g=25mm, L_c=26mm, W_c = 5.7mm, g =0.5mm,S =26mm, h = 1.6mm and ε_r = 4.4]

The impedance plot of the symmetrically shorted and that of proposed, asymmetrically shorted FGCPW are illustrated in Fig. 4.45. It is evident from the plot that the symmetrically shorted FGCPW is not resonating in the 1-6GHz band while the asymmetric short in the FGCPW results resonance at 2.2 GHz

4.4.4   Current distribution and radiation behavior

The surface current of the proposed antenna and that of an open ended coplanar waveguide, computed at the resonance is illustrated in Fig. 4.46. It is clear from the plot depicted in Fig.4.46 a, that the open ended coplanar waveguide has balanced current distributions at the resonance. The current distribution on either side of the gap between the center conductor and ground plane are equal in magnitude and opposite in direction. Therefore the field distribution in the far field will cancel out and results no radiation from the open ended coplanar waveguide.

The surface current distribution of the shorted CPW of same dimension is illustrated in Fig. 4.46 b. It is worth to note that the balanced current distribution in the non-radiating open-ended CPW has become unbalanced by the introduction of the short at the open end. This unbalance in the current distribution results reinforcement of the field at far field, which results radiation. Therefore the balanced CPW can act as an efficient radiator by introducing a short at the open-end.

The polarization of the proposed antenna can be predicted by analyzing the current distribution at the resonant frequency. A close examination in the current distribution reveals that the direction of the current vector at the top portion of the antenna is addictive in nature which results a horizontally polarized electromagnetic radiation.

The resonant length of the antenna is identified from the current distribution and it corresponds to $L_g + 2*W_g + \Delta = \lambda g$ where λg is effective wave length in the substrate.
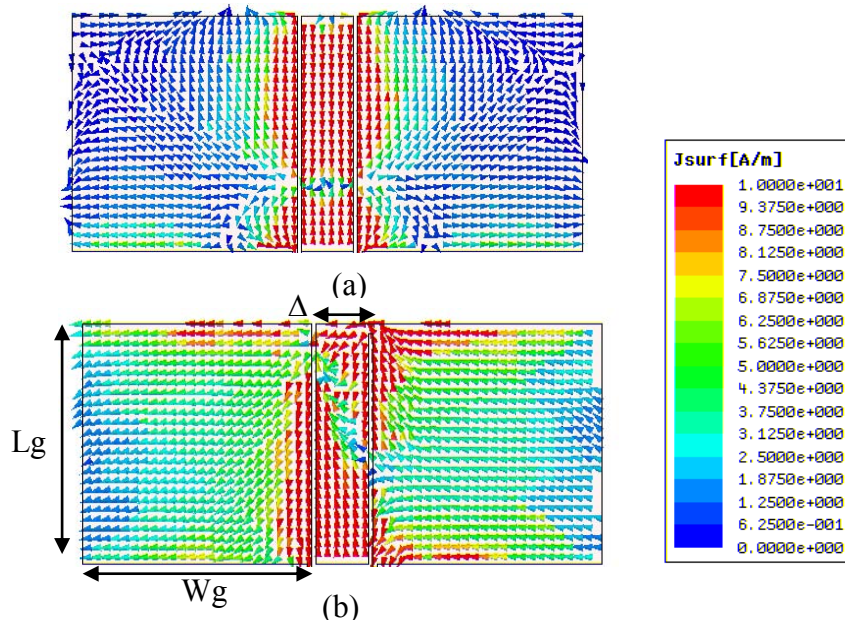
Fig. 4.46: Comparison of surface currents of the proposed antenna and open ended coplanar waveguide. (a) open CPW (b) Shorted CPW[L_g=26mm, W_g=25mm, L_c=26mm, W_c = 5.7mm, g =0.5mm,S =26mm, h = 1.6mm and ε_r = 4.4]

4.4.5   Polarization:

The transmission characteristics are measured at far field region with a highly linearly polarized horn antenna at bore-sight. The plot provided in Fig.4.47
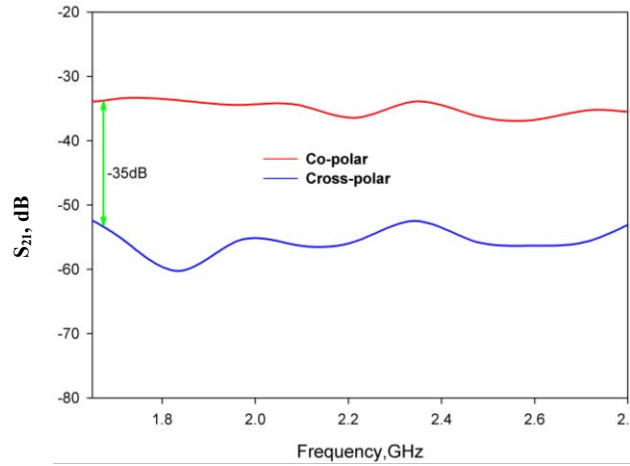
Fig.4.47 The S_{21} of the shorted FGCPW measured at far field [L_g=26mm, W_g=25mm, L_c=26mm, W_c = 5.7mm, g =0.5mm,S =26mm, h = 1.6mm and ε_r = 4.4]

It is clear from the plot that the device provides linearly polarized (x-polarization) radiation over the entire frequency region. The cross polarization level at the resonant frequency is observed to be better than 30dB.   The measurement results provide a concrete proof for the polarization predicted from the current density plot.

4.4.6   Radiation Pattern:

The 3D radiation pattern of the proposed coplanar antenna at the resonant frequency is computed through software simulation and plotted in Fig.4.48
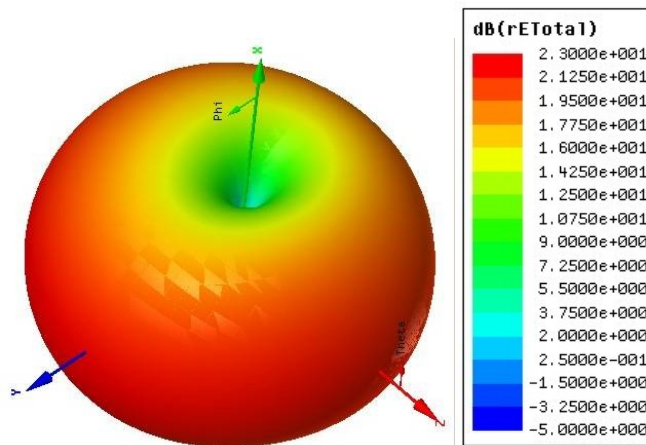
Fig.:4.48: Simulated 3D radiation pattern of the shorted FGCPW at the resonance frequency. [L_g=26mm, W_g=25mm, L_c=26mm, W_c = 5.7mm, g =0.5mm,S =26mm, h = 1.6mm and ε_r = 4.4]

The simulated 3D radiation pattern shown in the above Fig.ure reveals that the shorted FGCPW can provide good omni-directional radiation coverage suitable for wireless communication devices. It is worth to note that, compared to an open ended FGCPW resonating at a higher frequency mode, the shorted transmission line provides better radiation coverage.

The experimentally measured radiation patterns of the shorted Finite Ground coplanar antenna configuration at 2.19GHz are shown in the Fig. 4.49. The cross polarization along the maxima is better than 10dB in both the planes. The radiation along the YZ plane had broader radiation coverage compared to the XZ plane.
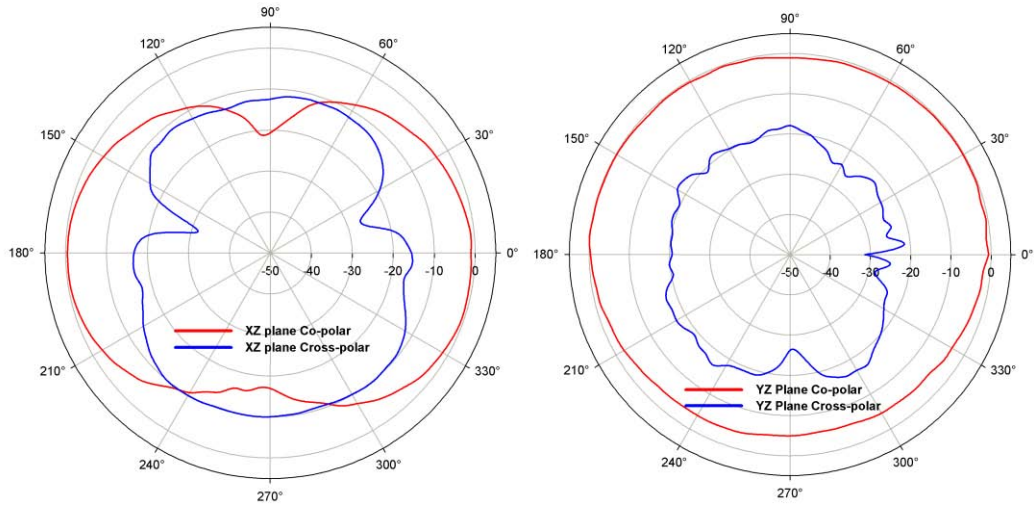
Fig. 4.49 Experimental radiation pattern of the shorted FGCPW at 2.19 GHz in two orthogonal planes, the resonant frequency in two orthogonal planes [L_g=26mm, W_g=25mm, L_c=26mm, W_c = 5.7mm, g =0.5mm,S =26mm, h = 1.6mm and ε_r = 4.4]

The radiation patterns are nearly omni-directional with isotropic radiation pattern in the YZ plane. Therefore the antenna can find applications in mobile communication systems.

4.4.7 Gain

The gain is measured using gain comparison method with the help of a standard horn antenna. The vector network analyzer, HP 8510c is used for the measurement. Fig. 4.50 depicts the measured gain of the antenna
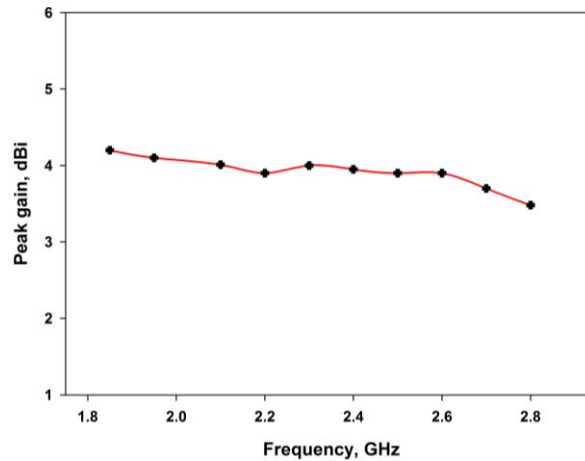
Fig. 4.50 Measured peak gain of the antenna [L_g=26mm, W_g=25mm, L_c=26mm, W_c = 5.7mm, g =0.5mm,S =26mm, h = 1.6mm and ε_r = 4.4]

It is understood from the measurement results that the shorted transmission line provides better gain compared to the open ended transmission line. The gain of the antenna remains almost stable throughout the operating band. Therefore the shorted transmission line can act as an effective radiator at the resonant frequency.

4.4.8   Parametric Analysis

In order to investigate the effect of various structural and substrate parameters, over the antenna characteristics, a parametric analysis is performed with the help of the simulation software. Results of the parametric analysis along with the concluding remarks for each study are depicted in the following sessions.

4.4.8.1 Effect of finite ground plane dimensions:

Effect of ground plane dimensions W_g and L_g are studied and conclusions are derived from the results.

4.4.8.1.1 Effect of Ground plane Width(W$_g$)

The finite ground plane width (W$_g$) of the shorted transmission line is varied from 20mm to 30mm (0.24λ_g to 0.36λ_g) to study its effect over the resonant frequency and bandwidth. The returnloss characteristics for different ground plane dimensions are depicted in Fig.4.51
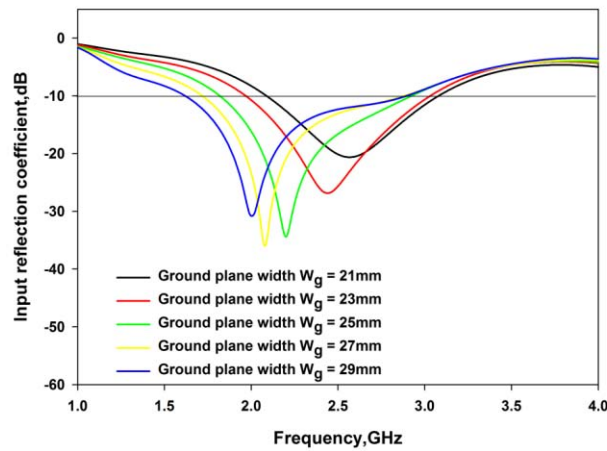
Fig. 4.51 Returnloss characteristics of the FGCPW antenna [L$_g$=26mm, L$_c$=26mm, W$_c$ = 5.7mm, g =0.5mm,S =26mm, h = 1.6mm and ε_r = 4.4]

It is observed from the returnloss characteristic that as W$_g$ varies from 20mmto 30mm (0.24λ_g to 0.36λ_g) the resonant band is found to be shifted to a lower resonant frequency region. This again conforms that the ground plane is also contributing for radiation.

(a)   (b)
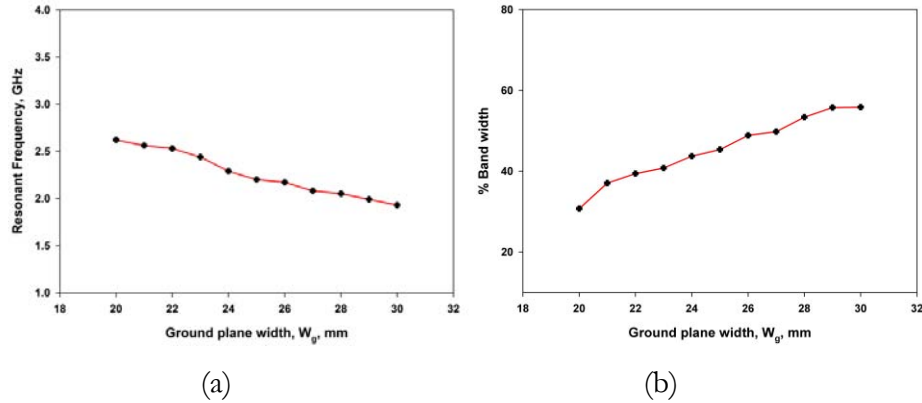
Fig. 4.52 Effect of finite ground plane width, wg, and variation of resonant frequency f_r of the shorted transmission line. [L_g=26mm, L_c=26mm, W_c = 5.7mm, g =0.5mm,S =26mm, h = 1.6mm and ε_r = 4.4]

It is observed from the parametric study that the width of the finite ground plane has reasonable effect over the resonant frequency. The variation of width from 20mm to 30mm (0.24λ_g to 0.36λ_g) results a frequency shift from 2.6 GHz to 1.9 GHz. This is because as W_g increases symmetrically, the resonant length increases two times and results rapid decrease in resonant frequency.

Influence of W_g over the bandwidth is also studied and illustrated in Fig.4.52b. It is found that as W_g increases from 20 mm to 30 mm (0.24λ_g to 0.36λ_g) the bandwidth varies from 30% to 58%.

4.4.8.1.2   Effect of Ground plane Length (L_g)

The influence of finite ground plane length, L_g is depicted in Fig. 4.53. A slight variation in resonant frequency is observed when the length of the ground plane varies from 20mm to 30mm (0.24λ_g to 0.36λ_g). It is observed that the

variation in L_g over the resonant frequency is feeble compared the frequency shift with W_g. This is because L_g contribute a small part in the total resonant length.
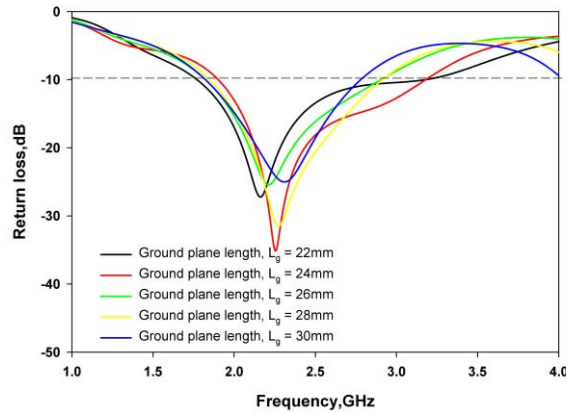
Fig. 4.53: Effect of Lg over the resonant frequency [W_g=25mm, L_c=26mm, W_c = 5.7mm, g =0.5mm,S =26mm, h = 1.6mm and ε_r = 4.4]

The influence of ground plane length over the bandwidth is plotted in Fig. 4.54.
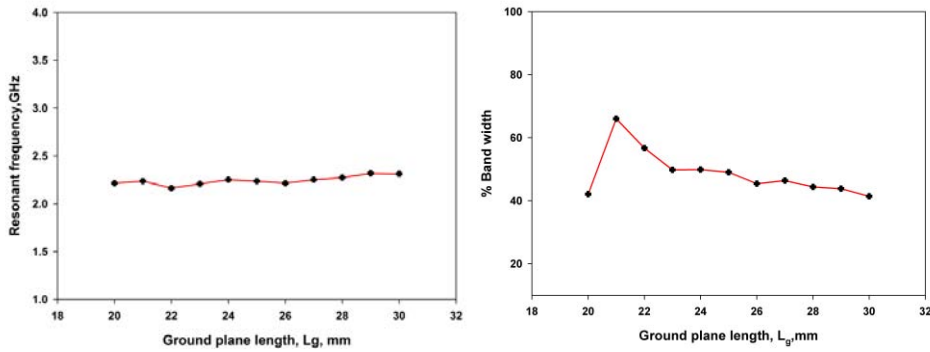
Fig. 4.54: Effect of lg over the bandwidth of the shorted FGCPW [W_g=25mm, L_c=26mm, W_c = 5.7mm, g =0.5mm,S =26mm, h = 1.6mm and ε_r = 4.4]

The analysis in the bandwidth variations with L_g reveals that as L_g varies from 21mm to 26mm ($0.25\lambda_g$ to $0.31\lambda_g$) a drastic variation in bandwidth occurred. The bandwidth remains quite stable thereafter.

4.4.8.2 Effect of Substrate parameters:

Parametric analysis of the substrate parameters – dielectric constant, εr and height of the substrate, h are conducted and the results are extracted.

4.4.8.2.1   Effect of dielectric constant of the substrate:

The dielectric constant of the substrate is varied from 2 to 12 to study its effect on returnloss characteristics of the radiator. Fig. 4.55 shows the variation in returnloss characteristics with εr and it is observed that the dielectric constant has a major effect over the returnloss.
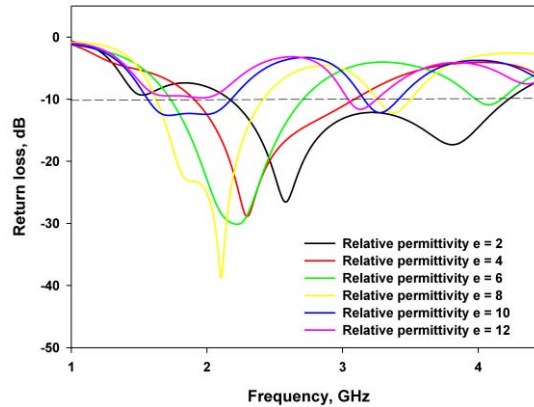
Fig. 4.55: Effect of dielectric constant over the returnloss characterestics and resonant frequency [L_g=26mm, W_g=25mm, L_c=26mm, W_c = 5.7mm, g =0.5mm,S =26mm and h = 1.6mm]

It is seen from the plot that as relative permittivity increases the resonant band is shifted to a lower frequency region. The corresponding variation in bandwidth is indicated in Fig. 4.56, which reveals that as dielectric constant of the

150

substrate moves from, 2 to 10 the bandwidth comes down from 65% to 35%. This may be because of the high value of Q as the dielectric constant of the substrate goes up.
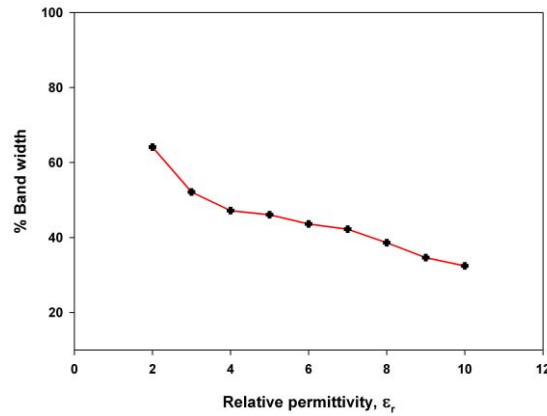
Fig.4.56 variation of banwidth with dielectric constant [L_g=26mm, W_g=25mm, L_c=26mm, W_c = 5.7mm, g =0.5mm,S =26mm and h = 1.6mm]

4.4.8.2.2   Effect of substrate thickness (h)

The effect of substrate thickness is depicted in Fig.4.57,
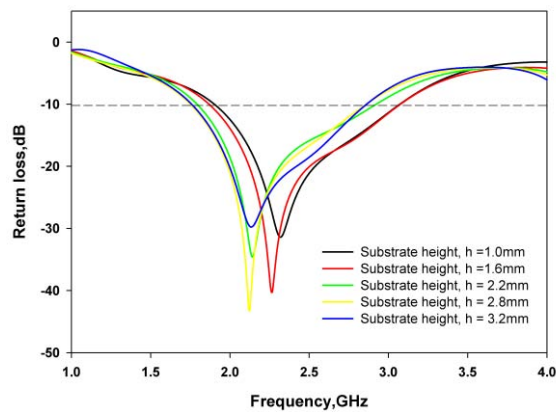
Fig. 4.54 (a)
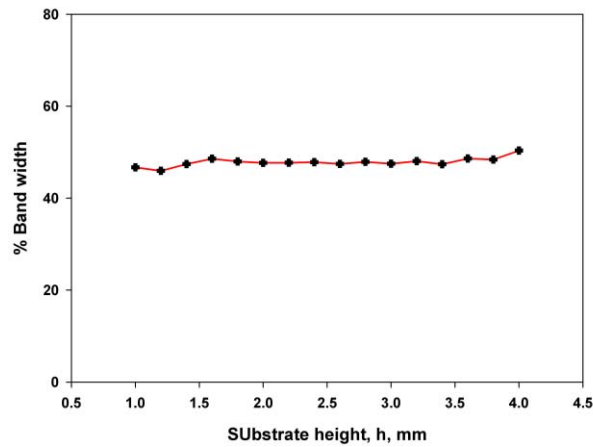
(b)

Fig. 4.57: Effect of substrate thickness over the returnloss characteristics, resonant frequency and bandwidth [L_g=26mm, W_g=25mm, L_c=26mm, W_c = 5.7mm, g =0.5mm,S =26mm and ε_r = 4.4]

The thickness of the substrate is varied from 1 to 4mm and observed that the variation in resonant frequency is only 250 MHz and the bandwidth is approximately 50MHz. Therefore the effect of substrate height has negligible effect on reflection characteristics and bandwidth.

4.4.8.3 Effect of shorting position:

The effect of shorting positions on the return loss characteristics of the antenna is depicted in Fig. 4.58 (a). Variation of the input impedance are plotted in Fig. 4.58.b.It is observed that the shorting position is affecting only the matching condition of the antenna.

Along the CPW line a standing wave pattern is generated. Depending on the location of the short its influence is tremendous. If the short is at the voltage minimum position the influence is minimum because short circuit has no effect. On the other hand if the short is placed at the voltage maximum, thus enforce the voltage to zero and hence the pattern is redistributed. This will effectively change the input impedance.

152
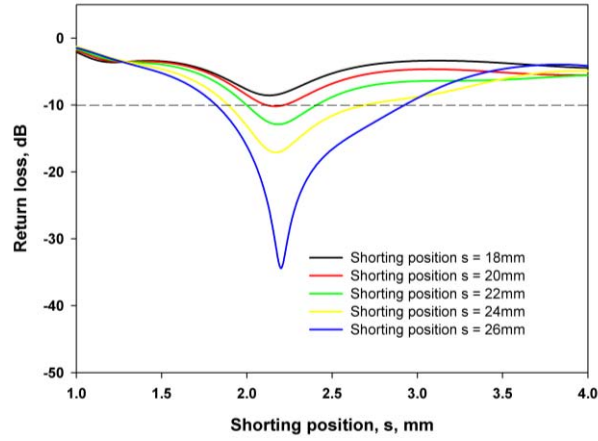
(a)
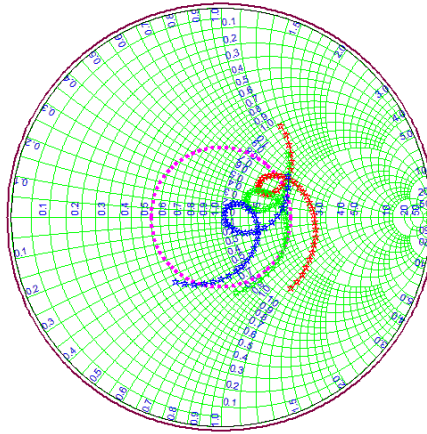
(b)

Fig.4.58 effect of shorting point (a)Return loss (b) input impedance variation [L_g=26mm, W_g=25mm, L_c=26mm, W_c = 5.7mm, g =0.5mm, h = 1.6mm and ε_r = 4.4]

The influence of s on the bandwidth performance of the antenna is depicted in Fig. 4.59. It is clear from the figure that the shoring point S significantly affects the bandwidth performance of the antenna. When S varies from 22mm to 26 mm ($0.26\lambda_g$ to $0.31\lambda_g$), the bandwidth of the antenna changes from 15% to 53 %. It can be concluded that the shorting point s is not affecting

153

the resonant frequency of the antenna significantly, but the impedance bandwidth characteristics is affected.
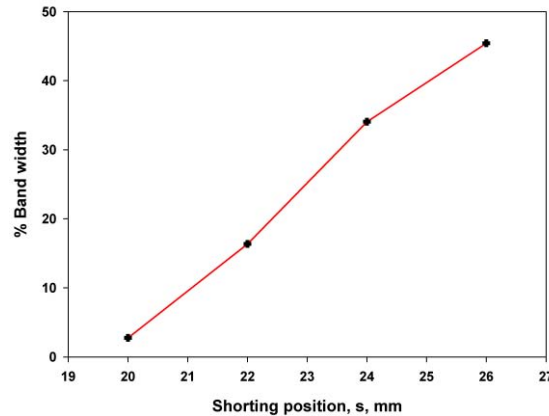
Fig. 4.59 Effect of shorting position on bandwidth [L_g=26mm, W_g=25mm, L_c=26mm, W_c = 5.7mm, g =0.5mm, h = 1.6mm and ε_r = 4.4]

4.4.9 Conclusions

The conclusions of the chapter are summarized below. These conclusions are used to design the wideband antenna element in the next chapter of the thesis.

1. An open circuited FGCPW has no resonance in the lower frequency band and not suitable for the application as an antenna.

2. An asymmetric short in the FGCPW can produce resonance in the lower frequency band while the symmetrically shorted FGCPW is not resonating in the 1-6GHz band.

3. The resonant length of the antenna is lg+2*wg+Δ = λg where λg is effective wave length in the substrate.

4. The impedance matching of the antenna is found to be get affected by the shorting position.

5   The current distribution reveals that the antenna provides horizontally polarized electromagnetic radiation.

6   The measured gain of the device is better than 3.5 dBi.

4.5 Development of a wideband coplanar antenna:

In order to address the wireless communication industry with a compact, wideband, omnidirectional antenna, investigations are carried out in the shorted coplanar antenna, discussed in the previous section[4.4] to improve the bandwidth while maintaining the compactness, radiation coverage and gain.

The analysis carried out in this module is summarized in table 4.9

Parameter	Measurements conducted
o finite ground dimensions (Lg,Wg)	Returnloss, Radiation Pattern, Current density plots, Gain and Efficiency
o Substrate parameters (ε_r, h)	
o shorting point(Gs)	
o Length of the center conductor(Lc)	
o Dimension of the shorting step	

Table 4.9 Summary of analysis

4.5.1 Antenna Geometry:

The geometry of the wideband coplanar antenna is illustrated in Fig. 4.60. The radiator is a uniplanar device whose cross sectional view is depicted in Fig. 4.60 b. It is fabricated on a substrate with dielectric constant $\varepsilon_r = 4.4$ and thickness h = 1.6mm. It is a 50 ohm shorted coplanar waveguide excited through a Sub Miniature Amphenol (SMA) connector. Various design parameters are gap, g = 0.5mm, Central conductor width, W_c = 5.7mm, Ground plane length, $L_g = 0.36\lambda_g$ (26mm), Ground plane width, $W_g = 0.34\lambda_g$ (25mm), Center conductor length, $L_c = 0.25\lambda_g$ (18mm), Stepped center conductor width, $W_s = 0.01 \lambda_g$ (1mm) and shorting gap, $G_s = 0.006 \lambda_g$ (0.5mm).
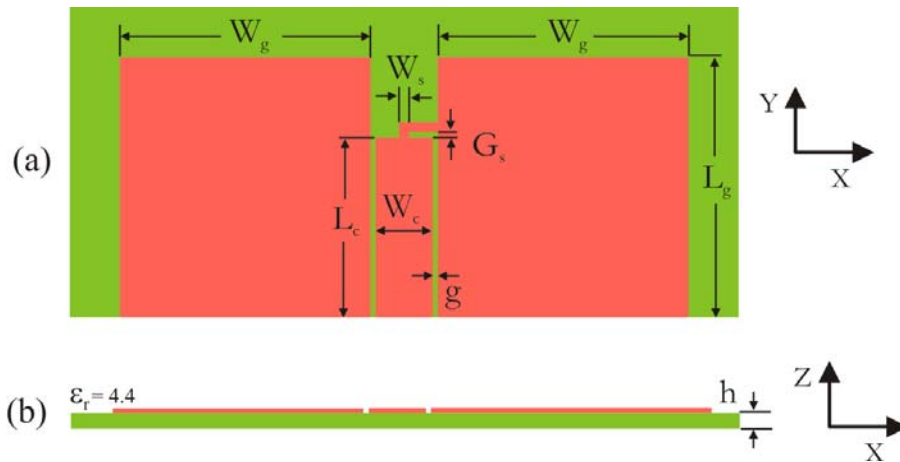
Fig. 4.60 Geometry of the wideband coplanar antenna.[L_g = 26mm, W_g = 25mm, L_c = 18mm, W_c = 5.7mm, g = G_s = 0.5mm, W_s = 1mm, h = 1.6mm and ε_r = 4.4]

The shorted coplanar antenna depicted in the previous chapter is modified by a stepped center strip shorted at the optimum position to achieve improved impedance bandwidth without much disturbing the radiation pattern and maintaining the compactness.

4.5.2. FDTD computational domain and optimum code parameters:

FDTD computation domain used for the theoretical analysis of the wideband FGCPW antenna is illustrated in Fig. 4.61.
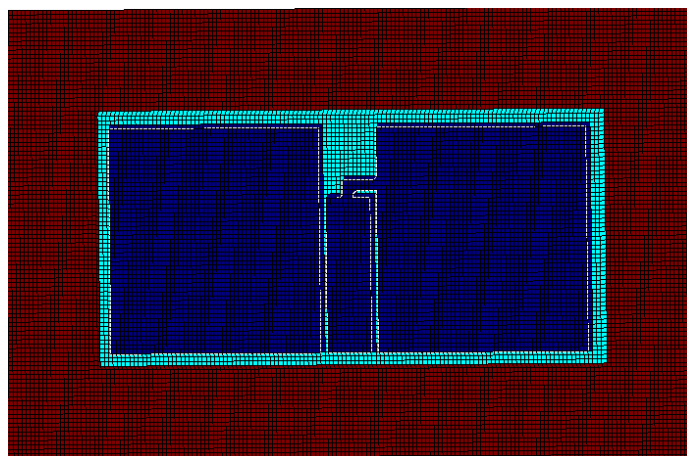
Fig.4.61Grid scheme wideband coplanar antenna.(2D grid)

The size of the computational domain filled with Yee-cells is Nx x Ny x Nz = 165 x 105 x 57 cells in which the antenna is modeled by 117 x 56 x 4 cells. In order to simulate the real condition the remaining cells are treated as air. Perfectly Matched Layer is employed as Absorbing Boundary Condition at the edges of the problem space. To excite the antenna a time domain gussion pulse is applied to the feed point and the results are extracted.

Optimum code parameters for the analysis is illustrated in Table 4.10

Time domain parameters	Geometrical Parameters
Gaussian Pulse Half width, T = 20ps Time delay,τ_d =3T Time step Δt = 0.66ps Number of time steps : 2000	Cell dimensions Δx =0.5mm, Δy=0.5mm Δz= 0.4mm.

Table 4.10 Optimum code parameters for the FDTD analysis

4.5.3 Return loss Characteristics:

The measured returnloss characteristics of the wideband coplanar antenna along with the simple shorted coplanar antenna discussed in the previous chapter is illustrated in Fig. 4.62 for comparison.
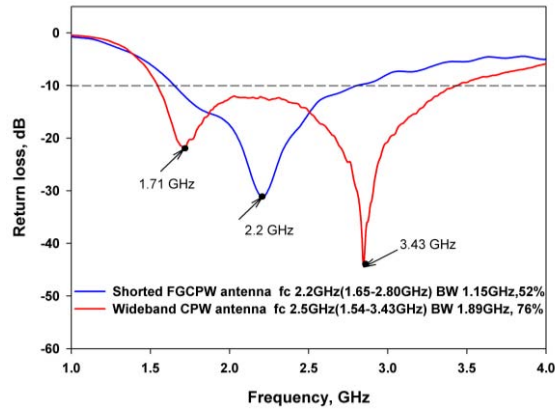
Fig. 4.62 Return loss characteristics of the simple shorted coplanar antenna and wideband coplanar antenna[L_g = 26mm, W_g = 25mm, L_c = 18mm, W_c = 5.7mm, g = G_s = 0.5mm, W_s = 1mm, h = 1.6mm and ε_r = 4.4]

It is observed from the plot that the simple short coplanar antenna exhibits resonance from 1.65GHz to 2.80GHz with a bandwidth of 1.15GHz, 53% while the modified short at the optimum position provides an impedance band from 1.54GHz to 3.43GHz with a bandwidth of 1.89GHz, 76%. Therefore the modified short provides a 23% improvement of bandwidth while maintaining the compactness. The reflection characteristics of the wideband coplanar antenna is observed to have two resonances at 1.71GHz and 2.89GHz, merged together to form wideband characteristics.

Fig.4.63 depicts the simulated, computed and measured return loss characteristics of the proposed antenna. It is observed that the results are in good agreement.
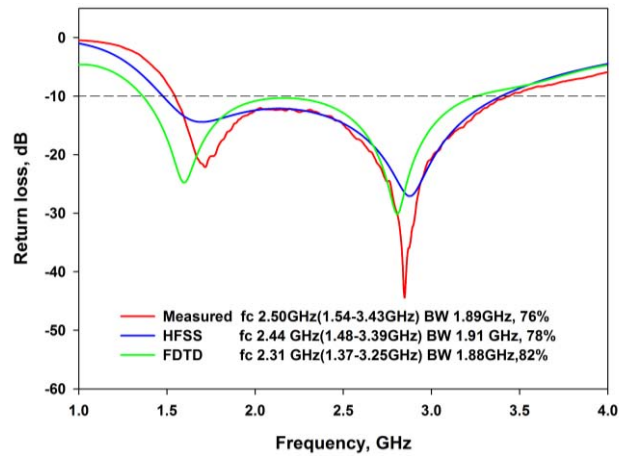
Fig.4.63 Theoretical, simulated and experimental returnloss characteristics of the wideband coplanar antenna [L_g = 26mm, W_g = 25mm, L_c = 18mm, W_c = 5.7mm, g = G_s = 0.5mm, W_s = 1mm, h = 1.6mm and ε_r = 4.4]

The theoretical result with FDTD, gives a 2:1 return loss band from1.19GHz to3.66GHz with a band width of 2.43GHz. The relative error in the FDTD plot compared to the experimental results is 2%. The error is mainly because of large cell size in the FDTD computation domain. It can be minimized by modeling the geometry with much small cell size. The impedance plot of the antenna is illustrated in Fig.4.64
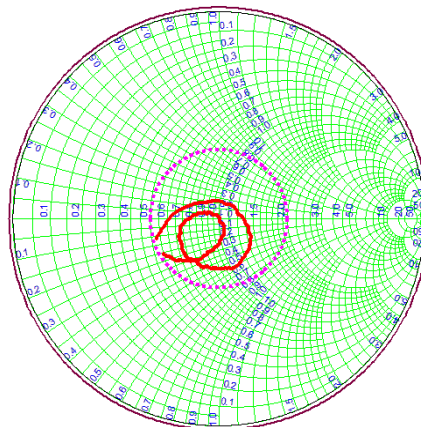
Fig. 4.64: The impedance plot of the proposed antenna.[L_g = 26mm, W_g = 25mm, L_c = 18mm, W_c = 5.7mm, g = G_s = 0.5mm, W_s = 1mm, h = 1.6mm and ε_r = 4.4]

4.5.4 Current distribution

The surface current density plot at two resonant frequencies in the wideband coplanar antenna is depicted in Fig. 4.65. A close examination of the current density plots is helpful for predicting the resonance and radiation behavior of the proposed antenna.

(a)

(b)
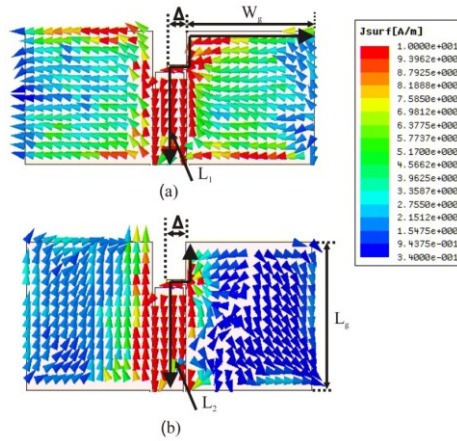
Fig. 4.65 Simulated current densities at 1.71 GHz and 2.89GHz [L_g = 26mm, W_g = 25mm, L_c = 18mm, W_c = 5.7mm, g = G_s = 0.5mm, W_s = 1mm, h = 1.6mm and ε_r = 4.4].

From the current density plot drawn at 1.71 GHz, depicted in Fig. 4.65(a), it is observed that the dimension (L_g +W_g+ Δ) contributes the first resonance while (Lg +Δ) in Fig. 4.65(b)contributes for the second resonance. These two resonant modes merge together to form the wide band characteristics. These conclusions about the wideband behavior of the proposed antenna are in agreement with the experimental results provided.

The direction of current in the top portion of the antenna predicts the polarization of the radiated field as x-polarization.

4.5.5 Radiation pattern

Fig. 4.66(a-f) illustrates the measured radiation pattern of the proposed antenna at different frequency points within the 2:1 VSWR band, including the lower and higher cut off frequencies
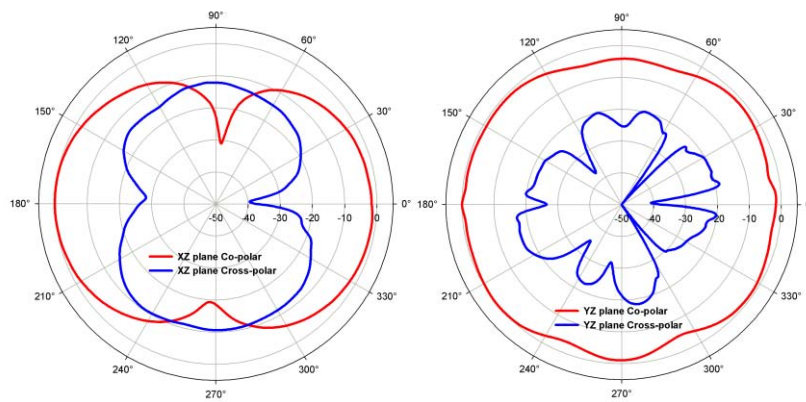
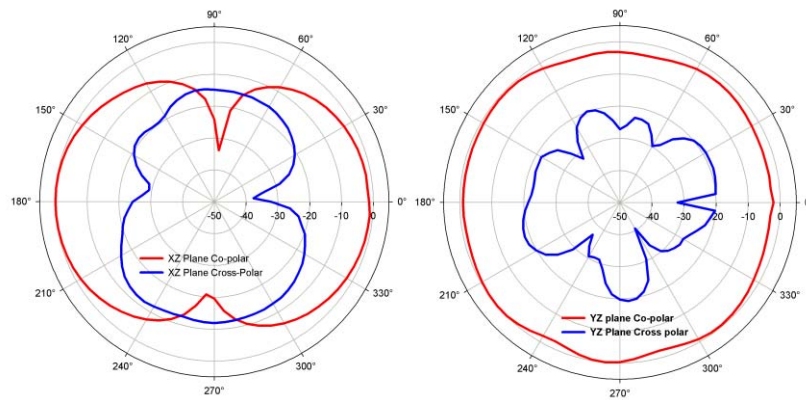Fig. 4.66(a) XZ and YZ plane radiation pattern of the wideband antenna at 1.54GHz

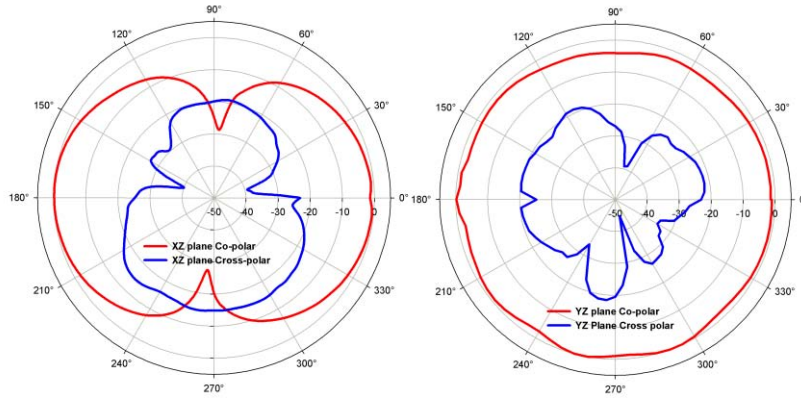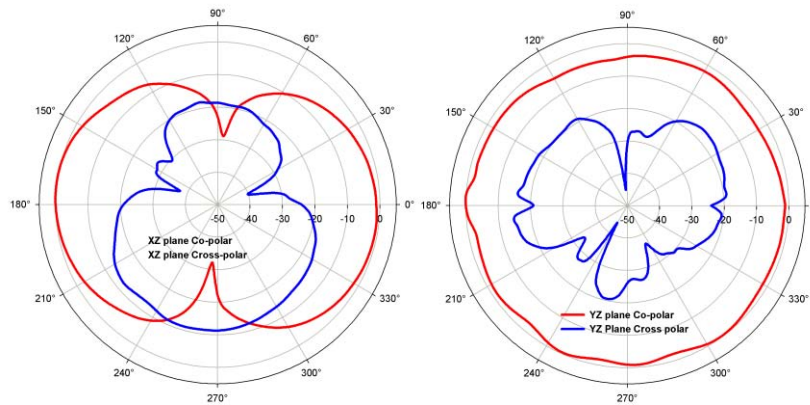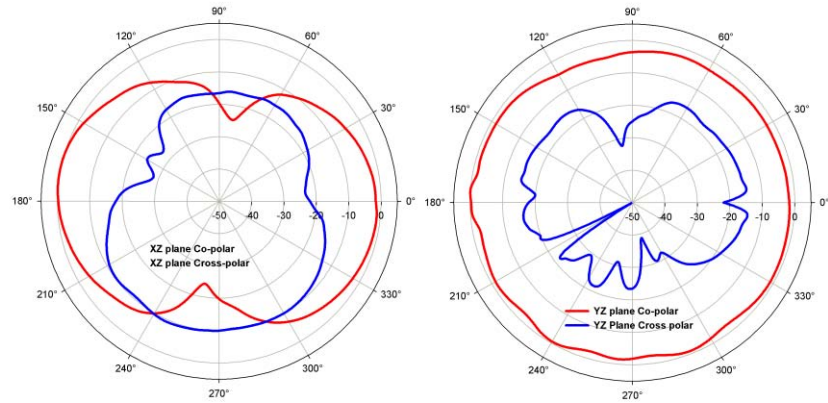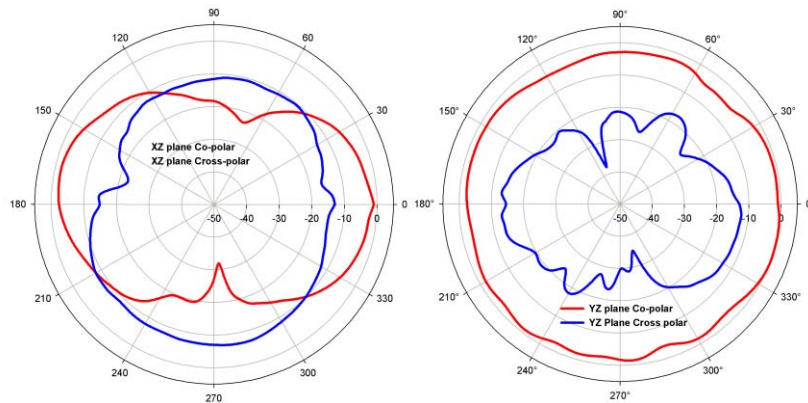Fig. 4.66(b) XZ and YZ plane radiation pattern of the wideband antenna at 1.71GHz

Fig. 4.66(c) XZ and YZ plane radiation pattern of the wideband antenna at 2.00GHz

Fig. 4.66(d) XZ and YZ plane radiation pattern of the wideband antenna at 2.50GHz.

Fig. 4.66(e) XZ and YZ plane radiation pattern of the wideband antenna at 2.89GHz

Fig. 4.66 (f) XZ and YZ plane radiation pattern of the wideband antenna at 3.43GHz[L_g = 26mm, W_g = 25mm, L_c = 18mm, W_c = 5.7mm, g = G_s = 0.5mm, W_s = 1mm, h = 1.6mm and ε_r = 4.4]

It is found from the measured radiation patterns at different frequency points in the VSWR band that the proposed antenna provides almost identical radiation patterns throughout the radiation band. It is also observed that the antenna radiation in YZ plane is non directional while that of the orthogonal plane is directional, which in turn provide nearly omnidiretionality suitable for wireless communication devices. From the experimental results it is also worth to note that

the modified coplanar antenna can provide a wideband resonance while maintaining the radiation pattern.

4.5.6 Polarization

The variation of received power from a highly linearly polarized horn antenna throughout the resonant band at both the polarization plane is depicted in the Fig.4.67
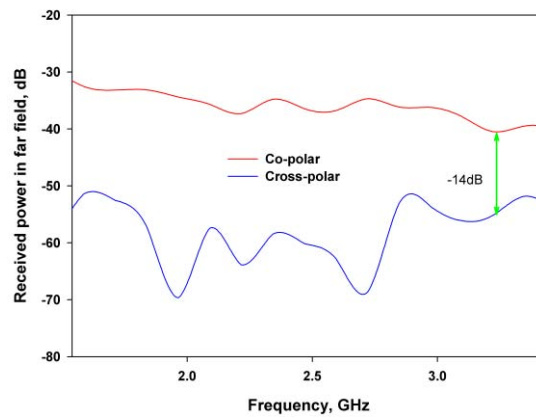

Fig. 4.67 Transmission (S21) characteristics of the wideband antenna[L_g = 26mm, W_g = 25mm, L_c = 18mm, W_c = 5.7mm, g = G_s = 0.5mm, W_s = 1mm, h = 1.6mm and ε_r = 4.4]

As predicted from the current density plot described earlier, the measurement results reveals that the radiated electromagnetic signal is linearly polarized along x-direction throughout the entire operating band. Across polarization level of better than -10dB is observed throughout the band.

4.5.7 Gain and Efficiency:

Gain of the wideband coplanar antenna is measured using gain comparison method and the efficiency of the antenna is measured through wheeler cap method. The gain of the radiator is depicted in Fig. 4.68.
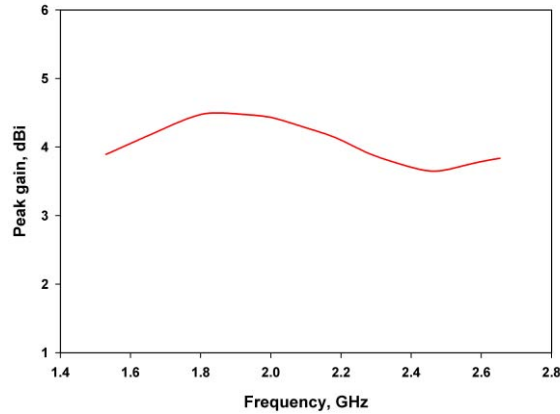
Fig. 4.68 Gain of the wideband coplanar antenna[L_g = 26mm, W_g = 25mm, L_c = 18mm, W_c = 5.7mm, g = G_s = 0.5mm, W_s = 1mm, h = 1.6mm and ε_r = 4.4]

The antenna gives a moderate gain greater than 3.5 dBi throughout the operating band. The maximum gain observed is 4.5dBi at 1.92GHz. It is also clear from the plot that the maximum variation of the gain is only 1dBi over the entire application band. Measured average efficiency of the antenna throughout the band is found to be 89%. Therefore the proposed antenna is an efficient radiator throughout the operating band.

4.5.8 Parametric analysis

The parametric analysis of the proposed antenna is conducted and effect of various antenna parameters over the antenna characteristics is studied. The results and discussion on various effects of different antenna elements are followed in this session.

4.5.8.1 Effect of finite ground dimensions:

The finite ground of the coplanar waveguide plays an important role in the antenna characteristics. The physical dimensions L_g and W_g and its effect over the reflection characteristics and bandwidth are studied in detail.

4.5.8.1.1 Effect of ground plane width (Wg)

The influence of ground plane width over the return loss characteristic of the antenna is shown in Fig. 4.69. In the present study the ground plane width is varied from 21mm to 31mm ($0.29\lambda_g$ to $0.42\lambda_g$) by maintaining other design parameters constant. It is observed from the plot that ground plane width has effect on both the resonant frequencies. It is worth to note that the antenna provides wide impedance bandwidth, when the W_g is in between 24mm ($0.33\ \lambda_g$) and 29mm ($0.4\ \lambda_g$). For W_g greater than 29mm ($0.4\ \lambda_g$), it is observed that first resonance moves to a lower frequency region and impedance matching becomes poor at the center portion of the impedance band. Similarly for W_g less than 24mm($0.4\ \lambda_g$) impedance matching at the lower frequency region becomes poor and in effect the bandwidth decreases drastically.
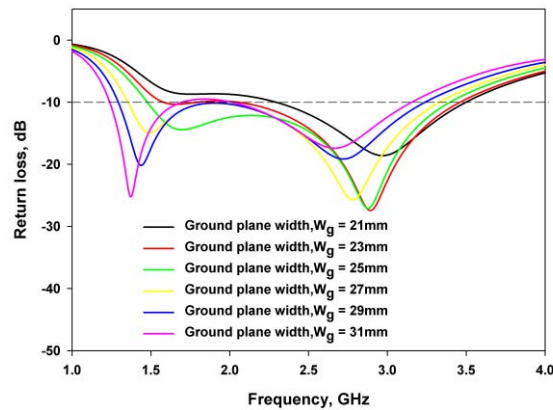

Fig. 4.69: Effect of ground plane width W_g on return loss characteristics of the wideband coplanar antenna[L_g = 26mm, L_c = 18mm, W_c = 5.7mm, g = G_s = 0.5mm, W_s = 1mm, h = 1.6mm and ε_r = 4.4]

The variation in resonant frequency with W_g is depicted in Fig. 4.70(a). It is observed from the plot that the variation in W_g from ($0.29\lambda_g$ to $0.42\lambda_g$) 21mm to 31mm (results a frequency shift from 1.7GHz to 1.4GHz for the first resonance while the second resonance sifts from 2.97GHz to 2.7GHz. This shift reveals the influence of resonant length over the resonant frequency as predicted through the current density plots.

The variation of bandwidth with the ground plane width is depicted in Fig. 4.70(b).
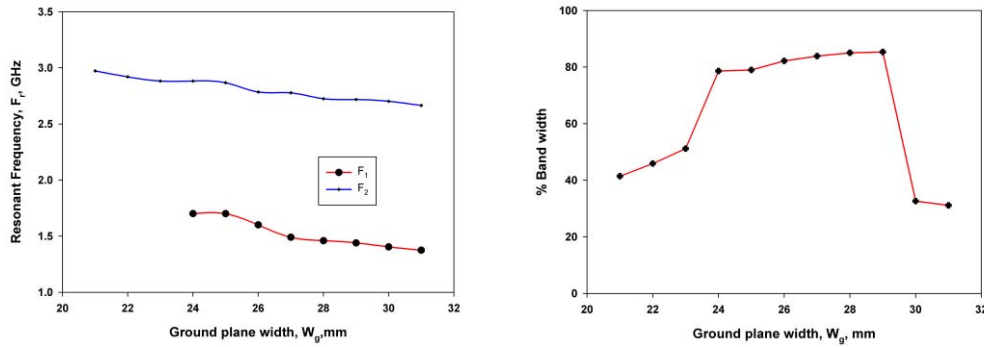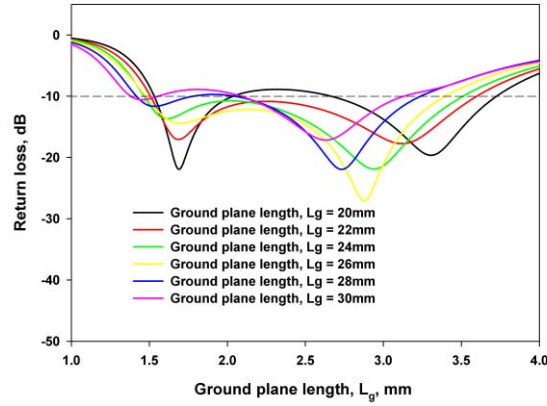

Fig. 4.70: Effect of ground plane width W_g on (a) resonant frequencies and (b) bandwidth[L_g = 26mm, W_g = 25mm, L_c = 18mm, g = G_s = 0.5mm, W_s = 1mm, h = 1.6mm and ε_r = 4.4]

It observed from the plot that when W_g changes from 24mm to 29 mm ($0.33\lambda_g$ to $0.40\lambda_g$) the bandwidth of the antenna varies from 75% to 85%. It can be concluded from the analysis that the proper merging of two resonant bands is the key element which determines the bandwidth of the proposed antenna.

4.5.8.1.2. Effect of ground plane length (L_g)

The variation in return loss characteristics, resonant frequencies and bandwidth with ground plane length are depicted in Fig. 4.71.

(a)
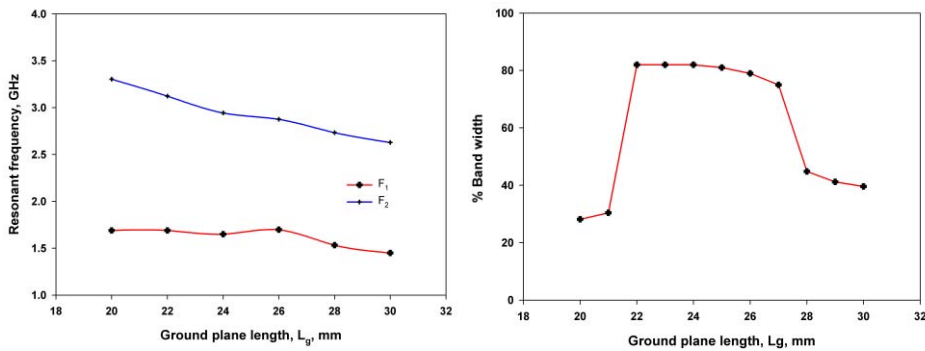
(b)   (b)

Fig. 4.71: Effect of ground plane width L_g on (a) returnloss characteristics (b)resonant frequencies and (c) bandwidth.[W_g = 25mm, L_c = 18mm, W_c = 5.7mm, g = G_s = 0.5mm, W_s = 1mm, h = 1.6mm and ε_r = 4.4]

It is observed from the return loss variations that as L_g increases both the resonant frequencies moves to a lower frequency region and the impedance matching of the lower frequency region, corresponds to first resonant mode becomes poorer. It is also clear from the bandwidth variations that the effective merging of two resonant modes is occurring for values in between 22mm and 27mm ($0.30\lambda_g$ and $0.37\lambda_g$). The variation in L_g by 5mm ($0.07\lambda_g$) results decrement of bandwidth by 7%.

4.5.8.2 Effect of shorting stub:

In this session we demonstrate the effect of shorting stub over the antenna characteristics. The gap between the shorting point and centre conductor (Gs), Width of the stepped centre conductor (Ws) and length of the centre conductor(Lc) are varied and their effect on retunloss characteristics and bandwidth are studied

4.5.8.2.1 Effect of shorting gap(Gs):

The variation of returnloss with shorting gap, Gs is depicted in Fig 4.72.
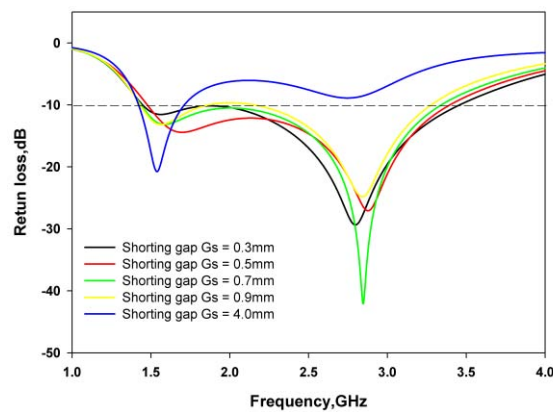

Fig. 4.72: Effect of Gs over the returnloss characterestics.[L_g = 26mm, W_g = 25mm, L_c = 18mm, W_c = 5.7mm, g = 0.5mm, W_s = 1mm, h = 1.6mm and ε_r = 4.4]

It is observed that the gap between shorting point and the center conductor has a crucial relevance on the returnloss characteristics of the proposed antenna. As the gap Gs varies from 0.3 mm to 4mm ($0.004\lambda_g$ to $0.05\lambda_g$) it is seen from the plot that the two resonances remains unaltered but it has effect over the impedance matching. Smaller values of Gs results more reflection in the lower side of the resonant band while larger values results more reflection in the higher side of the band. The antenna provides wideband performance of 79% when the gap is in between 0.5mm to 0.7mm ($0.006\lambda_g$ and $0.009\lambda_g$).
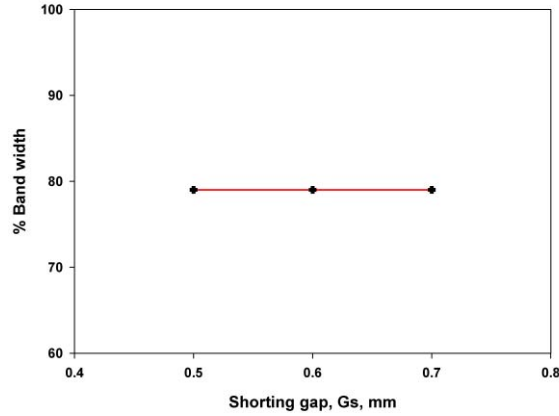
170

Fig. 4.73: Effect of gs over the Bandwidth[L_g = 26mm, W_g = 25mm, L_c = 18mm, W_c = 5.7mm, g = 0.5mm, W_s = 1mm, h = 1.6mm and ε_r = 4.4]

4.5.8.2.2 Effect of Stepped center conductor width(Ws):

The stepped center conductor width, W_s is varied, studied the influence over the antenna characteristics and plotted in Fig. 4.74.
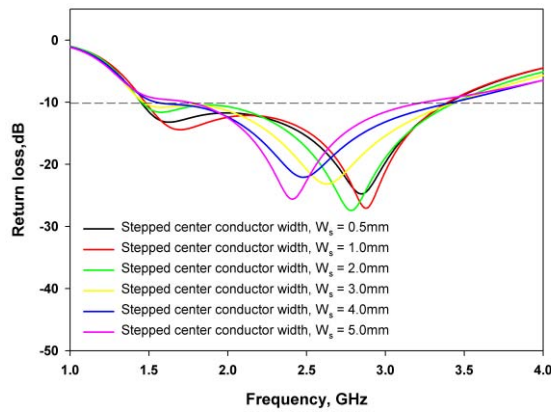

Fig. 4.74: Effect of W_s over the returnloss characteristics.[L_g = 26mm, W_g = 25mm, L_c = 18mm,Wc=5.7mm, g = G_s = 0.5mm, h = 1.6mm and ε_r = 4.4]

It is observed from the analysis that the bandwidth remains almost unaltered for the values from 1mm to 3mm. For higher values of Ws greater than 3mm (0.04 λ_g)it is seen that the bandwidth decreases drastically.
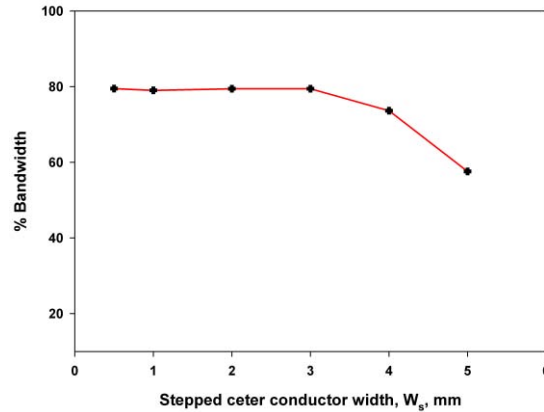
Fig. 4.75: Effect of W_s over the bandwidth [L_g = 26mm, W_g = 25mm, L_c = 18mm, W_c = 5.7mm, g = G_s = 0.5mm, h = 1.6mm and ε_r = 4.4]

4.5.8.2.3 Effect of Length of Center Conductor(L_c):

The length of the center conductor is varied from 12mm to 24mm (0.16 λ_g to 0.33 λ_g) to study its effect over different antenna characteristics. The variation in returnloss and bandwidth is shown in Fig. 4.76.
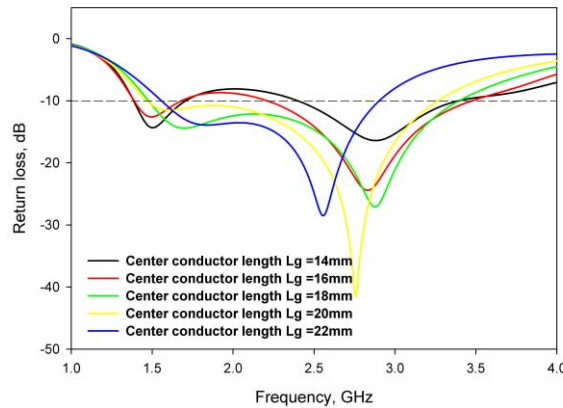

Fig. 4.76: Effect of center conductor length over the returnloss characteristics.[L_g = 26mm, W_g = 25mm, W_c = 5.7mm, g = G_s = 0.5mm, W_s = 1mm, h = 1.6mm and ε_r = 4.4]

It is observed from the returnloss variations that the antenna provides a wideband characteristics for higher values of L_c, that is for L_c >=18mm (0.25 λ_g).

It is seen from the bandwidth variations shown in Fig.4.77 that the higher values of L_c results reduction in bandwidth.
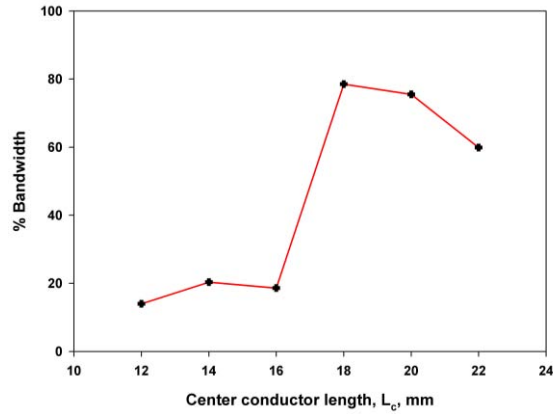

Fig. 4.77: Effect of center conductor length over the bandwidth[L_g = 26mm, W_g = 25mm, L_c = 18mm, W_c = 5.7mm, g = G_s = 0.5mm, W_s = 1mm, h = 1.6mm and ε_r = 4.4]

4.5.8.3 Effect of substrate parameters.

The influence of substrate parameters over the antenna characteristic is also studied through simulation.

4.5.8.3.1 Effect of substrate height.

Fig.4.78.a-b depicts the variation of the return loss and bandwidth with height of the substrate.
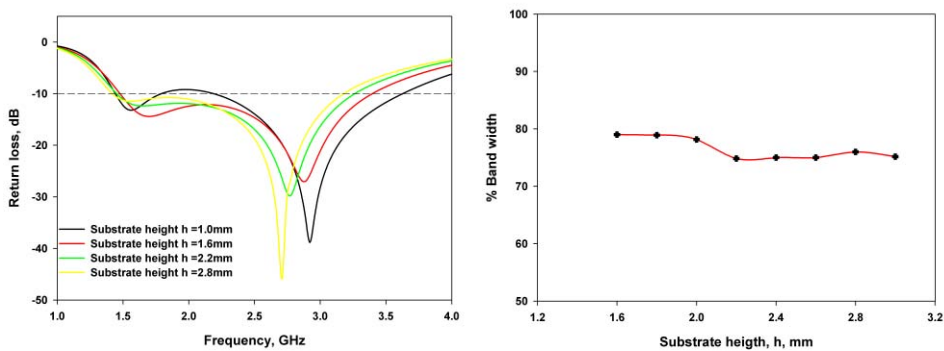

Fig. 4.78: Effectof substrate height over the (a) retunloss characteristiscs and (b) Bandwidth[L_g = 26mm, W_g = 25mm, L_c = 18mm, W_c = 5.7mm, g = G_s = 0.5mm, W_s = 1mm and ε_r = 4.4]

From the plot it is clear that the substrate height has an effect on both impedance matching and bandwidth of the resonant band. As far as the bandwidth is concerned, it remains almost unaltered for the values of h greater than 2.0mm.

4.5.8.3.2 Effect of Relative permittivity

The dielectric constant of the proposed antenna is varied from 2 to 11 and its effect over the bandwidth is studied. It is found that the bandwidth of the radiator decreases as the relative permittivity comes down. The bandwidth decrease is because of high Q of the device as dielectric constant increases.
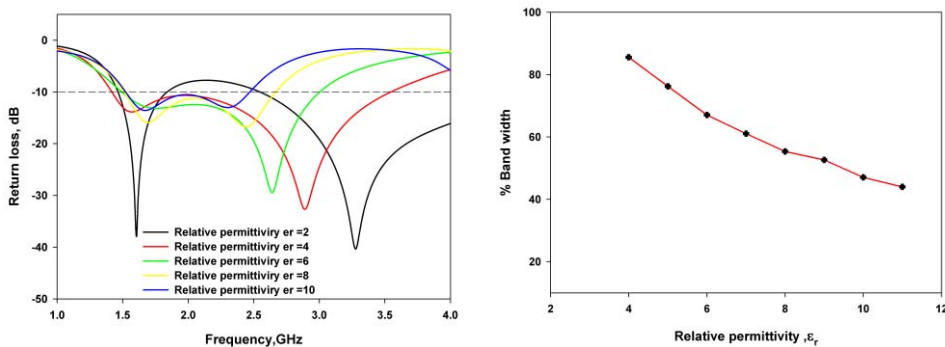

Fig. 4.79 : Influvance of returnloss charcteristics over the Bandwidth[L_g = 26mm, W_g = 25mm, L_c = 18mm, W_c = 5.7mm, g = G_s = 0.5mm, W_s = 1mm, h = 1.6mm]

4.5.9 Design Procedure:

The experimental and simulation analysis lead to the empirical relations for the wideband coplanar antenna. The following design procedures can be adopted to design the proposed antenna with good radiation characteristics.

1. Select a suitable substrate for the antenna with relative dielectric Er and thickness h.
2. The center strip width and gap is design for the characteristics impedance of 50Ohm with standard design equations.

3. The length of the center conductor can be calculated through the following equation,

$$L_{c(cm)} \approx \frac{7.5}{\sqrt{\varepsilon_{eff}} \times f_{(GHz)}}$$

4. The width(Wg) and length(Lg) of the finite ground plane can be estimated from,

$$W_{g(cm)} \approx \frac{10.2}{\sqrt{\varepsilon_{eff}} \times f_{(GHz)}} \quad , \qquad L_{g(cm)} \approx \frac{10.5}{\sqrt{\varepsilon_{eff}} \times f_{(GHz)}}$$

5. The gap, Gs can be calculated from the relation,

$$G_{s(cm)} \approx \frac{0.21}{\sqrt{\varepsilon_{eff}} \times f_{(GHz)}}$$

Where ε_{eff} is the effective permittivity given by,

$$\varepsilon_{eff} = \frac{\varepsilon_r + 1}{2}$$

The above equations are experimentally validated for different frequencies as shown in Table 4.11

Design Freq. (GHz)	Design Parameters(mm)				Exp. Band (GHz)	% BW
	L_g	W_g	L_c	G_s		
0.9	71	69	51	1.4	0.61-1.25	69
5.2	12	12	8.8	0.2	2.81-6.49	79

Table 4.11: Typical design parameters for different frequencies

4.5.10 Microstrip fed wideband coplanar Antenna:

The previous discussion on the development of the wideband coplanar antenna concludes that the finite ground coplanar wave guide can act as an efficient radiator. The conversion from the wave guiding device to an efficient radiator can be achieved by introducing a shorting stub in the waveguide.

175

However, in most practical situations, the integration with backend passives and microstrip transmission lines become a critical problem to be solved. In order to investigate the compatibility of the radiator with a microstrp line, the proposed antenna is coupled with a 50Ω transmission line and measured the critical antenna characteristics. The effective coupling to the microstrip transmission line is depicted in Fig. 4.80.
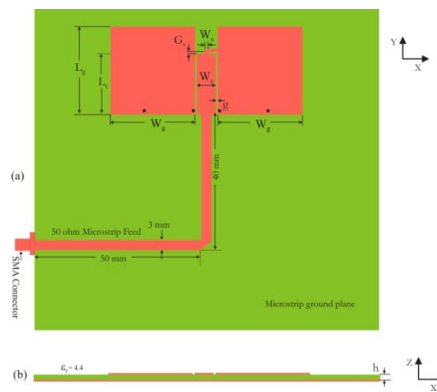

Fig.4.80 Microstrip fed coplanar antenna.

The major measurements carried out in the microstrip-integrated coplanar antenna are retunloss characteristics and radiation behavior. The corresponding returnloss characteristics of the microstrip line integrated along with that of wideband coplanar antenna is plotted in Fig.4.81 for comparison. It is observed that the integration of microstrip line to the proposed antenna makes only a feeble difference in the returnloss characteristics.
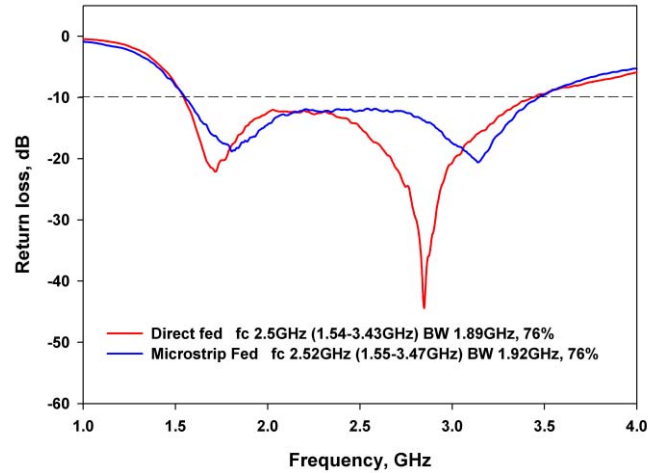
Fig. 4.81 Returnloss characteristics of microstrip integrated coplanar antenna and Direct fed Antenna.

In order to investigate the effect of microstrip line over the radiation characteristics the radiation pattern of the microstrip line fed coplanar antenna is measured and a comparison plot is illustrated in Fig. 4.82.

It is observed that both the radiation patterns are almost identical throughout the resonant band except for small variations seen in the higher band. Therefore we can conclude that the developed, wideband coplanar antenna is a potential candidate for microwave communication systems and it can be easily integrated MICs and MMICs without much variation in the antenna characteristics
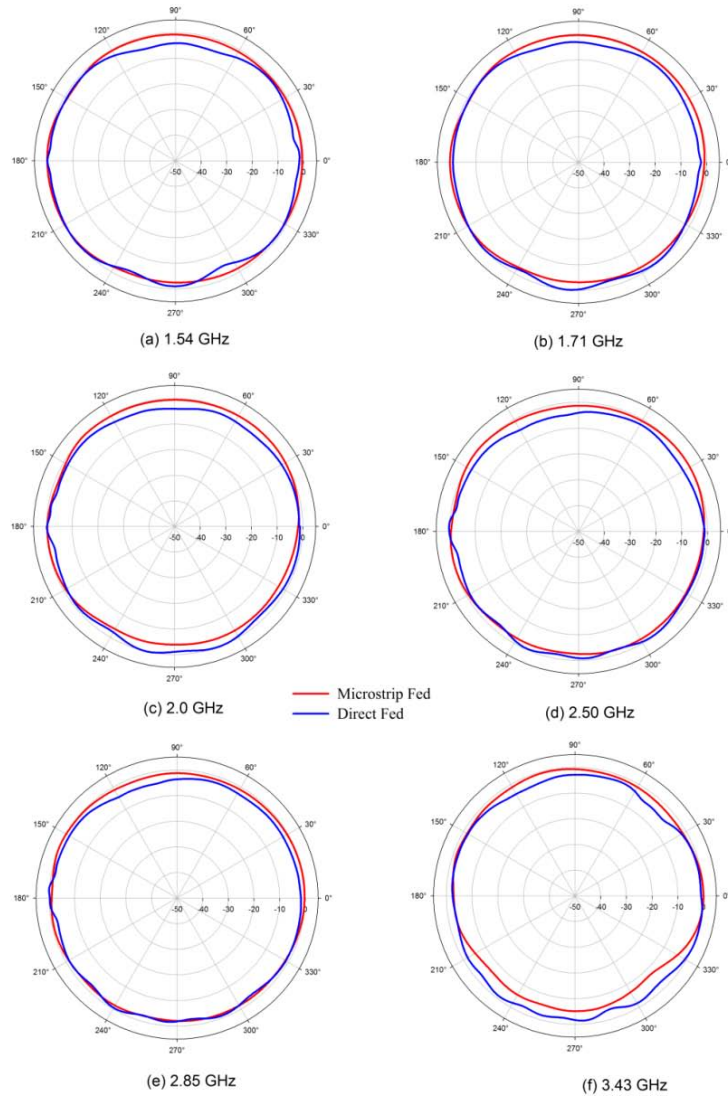
Fig. 4.82 Radiation pattern of microstrip integrated coplanar antenna and Direct (SMA) fed Antenna.

4.5.11 Conclusions:

A novel uniplanar shorted antenna is designed for wideband application. The simulated current density plot helps to predict the resonant path of the antenna along with its radiation characteristics. The antenna offers wide bandwidth greater than 75%, quasi omni-directional radiation coverage along with moderate gain and efficiency. The uniplanar design of the radiator provides easy integration with MMICs and back end passives.

.

Reference

[1] Jacub, G., Aanandan C.K, Mohanan P and Nair K.G., " Dual frequency miniature microstrip antenna", Electronics Letters, Vol.34, pp.1168-1170, 1998

Chapter Five

CONCLUSIONS

This chapter explains the conclusions brought out from the numerical and experimental investigations explained in the previous chapter. The salient features of the antennas are reported in this chapter. Suggestions for future work in this field are also provided.

5.1 Thesis Highlights

This chapter brings the thesis to a close by summarizing the results obtained out of the numerical as well as experimental investigations conducted on the resonance and radiation characteristics of Drum shaped monopole antenna, Funnel shaped monopole antenna and the shorted coplanar antenna. Aim of this work was to develop compact wideband antennas suitable for the present day today art.

An introduction to the over view of antennas, state of the art planar antenna technologies, different feeding techniques and introduction of coplanar waveguides have been discussed in chapter 1. The literature review presented in chapter 2 clearly convinces the importance of the work in this direction and the novelty of work presented. The materials and methodology employed for experimental investigations have been explained in chapter3.

Investigations on resonant characteristics of drum shaped monopole antenna, funnel shaped monopole antenna, conventional coplanar waveguide with simple short, modified short coplanar waveguide were presented in chapter 4. The FDTD results and experimental results were also presented. A design equation was also presented after the rigorous parametric analysis to design the antenna for any two bands of operation.

5.2 Inferences from investigations on Drum Shaped monopole antenna

- By loading the strip monopole with a drum shaped patch results improvement in the bandwidth.

- The resonant frequency is influenced by both the dimension of the strip monopole and the position and size of the drum shaped patch.

- The orientation of the patch over the monopole determines the polarization characteristics of the antenna.

- Single layer vertical orientation results optimum bandwidth with linearly polarized radiation pattern.

- The peak gain of the optimum orientation is found to be 5.8dBi.

5.3 Inferences from investigations on funnel shaped monopole Antenna

- A strip monopole loaded with funnel shaped patch provides similar bandwidth enhancement as in the case of drum shaped loading.

- The antenna provides almost 98 percentage bandwidth with linear polarization.

- When the antenna is energized, three distinct resonant modes are excited, which combines to form wideband characteristics.

- For lower resonant frequency all the antenna elements are contributing for the radiation. In the middle frequency region strip monopole and patch F1 contributes strongly to the radiation while patch F2 improves the overall impedance matching. At the higher frequency second harmonics of the strip is responsible for the radiation.

- The antenna offers reasonable gain over the entire band of operation with an average efficiency of 85%.

5.4 Inferences from the coplanar Antenna.

- An asymmetric short in the Finite Ground coplanar waveguide results a resonance in the lower frequency region.

- The resonance of the antenna is found to be get affected by the shorting position.

- By suitably modifying the short the bandwidth can be improved by 23%

- The FDTD method is utilized for the numerical computation in Matlab. The returnloss characteristics using FDTD code, Ansoft HFSS and measurements are in good agreement.

- The radiation pattern is found to be nearly omnidirection with moderate gain and efficiency.

- The unipolar design of the radiator provides easy integration with MMICs and backend passives.

5.5 Suggestions for future work in the field

Reconfigurable antennas are the other area where 'coplanar antenna' is found to be a good candidate. The varactor diodes integrated on the resonant path of the antenna element can tune its resonant frequency electronically. Active antenna concept can be implemented in 'coplanar antennas'. Transistors, diodes, MOSFETs etc. can be integrated on the antenna element for amplification, self oscillating systems etc. It is worth noting that the ground potential is available at the top layer of the antenna at the two lateral ground strips, thus avoids the use of vias for active device integration.

Appendix

Concept and Implementation based on FDTD

The Finite Difference Time Domain method is used for the theoretical analysis in this thesis; which is one of the most popular computational methods for the microwave engineering. It is simple to program, efficient and is easily adapted to the model in a verity of problems. K.S. Yee[1] proposed the method using central differences on a Cartesian grid staggered in both space and time. This method solves the Maxwell's equations in a differential form discretized in space and time and tracks the time-varying fields throughout the volume of space.

A.1 Basic Concepts:

A function in time and space can be written as,

$$F^{n}(i, j, k) = F(i\Delta x, j\Delta y, k\Delta z, n\Delta t) \rightarrow (1)$$

Where Δt is the increment in time, n is the time index and Δx, Δy, Δz are the space increments along the three coordinate,

The special derivatives of the function F in (1) can be written using central finite difference approximation as,

$$\frac{\partial F^{n}(i, j, k)}{\partial x} = \frac{F^{n}(i + 1/2, j, k) - F^{n}(i - 1/2, j, k)}{\Delta x} \rightarrow (2)$$

$$\frac{\partial F^{n}(i, j, k)}{\partial t} = \frac{F^{n+1/2}(i, j, k) - F^{n-1/2}(i, j, k)}{\Delta t} \rightarrow (3)$$

The basic formulation of FDTD method [2] is based on the differential formulation of Maxwell's Curl equations with piecewise, uniform, isotropic and homogeneous media.

$$\mu \frac{\partial H}{\partial y} = -\nabla \times E \rightarrow (4)$$

$$\varepsilon \frac{\partial E}{\partial t} = -\nabla \times H \rightarrow (5)$$

The above equations can be written in Cartesian coordinates as,

$$\frac{\partial \mathrm{H}x}{\partial t} = \frac{1}{\mu}\left(\frac{\partial \mathrm{E}y}{\partial z} - \frac{\partial \mathrm{E}z}{\partial y} \right) \rightarrow (6)$$

$$\frac{\partial \mathrm{H}y}{\partial t} = \frac{1}{\mu}\left(\frac{\partial \mathrm{E}z}{\partial x} - \frac{\partial \mathrm{E}x}{\partial z} \right) \rightarrow (7)$$

$$\frac{\partial \mathrm{H}z}{\partial t} = \frac{1}{\mu}\left(\frac{\partial \mathrm{E}x}{\partial y} - \frac{\partial \mathrm{E}y}{\partial x} \right) \rightarrow (8)$$

189

$$\frac{\partial \mathrm{E}x}{\partial t} = \frac{1}{\varepsilon}\left(\frac{\partial \mathrm{H}z}{\partial y} - \frac{\partial \mathrm{H}y}{\partial z} - \sigma \mathrm{E}x\right) \rightarrow (9)$$

$$\frac{\partial \mathrm{E}y}{\partial t} = \frac{1}{\varepsilon}\left(\frac{\partial \mathrm{H}x}{\partial z} - \frac{\partial \mathrm{H}z}{\partial x} - \sigma \mathrm{E}y\right) \rightarrow (10)$$

$$\frac{\partial \mathrm{E}z}{\partial t} = \frac{1}{\varepsilon}\left(\frac{\partial \mathrm{H}y}{\partial x} - \frac{\partial \mathrm{H}x}{\partial y} - \sigma \mathrm{E}z\right) \rightarrow (11)$$

By applying finite difference to the above scalar equations, the following equations can be derived,

$$H_y^{n+1/2}(i+1/2, j, k+1/2) = H_y^{n-1/2}(i+1/2, j, k+1/2)$$
$$+ \left[\frac{\Delta t}{\mu . \Delta x}\right]\left(E_z^n(i+1, j, k+1/2) - E_z^n(i, j, k+1/2)\right)$$
$$- \left[\frac{\Delta t}{\mu . \Delta z}\right]\left(E_x^n(i+1/2, j, k+1) - E_x^n(i+1/2, j, k)\right) \rightarrow (12)$$

$$H_z^{n+1/2}(i+1/2, j+1/2, k) = H_z^{n-1/2}(i+1/2, j+1/2, k)$$
$$+ \left[\frac{\Delta t}{\mu . \Delta y}\right]\left(E_x^n(i+1/2, j+1, k) - E_x^n(i+1/2, j, k)\right)$$
$$- \left[\frac{\Delta t}{\mu . \Delta x}\right]\left(E_y^n(i+1, j+1/2, k) - E_y^n(i, j+1/2, k)\right) \rightarrow (13)$$

$$E_x^{n+1}(i+1/2, j, k) = E_x^n(i+1/2 \, j, k)$$
$$+ \left[\frac{\Delta t}{\varepsilon . \Delta y}\right]\left(H_z^{n+1/2}(i+1/2, j+1/2, k) - H_z^{n+1/2}(i+1/2, j-1/2, k)\right)$$
$$- \left[\frac{\Delta t}{\varepsilon . \Delta z}\right]\left(H_y^{n+1/2}(i+1/2, j, k+1/2) - H_y^{n+1/2}(i+1/2, j, k-1/2)\right) \rightarrow (14)$$

$$H_x^{n+1/2}(i, j+1/2, k+1/2) = H_x^{n-1/2}(i, j+1/2, k+1/2)$$

$$+ \left[\frac{\Delta t}{\mu.\Delta z} \right] \left(E_y^n(i, j+1/2, k+1) - E_y^n(i, j+1/2, k) \right)$$

$$- \left[\frac{\Delta t}{\mu.\Delta y} \right] \left(E_z^n(i, j+1, k+1/2) - E_z^n(i, j, k+1/2) \right) \rightarrow (15)$$

$$E_z^{n+1}(i, j, k+1/2) = E_z^n(i, j, k+1/2)$$

$$+ \left[\frac{\Delta t}{\varepsilon.\Delta x} \right] \left(H_y^{n+1/2}(i+1/2, j, k+1/2) - H_y^{n+1/2}(i-1/2, j, k+1/2) \right)$$

$$- \left[\frac{\Delta t}{\varepsilon.\Delta y} \right] \left(H_x^{n+1/2}(i, j+1/2, k+1/2) - H_x^{n+1/2}(i, j-1/2, k+1/2) \right) \rightarrow (16)$$

$$E_y^{n+1}(i, j+1/2, k) = E_y^n(i, j+1/2, k)$$

$$+ \left[\frac{\Delta t}{\varepsilon.\Delta z} \right] \left(H_x^{n+1/2}(i, j+1/2, k+1/2) - H_x^{n+1/2}(i, j+1/2, k-1/2) \right)$$

$$- \left[\frac{\Delta t}{\varepsilon.\Delta x} \right] \left(H_z^{n+1/2}(i+1/2, j+1/2, k) - H_z^{n+1/2}(i-1/2, j+1/2, k) \right) \rightarrow (17)$$

A three dimensional cell called Yee lattice is proposed by Yee in which the Electric fields lie along the midpoint of the cell edges and the Magnetic fields are along the centre of the cell faces as shown in fig. A1
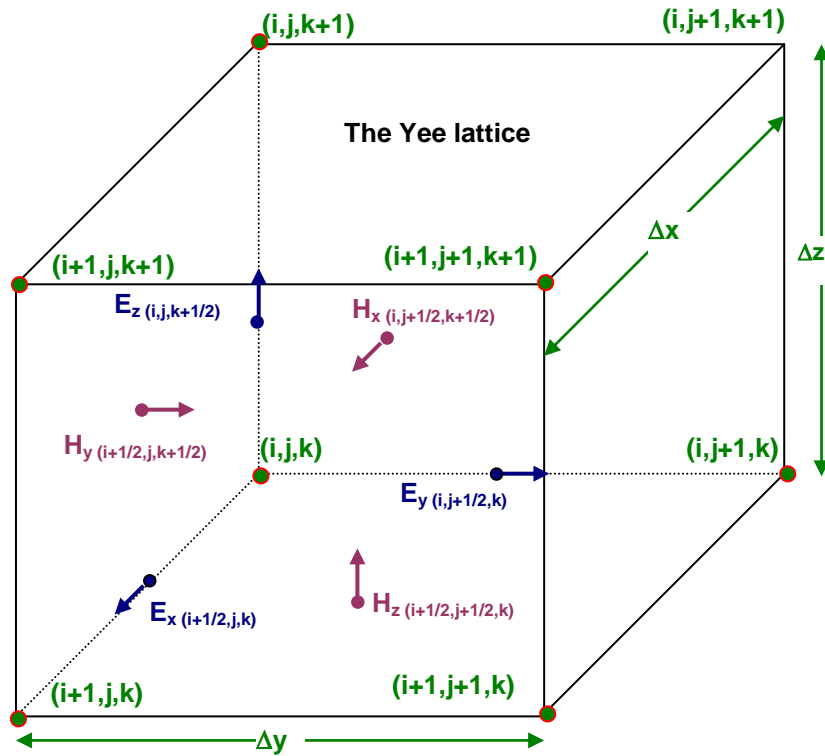
Fig. A1 Basic Yee Cell

The Electric and Magnetic fields are evaluated at alternate half time steps using the field equations 12-17 and each field components are calculated in each time step Δt. The updated value of a field component at any layer of the geometry is thus depends upon its value in the previous step and the previous value of the components of the other field at the adjacent special points.

In order to make the coding in a programming language easier, Sheen et al.[3] renamed the indices of the field components, eliminating the ½ index notations. This provides the value of each field component to be stored in a three dimensional array, with the array indices corresponding to the spatial indices. The modified equations are,

$$H_{x,i,j,k}^{n+1/2} = H_{x,i,j,k}^{n-1/2} + \frac{\Delta t}{\mu \Delta z}\left(E_{y,i,j,k}^{n} - E_{y,i,j,k-1}^{n}\right) - \frac{\Delta t}{\mu \Delta y}\left(E_{z,i,j,k}^{n} - E_{z,i,j-1,k}^{n}\right) \rightarrow (18)$$

$$H_{y,i,j,k}^{n+1/2} = H_{y,i,j,k}^{n-1/2} + \frac{\Delta t}{\mu \Delta x}\left(E_{z,i,j,k}^{n} - E_{z,i-1,j,k}^{n}\right) - \frac{\Delta t}{\mu \Delta z}\left(E_{x,i,j,k}^{n} - E_{x,i,j,k-1}^{n}\right) \rightarrow (19)$$

$$H_{z,i,j,k}^{n+1/2} = H_{z,i,j,k}^{n-1/2} + \frac{\Delta t}{\mu \Delta y}\left(E_{x,i,j,k}^{n} - E_{x,i,j-1,k}^{n}\right) - \frac{\Delta t}{\mu \Delta x}\left(E_{y,i,j,k}^{n} - E_{y,i-1,j,k}^{n}\right) \rightarrow (20)$$

$$E_{x,i,j,k}^{n+1} = E_{x,i,j,k}^{n} + \frac{\Delta t}{\varepsilon \Delta y}\left(H_{z,i,j+1,k}^{n+1/2} - H_{z,i,j,k}^{n+1/2}\right) - \frac{\Delta t}{\varepsilon \Delta z}\left(H_{y,i,j,k+1}^{n+1/2} - H_{y,i,j,k}^{n+1/2}\right) \rightarrow (21)$$

$$E_{y,i,j,k}^{n+1} = E_{y,i,j,k}^{n} + \frac{\Delta t}{\varepsilon \Delta z}\left(H_{x,i,j,k+1}^{n+1/2} - H_{x,i,j,k}^{n+1/2}\right) - \frac{\Delta t}{\varepsilon \Delta x}\left(H_{z,i+1,j,k}^{n+1/2} - H_{z,i,j,k}^{n+1/2}\right) \rightarrow (22)$$

$$E_{z,i,j,k}^{n+1} = E_{z,i,j,k}^{n} + \frac{\Delta t}{\varepsilon \Delta x}\left(H_{y,i+1,j,k}^{n+1/2} - H_{y,i,j,k}^{n+1/2}\right) - \frac{\Delta t}{\varepsilon \Delta y}\left(H_{x,i,j+1,k}^{n+1/2} - H_{x,i,j,k}^{n+1/2}\right) \rightarrow (23)$$

The leaf-frog algorithm proposed by Yee is employed for the discretization in space and time and is shown in fig.A2

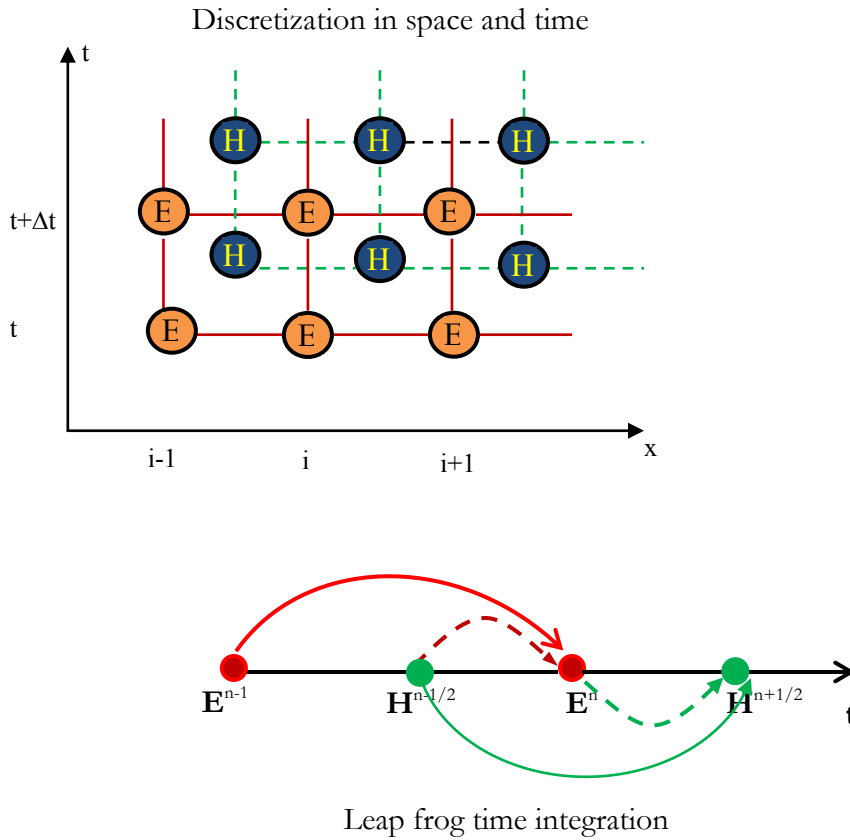Discretization in space and time

Leap frog time integration

Fig.A2 The FDTD technique by Yee.

A.2   Boundary conditions

As in the case of any computational electromagnetic method, FDTD technique requires complicated computational efforts and unlimited computational resources. In order to minimize the computational resources, the simulation domain is truncated and this results spurious fields from the boundaries unless appropriate techniques are employed to minimize this effects. The boundary condition should ensure that the outgoing wave is completely absorbed at the boundary, making domain appear infinite in extend with minimum numerical back reflection.

Perfectly matched layer (PML) boundary condition [4] is employed in theoretical modeling used in this thesis. In PML an artificial layer of absorbing

material is placed around the outer boundary of the computational domain. The plane wave incident from the FDTD free space to the PML region at an arbitrary angle is completely absorbed.

A.3 The Nyquist Criterion

The Nyquist sampling theorem states that there must be at least two samples per spatial period for adequate sampling [5]. In most cases the sampling is not exact and the smallest wavelength is not precisely determined and more than two samples per wavelength is suggested.

A.4 Stair case approximation for the source modeling.

The feeding point is modeled using Lubber's[6] stair case approach. The mesh transition from the electric field source location to the full width of the coplanar wave guide is modeled as shown in the fig. 3.6
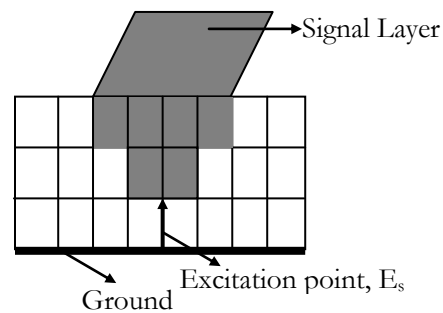
Fig. A3 Stair cased approach for the Feed modeling

It is seen from the stair cased transition in feed line that the substrate is discredited in order to incorporate more than one Yee cell. A gap feed model can be obtained by applying the excitation field between the microstrip line and the ground plane using a stair cased mesh transition

A.5 The FDTD Flowchart:
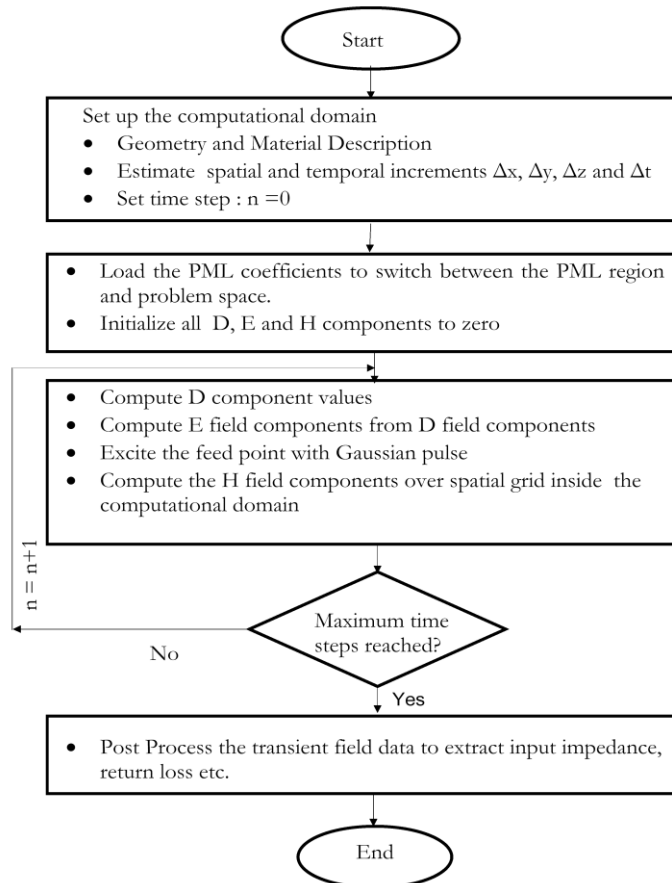
The FDTD flow chart is illustrated in fig. A4

Fig. A4 The FDTD flowchart.

References:

[1] K.S.Yee, "Numerical solution of initial boundary value problems involving Maxwell's equations in isotropic media," IEEE Trans. Antennas Propagat. Vol.14, no.4, pp.302-307, May 1966.

[2] Andrew F Peterson, Scott L Ray and Raj Mittra, " Computational methods for electromagnetic, " University press, India, 2001.

[3] David M. Sheen, Sami M.Ali, Mohamed D. Abouzahra and Jin Au Kong, "Application of the three dimensional finite difference time domain method to the analysis of planar Microstrip circuits, " IEEE Trans. Microwave Theory and Tech., Vol. 38, pp. 849-857.

[4] Jean Pierre Berenger, " A perfectly matched layer for the absorption of electromagnetic waves", Journal of Computational physics, 114, pp.185-200, 1994.

[5] Allen Taflov, " Computational electromagnetic: The Finite Difference Time Domain method", Artech house publishers, London, 1995.

[6] R.J. Luebbers and H.S. Langdon, " A Simple feed model that reduces time steps needed for FDTD antenna and Microstrip calculatons", IEEE Trans. Antennas Propagat., Vol.44, pp.1000-1005, July 1996.

LIST OF PUBLICATIONS

International Journal

1. **P.C. Bybi**, Gijo Augustin, B. Jitha, C.K. Aanandan, K.Vasudevan and P.Mohanan, *"A Quasi-omnidirectional antenna for modern wireless communication gadgests"*, **IEEE Antennas and Wireless Propagation Letters**, Vol.7, pp.504-507, 2008

2. Gijo Augustin, **P.C. Bybi**, V.P. Sarin, P.Mohanan, C.K. Aanandan and K Vasudevan, *"A Compact Dual band Planar Antenna for DCS-1900/PCS/PHS, WCDMA/IMT-2000 and WLAN Applications"*, **IEEE Antennas and Wireless Propagation Letters**, Vol.7, pp.108-111,2008.

3. B.Jitha, **P.C. Bybi**, C.K. Aanandan and P.Mohanan, " Microstrip band rejection filter using open loop resonator", **Microwave and optical technology letters**, Vol.50, No.6, pp.1550-1551, 2008

4. **P.C. Bybi**, Gijo Augustin, B. Jitha, Binu Paul, C.K.Aanandan , K. Vasudevan and P.Mohanan, "Compact Monopole Excited Drum Shaped Antenna for AWS/ DCS/ PCS/ DECT/ 3G/ UMTS/ BLUETOOTH Application," **International Journal on Wireless and optical communications**, Vol. 4, No.2,pp. 195-206, 2007.

5. **P.C. Bybi**, B. Jitha, P.Mohanan and C.K.Aanandan, "Wide Band Planar Antenna for New Generation Mobile Applications," **International Journal of Antennas and Propagation**, Vol.2007,pp.1-7, 2007

6. M.N. Suma, **P.C. Bybi**, P.Mohanan, "A wideband Hybrid printed monopole/Rectangular patch antenna," **International Journal on Wireless and Optical Communications**, Vol. 4, No.1, pp. 53-59, 2007.

7. Shameena V.A., Suma M.N., Raj Rohith K., **Bybi P.C.** and Mohanan, P ,"Compact ultra-wideband planar serrated antenna with notch band ON/OFF control," **IEE Electronics Letters**, Vol. 42, No. 23, pp. 1323 – 1324, 2006.

8. Suma, M.N, Raj, R.K, Joseph, M, **Bybi P.C**, Mohanan P, "A compact dual band planar branched monopole antenna for DCS/2.4-GHz WLAN applications," **Microwave and Wireless Components Letters**, Vol. 16, No. 5, pp. 275 – 277, 2006.

9. M. N. Suma, **P. C. Bybi**, and P. Mohanan ,"A wideband printed monopole antenna for 2.4-GHz WLAN applications", *Microwave and Optical Technology Letters,*Vol. 48, No.5, pp. 871-873, 2006.

10. M.N. Suma, Rohith K Raj, Manoj Joseph, **P.C. Bybi** and P.Mohanan, " A Compact Dual Band Planar Branched Monopole Antenna for DCS/2.4-GHz WLAN Applications", *IEEE Microwave and Wireless Components Letters*, Vol.16, No.5, 2006.

International Conference

1. **P.C. Bybi,** B. Jitha, C.K. Aanandan, K.Vasudevan, P.Mohanan, "A Compact wideband Antenna for modern wireless communication systems," Proceedings of URSI General Assembly 20008, Chicago, USA.

2. G. Augustin, **P.C. Bybi**, V.P. Sarin, M.S. Nisha, P.Mohanan, C.K. Aananda, K.Vasudevan, " Compact dual band antenna for handheld wireless communication gadgets," Proceedings of IEEE Antennas and Propagation Society International Symposium 2008, Sandiago, USA.

National Conference

1. P.C.Bybi, G. Augustin, B.Jitha, Binu Paul, C.K. Aanandan, K Vasudevan and P.Mohanan "Compact Drum Shaped Monopole Antenna for New Generation Mobile Applications", Proc. Of National Symposium on Antennas and Propagation (APSYM2006), pp.249-252, Dec. 2006.

Citations

1. Reference to the paper "A compact Dual Band Planar Branched Monopole Antenna for DCS/2.4GHz WLAN Applications", Suma M.N, Rohith K.Raj, Manoj Joseph, **Bybi P.C** and P.Mohanan, *IEEE Microwave and Wireless Components Letters* Vol.16, No.5, May 2006. pp 275-277.in the paper entitled "Dual Wideband Printed Monopole Antenna for WLAN/WiMAX Applications". Chien-Yuan Pan, Tzyy-Sheng Horng, Wen-Shan Chen and Chien-Hsiang Huang, *IEEE Antennas and Wireless Propagation Letters*, VOL. 6, 2007.

2. Reference to the paper"A wide Band Printed Monopole antenna for 2.4GHz WLAN Applications". Suma M.N, **Bybi P.C** and P.Mohanan, *Microwave and Optical Technology Letters* Vol.48, No.5, May 2006. pp 871-873 in the Master's Thesis entitled "Design and Application of Planar Dual-band S-shaped Monopole Antennas for WLAN" by Chuen-shian Yan, Electrical Engineering Department.

3. Reference to the paper " A compact Dual Band Planar Branched Monopole Antenna for DCS/2.4GHz WLAN Applications" Suma M.N, Rohith K.Raj, Manoj Joseph, **Bybi P.C** and P.Mohanan, *IEEE Microwave and Wireless Components Letters* Vol.16, No.5, May 2006. pp 275-277 in the Master's Thesis entitled "Design and Application of Planar Dual-band S-shaped Monopole Antennas for WLAN" by Chuen-shian Yan, Electrical Engineering Department.

4. Reference to the paper"A wide Band Printed Monopole antenna for 2.4GHz WLAN Applications". Suma M.N, **Bybi P.C** and P.Mohanan, *Microwave and Optical Technology Letters* Vol.48, No.5, May 2006. pp 871-873 in the paper entitled "Analysis and Application of an On-Package Planar Inverted-F Antenna"in IEEE Transactions on Antennas And Propagation, Vol. 55, No. 6, June 2007 authored by Ching-Wei Ling, Chia-Yu Lee, Chia-Lun Tang, and Shyh-Jong Chung.

RESUME OF THE AUTHOR

BYBI P.C.

Research Scholar,
CREMA, Department of Electronics,
Cochin University of Science and Technology,
Kochi, India – 682 022.
Tel   : +91-484-2576418
Mobile : +91-9495129729
Email   : bybi@ieee.org

Objective:

To pursue research activities in the field of planar wideband antennas for communication gadgets.

Education :

M.Sc. Applied Electronics
Bharathiar University, Coimbatore, India
Duration : 2001-2003
Score :76.6% - First Class and Fourth Rank

B.Sc. Electronics
M.G. University , Kottayam, India
Duration : 1998-2001
Score :82.4% - First Class with Distinction

Participation in National / International Conferences

Participated and presented research paper in XXIX URSI General Assembly, 7-16 August 2008, held at Chicago, Illinois, USA.

Participated and presented research paper in National Symposium on Antennas and Propagation(APSYM), December 2006 held at department of Electronics, CUSAT, India.

Publications:

International Journal   : 10
International Conference   : 2
National Conference   : 1

Academic Honours

Awarded Research Fellowship for Meritorious Students(RFSMS) by University Grants Commission(UGC) Government of India in the year 2007.

Recipient of University IVth Rank for M.Sc. Applied Electronics examination conducted by the Bharathiyar University, India.

Teaching Experience:

Two years of teaching experience for M.Sc. Applied Electronics at Jai Bharath College of Arts and Science, Affiliated to M.G. University, Kottayam, India.

Computer Proficiency:

Programming Languages: Matlab, C, Fortran.
RF CAD Packages   : Ansoft HFSS, Zeland IE3D, CST Microwave-Studio, Flomerics Microstripes.

Membership in Professional Bodies

Student Member- Institute of Electronics and Electrical Engineers (IEEE)

INDEX